



Norwegian University of
Science and Technology

Catalysis for Control of Methane Slip in Marine Machinery

Using a Palladium based Catalyst

Helene Mørkkåsa Sandvik

Chemical Engineering and Biotechnology

Submission date: June 2016

Supervisor: Hilde Johnsen Venvik, IKP

Co-supervisor: Rune Lødeng, IKP

Norwegian University of Science and Technology
Department of Chemical Engineering

Preface

This report is written for my Master's Thesis in the course TKP4900 Chemical Process Technology at the Department of Chemical Engineering, at the University of Science and Technology (NTNU). It is an extension of my Specialization Project in the course TKP4510 Catalysis and Petrochemistry. The project, including laboratory work, has been performed during the fall 2015 and spring 2016 at NTNU, with Professor Hilde Venvik as main supervisor and co-supervisors Senior Scientist Rune Lødeng at SINTEF and Research Scientist Jia Yang at SINTEF. It is affiliated with a new project awarded by the Research Council of Norway TRANSPORT 2025 program, which includes finding measures to reduce NO_x formation. A part of that work is to find catalysts for methane slip, and therefore this project included synthesis, characterization and testing of the active catalyst palladium. The catalyst was tested for the methane oxidation reaction in a rig at NTNU, build by Professor Hilde Venvik and prepared by Research Scientist Jia Yang at SINTEF.

I would like to thank my supervisor Professor Hilde Venvik for help and discussions during the project, Senior Scientist Rune Lødeng at SINTEF for always having good theories and ideas, and Research Scientist at SINTEF Jia Yang for the preparations of the rig, always answering questions and helping out at the lab. Lastly, I would like to thank Hanna Marie Storrvik for cooperation and helpful discussions during the project.

I declare that this is an independent work according to the exam regulations of the Norwegian University of Science and Technology (NTNU).

Trondheim, June 3rd, 2016



Helene Sandvik

Abstract

In a world distributing more and more liquefied natural gas (LNG), due to its advantages within health, environment and energy compared to gasoline and diesel, it is favourable to research more within this area. The main objective of this study is to find an extra route to the conventional high-temperature burning of methane (main component in LNG) in the marine machinery, in which produces noxious by-products. The engines existing today achieves very low NO_x -emissions at high efficiency, but emits low concentrations of CH_4 . Methane is a greenhouse gas with 20 times the global warming potential of CO_2 and measures to improve the methane slip abatement by catalytic oxidation of methane using palladium supported catalysts will be studied. Pure palladium catalysts are expensive, therefore the studied catalysts are supposed to be used as references when exploring the opportunities within activity of palladium based catalysts mixed with other metals, such as nickel, or catalysts using small amounts of palladium or not using palladium at all.

Three catalysts were prepared using incipient wetness impregnation with a solution of palladium nitrate and γ -alumina, including two 0.2 wt% Pd/ Al_2O_3 catalysts and one 2.0 wt% Pd/ Al_2O_3 catalyst. The catalysts were characterized using Nitrogen Adsorption, X-Ray Fluorescence, Chemisorption with H_2 and CO , X-Ray Diffraction and Thermogravimetric Analysis, to find the catalysts' chemical and physical properties. Their activities were tested by loading the catalysts into a reactor and install it in a setup for methane oxidation. The gas feed consisted of various compositions of methane, oxygen and nitrogen at 1 bar and the temperature was raised from room temperature and up to the temperature needed to achieve practically complete methane conversion. Deactivation experiments were also performed by running the reactions in series and comparing the temperatures where 100% methane conversion was achieved, $T_{100\%}$. An increased $T_{100\%}$ can reveal the extent of the catalysts deactivation, as the reaction is irreversible and extremely exothermic.

The results from the testing showed that the catalyst with the highest loading, i.e. 2.0 wt% Pd/ Al_2O_3 , performed the best when comparing the catalysts at the same reference conditions, such as using fresh catalyst, a constant total molar feed flow equal to 200 NmL/min and inlet gas composition of methane/oxygen/nitrogen equal to 2%/10%/88%. The $T_{100\%}$ was increased from 437 °C to 541 °C for the 2.0 wt% and 0.2 wt% catalysts, respectively. The lowest $T_{100\%}$ equal to 317 °C was achieved when the air/fuel-ratio was 10 and the inlet gas flow composition of methane/oxygen/nitrogen was 0.1%/1%/98.9%. The catalysts showed the same trends where the lowest $T_{100\%}$ was achieved under lean conditions and air/fuel-ratio equal to 10. The results suggest that the palladium particles are more active in an oxygen rich environment, i.e. lean burn and A/F-ratio equal to 10, and it may correspond to bulk- or surface-oxidation of the Pd particles becoming more active. The TGA-results showed that the palladium stores a lot

of oxygen. No by-products such as CO were detected, hence the selectivity is equal to 100% under all conditions. The high activity can be explained by well dispersed metal particles on the γ -alumina surface, which is in agreement with the CO-chemisorption and XRD results. As the XRD and XRF did not show any impurities and it is therefore expected that the preparation method was good enough to remove organic molecules and nitrates.

The observed activity loss when testing the catalysts for deactivation may be due to sintering, and further analyses on the spent catalysts should be performed. The $T_{100\%}$ increased by 83 °C after all runs had completed for the 0.2 wt% compared to the 2.0 wt% which increased by 32 °C. The ignition temperatures of the reactions are supposed to be at almost the same temperature as the outlet of the machinery to save energy, and the observed temperatures were relatively low.

Sammendrag

I en verden der mer og mer flytende naturgass (LNG) blir distribuert, grunnet dens fordeler innenfor helse, miljø og energi i forhold til bensin og diesel, er det gunstig å forske mer på dette området. Hovedmålet med denne oppgaven er å finne en ekstra vei til den konvensjonelle høy-temperaturs forbrenningen av metan (hovedkomponenten i LNG) i det marine maskineriet, som produserer giftige nitrogenholdige biprodukter. Dagens maskiner oppnår veldig lave NO_x -utslipp ved høy virkningsgrad men slipper ut konsentrasjoner av metan. Metan er en klimagass med 20 ganger mer global oppvarmingspotensial i forhold til CO_2 , og tiltak for å forbedre fangsten av metanslipp ved katalytisk oksidasjon av metan ved bruk av palladiumbaserte katalysatorer og γ -alumina bærere er ettertraktet. Katalysatorer laget av ren palladium er dyre, derfor vil katalysatorene i denne oppgaven bli brukt for sammenligning mot palladium-baserte katalysatorer laget av en metallblandinger, katalysatorer med en liten mengde palladium eller katalysatorer uten palladium.

Tre katalysatorer ble fremstilt ved å fuktighetsimpregnere (incipient wetness impregnation) γ -alumina bærere hvor palladiumnitrat ble påført i vannløsningen, inkludert to 0.2 wt% Pd/ Al_2O_3 katalysatorer og en 2.0 wt% Pd/ Al_2O_3 katalysator. Katalysatorene ble karakterist ved hjelp av nitrogenadsorpsjon, røntgenfluorescens, hydrogen- og karbonmonoksidkjemisorpsjon, røntgenkrystallografi og termogravimetrisk analyse, for å finne katalysatorenes kjemiske og fysiske egenskaper. Aktiviteten ble testet ved å putte katalysator i en reaktor som ble installert på en rigg. Fødegassen besto av ulike sammensetninger av metan, oksygen and nitrogen ved 1 bar og temperaturen ble økt fra romtemperatur og opp til temperaturen som trengtes for å oppnå nesten fullstendig metan omdanning. Deaktiveringseksperimenter ble også gjort ved å kjøre reaksjonene i serier for å sammenligne temperaturene hvor 100% metanomdannelse ble oppnådd, $T_{100\%}$. En økt verdi av $T_{100\%}$ kan avsløre omfanget av katalysatorenes deaktivering, fordi reaksjonen er irreversibel og ekstremt eksoterm.

Resultatene fra testingen viste at katalysatoren med den høyeste palladiummengden, altså 2.0 wt% Pd/ Al_2O_3 , presterte best når katalysatorene ble sammenlignet ved de samme referansebetingelser, sånn som bruk av ny katalysator, konstant molar fødegass lik 200 NmL/min og fødegassammensetning av metan/oksygen/nitrogen lik 2%/10%/88%. $T_{100\%}$ økte fra 437 °C til 541 °C for henholdsvis 2.0 vekt% og 0.2 vekt% katalysatorene. Den laveste $T_{100\%}$ ble oppnådd med en luft/metan-ratio (A/F) lik 10. Resultatene foreslår at palladiumpartiklene er mer aktive i en oksygenrik atmosfære, altså A/F lik 10, som kan forklares ved bulk- eller overflateoksidasjon av palladiumpartiklene som blir mer aktive. TGA-resultatene viste at palladium inneholder en god del oksygen. Ingen biprodukter sånn som CO ble detektert, derav er CO_2 -selektiviteten lik 100% for alle reaksjonsbetingelser. Den høye aktiviteten kan forklares av godt dispergerte metallpartikler på γ -aluminaoverflaten, som også er i overenstemmelse med

CO-kjemisorpsjon og XRD resultatene. Siden XRD og XRF ikke viste noen urenheter, er det antatt at syntetiseringsmetoden var god nok for å bli kvitt organiske og nitrøse forbindelser.

Det observerte aktivitetstapet når katalysatorene ble testet for deaktivering kan forklares ved sintring, og videre analyser av de brukte katalysatorene bør gjøres. For 0.2 vekt%, økte $T_{100\%}$ med 83 °C etter at alle reaksjonene hadde kjørt, sammenlignet med 2.0 vekt%-katalysatoren som kun økte med 32 °C. Initiertemperaturer for reaksjonen bør være ca like temperaturen ut av det marine maskineriet for å spare energi. De observerte temperaturene var relativt lave.

Contents

1	Introduction	1
2	Theory	3
2.1	Palladium as an active metal	3
2.2	γ -alumina support	3
2.3	Methane oxidation	4
2.3.1	Reactions and Kinetics	4
2.3.2	Reaction Mechanisms	5
2.4	Preparation of supported catalyst	5
2.4.1	Incipient Wetness Impregnation	5
2.4.2	Drying	6
2.4.3	Calcination	6
2.5	Catalyst characterization	6
2.5.1	Nitrogen Adsorption	6
2.5.2	X-Ray Fluorescence	8
2.5.3	Chemisorption	8
2.5.4	Temperature Programmed Reduction	11
2.5.5	X-Ray Diffraction	13
2.5.6	Thermogravimetric Analysis	14
2.6	Catalyst Testing	15
2.6.1	Powder vs pellets catalyst	15
2.6.2	Gas Chromatograph	15
2.6.3	Activity and selectivity	16
2.6.4	Turnover-frequency	16
2.6.5	Gas Hourly Space Velocity	17
2.6.6	Residence Time	17
2.6.7	Heterogeneous Catalyst Deactivation	17
3	Experimental	19
3.1	Risk evaluation	19
3.2	Catalyst Preparation	19
3.3	Catalyst Characterization	20
3.3.1	Nitrogen Adsorption	20
3.3.2	X-Ray Fluorescence	20
3.3.3	Chemisorption	21

3.3.4	X-Ray Diffraction	22
3.3.5	Thermogravimetric Analysis	22
3.4	Activity Measurements	24
4	Results and discussion	28
4.1	Catalyst Characterization	28
4.1.1	Nitrogen Adsorption	28
4.1.2	Chemisorption	29
4.1.3	X-Ray Fluorescence	32
4.1.4	X-Ray Diffraction	33
4.1.5	Thermogravimetric Analysis	34
4.2	Activity Measurements	35
5	Conclusions	45
6	Suggestions for further work	47
	Appendix	I
A	Risk assessment	I
B	Calculation of amount of Pd(NO₃)₂ × H₂O used	III
C	Calculation of the amount of water needed	IV
D	Exact catalyst mass used for the experiments	V
D.1	Nitrogen Adsorption	V
D.2	X-Ray Fluorescence	V
D.3	Chemisorption	VI
D.4	Thermogravimetric Analysis	VI
D.5	Catalyst Testing	VI
E	H₂-Chemisorption results using the 2nd isotherm	VII
F	Pore Size Distribution	VIII
G	XRF-results	X
H	Weight% of Palladium in the XRF-results	XV
I	TGA-measurements: weight changes	XVI

J	Sketch of the methane oxidation reactor	XVIII
K	MFC calibration data	XIX
L	Temperature measurements in the catalyst bed	XXII
M	Gas Hourly Space Velocity calculations	XXXI
N	Results from methane oxidation testing	XXXII
N.1	0.2 wt% Pd/Al ₂ O ₃ SP catalyst	XXXII
N.2	0.2 wt% Pd/Al ₂ O ₃ MT catalyst	XXXIII
N.3	2.0 wt% Pd/Al ₂ O ₃ MT catalyst	XXXVI
O	Conversion Calculations	XLI
P	Check of the mass balances from the reaction	L

List of Symbols

Variable	Description	Unit
V_{SOL}	Volume of solution	m^3
V_{PT}	Pore volume	m^3
T	Temperature	$^{\circ}C$
p	Pressure	bar
p^0	Equilibrium pressure of condensed gas	bar
n_m	Monolayer capacity	mm^3
n_{ads}	Volume each molecule occupies	$mm^3/\text{molecule}$
C	Parameter related with the energy of adsorption	-
A_s	Specific surface area	m^2
a_m	Area occupied by one molecule in the monolayer	m^2
N_A	Avogadro's number	mol^{-1}
m_{cat}	Mass of catalyst	kg
V_m	Molar volume	m^3/mol
D	Dispersion	%
v_{ads}	Volume of gas adsorbed	mol/g_{cat}
Mm	Molecular weight	g/mol
F	Adsorption stoichiometry	-
x_m	Metal weight fraction in the catalyst	-
d	Average particle size	m
f	Factor describing the particle shape	-
V_{sp}	Specific volume of metal particle	m^3
S_m	Specific surface area of the metal	m^2
ΔG	Change in Gibbs free energy	J
ΔG^0	Change in Gibbs free energy under standard conditions	J
n	Number of moles	Mole
R	Gas constant	J/K mol
p_{H_2O}	H_2O Partial pressure	bar
$p_{H_2O,eq}$	The equilibrium partial pressure of H_2O	bar
τ	Volume-weighted crystalline thickness	-
τ	Residence time	s
K	Constant	-
λ	Line broadening of XRD diagram	nm
β	Radiation wavelength	nm
θ	Angle of diffraction	$^{\circ}$
X_{CH_4}	Methane conversion	-
$F_{i,in}$	In flow of component i	NmL/min
$F_{i,out}$	Out flow of component i	NmL/min
mol% i	Mole percent of component i	%
u_0	Volumes of feed as gas at STP/hr	Nml/min
GHSV	Gas Hourly Space Velocity	s^{-1}

Abbreviations

BET	Brunauer-Emmet-Teller
BJH	Barret, Joyner and Halenda
ER	Eley-Rideal reaction mechanism
FID	Flame Ionization Detector
GC	Gas Chromatograph
HSE	Health, Safety and Environment
LFC	Level Flow Controller
LH	Langmuir-Hinshelwood reaction mechanism
LNG	Liquefied natural gas
MFC	Mass Flow Controller
MvK	Mars-van Krevelen reaction mechanism
NG	natural gas
NO _x	noxious by-products
NTNU	the Norwegian University of Science and Technology
PC	Pressure Controller
PHA	Pulse Height Analyzer
SEM	Scanning Electron Microscope
TEM	Transmission Electron Microscope
XRPD	X-Ray Powder Diffraction
TCD	Thermal Conductivity Detector
TGA	Thermogravimetric Analysis
TOF	Turnover Frequency
TPR	Temperature-Programmed Reduction
WDXRF	Wavelength Dispersive X-Ray Fluorescence
XRD	X-Ray Diffraction
XRF	X-Ray Fluorescence
GHSV	Gas Hourly Space Velocity
SP	Specialization Project
MT	Master's Thesis

List of Figures

1	An illustration of the γ -alumina cubic defect spinel structure unit cell, in which the aluminium atoms occupy both the tetrahedral and octahedral sites as small, yellow spheres and the oxygen atoms are arranged in a cubic close packing as green spheres. The illustration is adapted from The University of Groningen.[17]	4
2	Pore and particle profiles after drying at different rates. The Figure is adapted from a lecture in the Specialization Course TKP4515 Catalysis and Petrochemistry fall 2015 at NTNU.	6
3	An illustration of chemisorption and the isotherms obtained from increasing the pressure the sample is exposed to. The highest isotherm symbolizes how the volume of gas which is chemisorbed and physisorbed. The lower isotherm is the physisorbed gas volume. The difference between the isotherms, the regression line in the middle, is the volume of gas chemisorbed. The Figure is obtained from HSE lectures at the Catalysis and Petrochemistry group during fall 2015 at NTNU held by Cristian Ledesma.[27]	9
4	A TPR-profile where the hydrogen consumption of a Pd/ γ -Al ₂ O ₃ catalyst is measured as a function of temperature (°C). The result is obtained from an article by B. Wang et al. [32].	12
5	The equilibrium diagram for the system Al-Al ₂ O ₃ in various pressures of H ₂ -H ₂ O at 500-2000 °C. It also shows a phase transformation of γ -alumina to α -alumina at high temperatures. By adjusting the pressure and the temperature the alumina can be reduced to liquid or solid aluminium. The Figure is adapted from <i>The Possible Reduction of Alumina to Aluminum Using Hydrogen</i> [33] . . .	12
6	X-rays scattered from the crystalline solid interfere, producing a diffracted beam. The Figure is obtained from the University of Delaware.[36] λ is the wavelength of the X-rays, d is the distance between two lattice planes, θ is the angle between the incoming X-rays and the normal to the reflecting lattice plane.	13
7	The procedure of oxidation and reduction of Palladium supported on Al ₂ O ₃ under different atmospheres, including hydrogen (25% H ₂ /75% Ar), argon and air (20% O ₂ /80% N ₂) at different temperatures. The palladium will alter between the oxidized state, PdO and the reduced state, Pd ⁰	14
8	Block diagram of a chromatographic system, adapted from the book named Gas Chromatography[42]. It includes a sample introduction device which introduces the sample into the inlet. The gas flows through the column, before a detector detects the composition of the out flow, and sends the signal to a computer.	16

9	An illustration of the temperature profile as a function of time(min) of the TGA with the exposed gases and the hold-time (minutes) shown below the curve. The curve is divided in isothermal and dynamic parts, where the rate is 5°C/min in the dynamic parts. The gases are hydrogen (25% H ₂ /75% Ar), argon (Ar) and Air (20% O ₂ /80% N ₂).	23
10	The flow diagram of the methane oxidation process, where MFC and PC are controllers of the mass flows, level and pressure, respectively. The GC is the gas chromatography. The inlet gases used for this work are nitrogen, air and methane and the flows are opened by control valves. Several vents are present to release the reactants, products and by-products if required.	24
11	An illustration of the temperature profile of the catalyst testing, with 25 to 50 °C intervals, hold-up times of 20 to 30 minutes and a rate of 5 °C/min.	26
12	The XRD patterns for the alumina support (black line), 2 wt% Pd/Al ₂ O ₃ MT catalyst (purple line), the 0.2 wt% SP catalyst(dark green line) and 0.2 wt% MT catalyst (light green line). The lines marked red and blue are crystal reflections for γ-Al ₂ O ₃ and palladium, respectively. The graph is shown as counts per minute (CPS) as a function of 2θ. The Y Offset is adjusted to fit all the results in the same plot by position the objects above or below the baseline.	33
13	TGA measurement of 2.0 wt% Palladium supported Al ₂ O ₃ catalyst. The blue and red line are the change in weight% of the catalyst and the temperature as a function of time, respectively. The procedure of oxidation and reduction of Palladium supported on Al ₂ O ₃ under different atmospheres, including hydrogen (25% H ₂ /75% Ar), argon and air (20% O ₂ /80% N ₂) at different temperatures. An illustration can be found in Section 2.5.6 in Figure 7. The catalyst is reduced for three hours up to 350 °C, oxidized for five hours up to 700 °C and lastly reduced for three hours up to 350 °C. The palladium will alter between being an oxygen-carrier, PdO, and the reduced state, Pd ⁰ . It starts on the baseline equal to 100 wt% each time the gases are switched.	35
14	The temperature profile of the 2.0 wt% Pd/Al ₂ O ₃ MT catalyst at each setpoint hold-up temperature when testing the catalyst for methane oxidation using a total molar flow equal to 200 NmL/min and gas feed composition of methane, oxygen and nitrogen equal to 2%, 10% and 88%, respectively. The setpoint temperatures were every 50 °C from 250 to 500 °C. The catalyst bed was 2 cm in height and the measurements were performed at axial length across the catalyst bed equal to 0 cm, 1 cm and 2 cm.	36

15	The methane converted (%) in the catalytic combustion of methane over the 0.2 wt% Pd/Al ₂ O ₃ SP catalyst as a function of the catalyst bed temperature (°C) with a GHSV equal to 59400 NmL/g _{cat} h. The temperature was ramped for 5°C/min and the temperature was held for 30 minutes every 50 °C. The total molar flow is 200 NmL/min and the flow reactant feed CH ₄ /O ₂ /N ₂ is 4/20/176 (2%/10%/88%) NmL/min. The red curve symbolizes when the reaction was heated up to 550 °C and the blue curve when it was cooled from 550 to 250 °C.	38
16	The methane converted (%) in the catalytic combustion of methane over the 0.2 wt% Pd/Al ₂ O ₃ MT catalyst as a function of the catalyst bed temperature (°C) with a GHSV equal to 58000 NmL/g _{cat} h. The temperature was ramped for 5°C/min and the temperature was held for 20-30 minutes every 50 °C.	40
17	The methane converted (%) in the catalytic combustion of methane over the 0.2 wt% Pd/Al ₂ O ₃ MT catalyst as a function of the catalyst bed temperature (°C) with a GHSV equal to 58800 NmL/g _{cat} h for reaction number 1 to 8 and 59400 NmL/g _{cat} h for reaction number 9 and 10, as described in Table 3. The temperature was ramped for 5°C/min and the temperature was held for 20-30 minutes every 50 °C.	43
18	The risk evaluation due to the experimental work done, including synthesis, characterization and testing of the catalysts for methane oxidation under application relevant conditions.	I
19	The risk evaluation due to the experimental work done, including synthesis, characterization and testing of the catalysts for methane oxidation under application relevant conditions and the likelihoods and consequences of potential accidents.	II
20	The pore volume (cm ² /g · Å) distribution as a function of the pore size (Å) for alumina based on desorption branch using BJH model. The pore diameter is given in a logarithmic scale.	VIII
21	The pore volume (cm ² /g · Å) distribution as a function of the pore size (Å) for the 0.2 wt% Pd/Al ₂ O ₃ SP catalyst based on desorption branch using BJH model. The pore diameter is given in a logarithmic scale.	VIII
22	The pore volume (cm ² /g · Å) distribution as a function of the pore size (Å) for the 0.2 wt% Pd/Al ₂ O ₃ MT catalyst based on desorption branch using BJH model. The pore diameter is given in a logarithmic scale.	IX
23	The pore volume (cm ² /g · Å) distribution as a function of the pore size (Å) for the 2.0 wt% Pd/Al ₂ O ₃ MT catalyst based on desorption branch using BJH model. The pore diameter is given in a logarithmic scale.	IX

- 24 The intensity (kcps)(blue line) measured as a function of 2θ up to $2\theta=88$ for 0.2 wt% Pd/Al₂O₃ SP, where palladium and alumina compounds were detected (green writing). Palladium compounds were detected around around 15-20 2θ . Iron compound was detected around 2θ equal to 57. X
- 25 The intensity (kcps)(blue line) of 0.2 wt% Pd/Al₂O₃ SP as a function of 2θ , where the results are not continuous, but only showed for the most common compounds. The XRF detected palladium and alumina. There are no traces of calcium, potassium, chlorine, sulfur, phosphorus, silicon, magnesium, sodium or fluorine. X
- 26 The intensity (kcps)(blue line) measured as a function of 2θ up to $2\theta=88$ for the second made 0.2 wt% Pd/Al₂O₃ MT, where palladium and alumina compounds were detected (green writing) and traces of silica, sulfur and silver. Palladium compounds were detected around around 15-20 2θ .Iron compound was detected around 2θ equal to 57. XI
- 27 The intensity (kcps)(blue line) of the second made 0.2 wt% Pd/Al₂O₃ MT as a function of 2θ , where the results are not continuous, but only showed for the most common compounds. The XRF detected palladium and alumina. There were also detected traces of silicon, potassium, silver and sulfur. There are no traces of calcium, chlorine, phosphorus, magnesium, sodium or fluorine. XI
- 28 The intensity (kcps)(blue line) measured as a function of 2θ up to $2\theta=88$ for 2.0 wt% Pd/Al₂O₃ MT, where palladium and iron were detected (green writing). Palladium compounds were detected around around 15-20 2θ and iron compounds were detected around 2θ equal to 57. XII
- 29 The intensity (kcps)(blue line) of 2.0 wt% Pd/Al₂O₃ MT as a function of 2θ , where the results are not continuous, but only showed for the most common compounds. The XRF detected palladium and alumina, and traces of potassium. There are no traces of calcium, chlorine, sulfur, phosphorus, silicon, magnesium, sodium or fluorine. XII
- 30 The intensity (kcps)(blue line) measured as a function of 2θ up to $2\theta=88$ for alumina, where palladium compounds were detected (green writing). Palladium compounds were detected around around 15-20 2θ .Iron compound was detected around 2θ equal to 57. XIII
- 31 The intensity (kcps)(blue line) of alumina as a function of 2θ , where the results are not continuous, but only showed for the most common compounds. The XRF detected alumina, and traces of potassium and tin. There are no traces of calcium, chlorine, sulfur, phosphorus, silicon, magnesium, sodium or fluorine. . XIII

32	The intensity (kcps)(blue line) measured as a function of 2θ up to $2\theta=88$ for the binder (HBO_3), where palladium compounds were detected (green writing). Palladium compounds were detected around 15-20 2θ	XIV
33	The intensity (kcps)(blue line of the binder (HBO_3) as a function of 2θ , where the results are not continuous, but only showed for the most common compounds. The XRF detected palladium and silicon. There are no traces of calcium, potassium, chlorine, sulfur, phosphorus, magnesium, sodium or fluorine.	XIV
34	An illustration of the temperature profile as a function of time of the TGA with exposed gases and hold-up times. The red numbers illustrate the reaction conditions where the data for mass change are calculated from.	XVII
35	A sketch of the reactor with dimensions which is used when 0.2 and 2.0 wt% palladium supported catalysts are tested during methane oxidation.	XVIII
36	The calibration curve of the air flow as a function of the % setpoint of the mass flow controller, where the trend line equation is shown.	XIX
37	The calibration curve of the Methane flow as a function of the % setpoint of the mass flow controller, where the trend line equation is shown.	XIX
38	The calibration curve of the Nitrogen flow as a function of the % setpoint of the mass flow controller, where the trend line equation is shown.	XIX
39	The methane converted (%) in the catalytic combustion of methane over the 0.2 wt% Pd/ Al_2O_3 SP catalyst as a function of the catalyst bed temperature ($^\circ\text{C}$) with a GHSV equal to 59400 $\text{NmL}/\text{g}_{cat}\text{h}$. The temperature was ramped for $5^\circ\text{C}/\text{min}$ and the temperature was held for 30 minutes every 50°C . The feed flow was constant equal 200 NmL/min and the composition of $\text{CH}_4/\text{O}_2/\text{N}_2$ is 4/20/176 (2%/10%/88%) NmL/min . The red curve symbolizes when the reaction was heated up to 550°C and the blue curve when it was cooled from 550°C to 250°C	XXXII
40	The methane converted (%) in the catalytic combustion of methane over the 0.2 wt% Pd/ Al_2O_3 MT catalyst as a function of the catalyst bed temperature ($^\circ\text{C}$) with a GHSV equal to 58000 $\text{NmL}/\text{g}_{cat}\text{h}$. The temperature was ramped for $5^\circ\text{C}/\text{min}$ and the temperature was held for 20 minutes every 50°C . The flow reactant feed $\text{CH}_4/\text{O}_2/\text{N}_2$ is 4/20/176 (2%/10%/88%) NmL/min . The red curve symbolizes when the reaction was heated up to 600°C and the blue curve when it was cooled from 600°C to 250°C	XXXIII

- 41 The methane converted (%) in the catalytic combustion of methane over the 0.2 wt% Pd/Al₂O₃ MT catalyst as a function of the catalyst bed temperature (°C) with a GHSV equal to 58000 NmL/g_{cat}h. The temperature was ramped for 5°C/min and the temperature was held for 20 minutes every 50 °C. The flow reactant feed CH₄/O₂/N₂ is 2/20/178 (1%/10%/89%) NmL/min. The red curve symbolizes when the reaction was heated up to 600 °C and the blue curve when it was cooled from 600 °C to 250 °C. XXXIII
- 42 The methane converted (%) in the catalytic combustion of methane over the 0.2 wt% Pd/Al₂O₃ MT catalyst as a function of the catalyst bed temperature (°C) with a GHSV equal to 58000 NmL/g_{cat}h. The temperature was ramped for 5°C/min and the temperature was held for 20 minutes every 50 °C. The flow reactant feed CH₄/O₂/N₂ is 2/10/188 (1%/5%/96%) NmL/min. The red curve symbolizes when the reaction was heated up to 600 °C and the blue curve when it was cooled from 600 °C to 250 °C. XXXIV
- 43 The methane converted (%) in the catalytic combustion of methane over the 0.2 wt% Pd/Al₂O₃ MT catalyst as a function of the catalyst bed temperature (°C) with a GHSV equal to 58000 NmL/g_{cat}h. The temperature was ramped for 5°C/min and the temperature was held for 20 minutes every 50 °C. The flow reactant feed CH₄/O₂/N₂ is 1/5/194 (0.5%/2.5%/97%) NmL/min. The red curve symbolizes when the reaction was heated up to 600 °C and the blue curve when it was cooled from 600 °C to 250 °C. XXXIV
- 44 The methane converted (%) in the catalytic combustion of methane over the 0.2 wt% Pd/Al₂O₃ MT catalyst as a function of the catalyst bed temperature (°C) with a GHSV equal to 58000 NmL/g_{cat}h. The temperature was ramped for 5°C/min and the temperature was held for 20 minutes every 25-50 °C. The flow reactant feed CH₄/O₂/N₂ is 1/10/189 (0.5%/5%/97%) NmL/min. The red curve symbolizes when the reaction was heated up to 600 °C and the blue curve when it was cooled from 600 °C to 250 °C. XXXV
- 45 The methane converted (%) in the catalytic combustion of methane over the 0.2 wt% Pd/Al₂O₃ MT catalyst as a function of the catalyst bed temperature (°C) with a GHSV equal to 58000 NmL/g_{cat}h. The temperature was ramped for 5°C/min and the temperature was held for 20 minutes every 25-50 °C. The flow reactant feed CH₄/O₂/N₂ is 4/20/176 (2%/10%/88%) NmL/min. The red curve symbolizes when the reaction was heated up to 650 °C and the blue curve when it was cooled from 650 °C to 250 °C. XXXV

- 46 The methane converted (%) in the catalytic combustion of methane over the 2.0 wt% Pd/Al₂O₃ MT catalyst as a function of the catalyst bed temperature (°C) with a GHSV equal to 58800 NmL/g_{cat}h. The temperature was ramped for 5°C/min and the temperature was held for 20 minutes every 50 °C. The flow reactant feed CH₄/O₂/N₂ is 4/20/176 (2%/10%/88%) NmL/min. The red curve symbolizes when the reaction was heated up to 500 °C and the blue curve when it was cooled from 500 °C to 200 °C. The tests were ran in series where this was run number one. XXXVI
- 47 The methane converted (%) in the catalytic combustion of methane over the 2.0 wt% Pd/Al₂O₃ MT catalyst as a function of the catalyst bed temperature (°C) with a GHSV equal to 58800 NmL/g_{cat}h. The temperature was ramped for 5°C/min and the temperature was held for 20 minutes every 50 °C. The flow reactant feed CH₄/O₂/N₂ is 4/20/176 (2%/10%/88%) NmL/min. The red curve symbolizes when the reaction was heated up to 500 °C and the blue curve when it was cooled from 500 °C to 200 °C. The tests were ran in series where this was run number two. XXXVI
- 48 The methane converted (%) in the catalytic combustion of methane over the 2.0 wt% Pd/Al₂O₃ MT catalyst as a function of the catalyst bed temperature (°C) with a GHSV equal to 58800 NmL/g_{cat}h. The temperature was ramped for 5°C/min and the temperature was held for 20 minutes every 50 °C. The flow reactant feed CH₄/O₂/N₂ is 2/20/178 (1%/10%/89%) NmL/min. The red curve symbolizes when the reaction was heated up to 500 °C and the blue curve when it was cooled from 500 °C to 250 °C. The tests were ran in series where this was run number three. XXXVII
- 49 The methane converted (%) in the catalytic combustion of methane over the 2.0 wt% Pd/Al₂O₃ MT catalyst as a function of the catalyst bed temperature (°C) with a GHSV equal to 58800 NmL/g_{cat}h. The temperature was ramped for 5°C/min and the temperature was held for 20 minutes every 50 °C. The flow reactant feed CH₄/O₂/N₂ is 4/20/176 (2%/10%/88%) NmL/min. The red curve symbolizes when the reaction was heated up to 500 °C and the blue curve when it was cooled from 500 °C to 250 °C. The tests were ran in series where this was run number four. XXXVII

- 50 The methane converted (%) in the catalytic combustion of methane over the 2.0 wt% Pd/Al₂O₃ MT catalyst as a function of the catalyst bed temperature (°C) with a GHSV equal to 58800 NmL/g_{cat}h. The temperature was ramped for 5°C/min and the temperature was held for 20 minutes every 50 °C. The flow reactant feed CH₄/O₂/N₂ is 2/10/188 (1%/5%/94%) NmL/min. The red curve symbolizes when the reaction was heated up to 500 °C and the blue curve when it was cooled from 500 °C to 200 °C. The tests were ran in series where this was run number five. XXXVIII
- 51 The methane converted (%) in the catalytic combustion of methane over the 2.0 wt% Pd/Al₂O₃ MT catalyst as a function of the catalyst bed temperature (°C) with a GHSV equal to 58800 NmL/g_{cat}h. The temperature was ramped for 5°C/min and the temperature was held for 20 minutes every 50 °C. The flow reactant feed CH₄/O₂/N₂ is 1/5/194 (0.5%/2.5%/97%) NmL/min. The red curve symbolizes when the reaction was heated up to 500 °C and the blue curve when it was cooled from 500 °C to 250 °C. The tests were ran in series where this was run number six. XXXVIII
- 52 The methane converted (%) in the catalytic combustion of methane over the 2.0 wt% Pd/Al₂O₃ MT catalyst as a function of the catalyst bed temperature (°C) with a GHSV equal to 58800 NmL/g_{cat}h. The temperature was ramped for 5°C/min and the temperature was held for 20 minutes every 50 °C. The flow reactant feed CH₄/O₂/N₂ is 1/10/189 (0.5%/5%/94.5%) NmL/min. The red curve symbolizes when the reaction was heated up to 450 °C and the blue curve when it was cooled from 450 °C to 250 °C. The tests were ran in series where this was run number seven. XXXIX
- 53 The methane converted (%) in the catalytic combustion of methane over the 2.0 wt% Pd/Al₂O₃ MT catalyst as a function of the catalyst bed temperature (°C) with a GHSV equal to 58800 NmL/g_{cat}h. The temperature was ramped for 5°C/min and the temperature was held for 20 minutes every 50 °C. The flow reactant feed CH₄/O₂/N₂ is 4/20/176 (2%/10%/88%) NmL/min. The red curve symbolizes when the reaction was heated up to 500 °C and the blue curve when it was cooled from 500 °C to 250 °C. The tests were ran in series where this was run number eight. XXXIX

- 54 The methane converted (%) in the catalytic combustion of methane over the 2.0 wt% Pd/Al₂O₃ MT catalyst as a function of the catalyst bed temperature (°C) with a GHSV equal to 59400 NmL/g_{cat}h. The temperature was ramped for 5°C/min and the temperature was held for 20 minutes every 50 °C. The flow reactant feed CH₄/O₂/N₂ is 0.2/1/198.8 (0.1%/0.5%/99.4%) NmL/min. The red curve symbolizes when the reaction was heated up to 400 °C and the blue curve when it was cooled from 400 °C to 200 °C. A gas bottle with 5% CH₄ in N₂ was used to achieve lower methane concentrations and were tested using a fresh catalyst. XL
- 55 The methane converted (%) in the catalytic combustion of methane over the 2.0 wt% Pd/Al₂O₃ MT catalyst as a function of the catalyst bed temperature (°C) with a GHSV equal to 59400 NmL/g_{cat}h. The temperature was ramped for 5°C/min and the temperature was held for 20 minutes every 50 °C. The flow reactant feed CH₄/O₂/N₂ is 0.2/2/197.8 (0.1%/1%/98.9%) NmL/min. The red curve symbolizes when the reaction was heated up to 375 °C and the blue curve when it was cooled from 375 °C to 200 °C. A gas bottle with 5% CH₄ in N₂ was used to achieve lower methane concentrations. The same catalyst as used to achieve the results in Figure 54 was used. XL

List of Tables

1	The analyse conditions using Chemisorption ASAP 2020 (SINTEF) at NTNU. The adsorptive was hydrogen, flows of hydrogen (H ₂) and helium (He) were used and the sample was evacuated with vacuum. The analyses were performed on 0.2 wt% palladium supported catalyst SP.	21
2	The analyse conditions using Chemisorption ASAP 2020 (SINTEF) at NTNU. The adsorptive was carbon monoxide, flows of hydrogen (H ₂) and helium (He) were used and the sample was evacuated with vacuum. The analyses were performed on the 0.2 wt% Pd/Al ₂ O ₃ SP and 0.2 wt% and 2.0 wt% palladium supported catalysts MT.	22
3	The feed flow compositions for reactions with different reaction conditions. The compositions differ with a CH ₄ :O ₂ -ratio equal to 1:5 and 1:10, i.e. rich and very rich oxygen environment. The reactions were ran from around 200 to around 650 °C, depending on the activity, with temperature intervals of 25 to 50 °C, rate at five °C/min and hold-up times of 20 to 30 minutes. The total feed flow were held constant at 200 NmL/min, where the composition of methane, oxygen and nitrogen were varied and consequently the set points. The calculations of the MFC set points to achieve the desired feed flows can be found in Appendix K.	26
4	The physical-chemical properties of the prepared 0.2 wt% Pd/Al ₂ O ₃ SP, 0.2 wt% Pd/Al ₂ O ₃ MT and 2.0 wt% Pd/Al ₂ O ₃ MT catalysts found by Nitrogen Adsorption using BET and BJH. Catalyst SP and MT are performed during fall 2015 for the Specialization Project and for the Master's Thesis during spring 2016, respectively. The results are shown for desorption and adsorption isotherms, respectively. Where one number is presented, the number is obtained from the desorption isotherm.	29
5	The physical-chemical properties of the 0.2 wt% Pd/Al ₂ O ₃ SP catalyst prepared during the Specialization Project during fall 2015 found by H ₂ chemisorption. Chemisorption was performed two times. The results are shown for the total adsorbed amount. The analysis conditions are found in Table 1.	30
6	The physical-chemical properties of prepared 0.2 wt% Pd/Al ₂ O ₃ SP, 0.2 wt% Pd/Al ₂ O ₃ MT and 2.0 wt% Pd/Al ₂ O ₃ MT catalysts found by CO chemisorption. Chemisorption were performed two times for each catalyst for repetition of the experiments. The results are shown for the total adsorbed amount. The analysis conditions are found in Table 2.	31

7	The mass% of the compounds detected of the 0.2 wt% Pd/Al ₂ O ₃ SP, 0.2 wt% Pd/Al ₂ O ₃ MT, 2.0 wt% Pd/Al ₂ O ₃ MT catalysts, alumina and the binder (HBO ₃) using X-Ray Fluorescence. The intensity is measured in kilo counts per second(kcps). The mass% of pure Pd is calculated based on the mass% of PdO. The calculations can be found in Appendix H.	32
8	The methane converted as a function of the catalyst bed temperature to achieve 10%, 50% and 100% converted methane, labelled T _{10%} , T _{50%} and T _{100%} , respectively. The 0.2 wt% Pd/Al ₂ O ₃ SP catalyst was only tested under the reference conditions described in Section 3.4. The reaction number corresponds to the reaction number and consequently reaction conditions described in the table. The fraction of the feed gas containing methane, oxygen and nitrogen is changed for each reaction and the total molar feed flow is 200 NmL/min. The GHSV is calculated using the amount of fresh catalyst and is 59400 NmL/g _{cat} h.	37
9	The methane converted as a function of the catalyst bed temperature to achieve 10%, 50% and 100% converted methane, labelled T _{10%} , T _{50%} and T _{100%} , respectively. The catalyst, 0.2 wt% Pd/Al ₂ O ₃ MT was ran in reaction series as described in Table 3. The reaction number corresponds to the reaction number and consequently reaction conditions described in the table. The fraction of the feed gas containing methane, oxygen and nitrogen is changed for each reaction and the total molar feed flow was kept constant equal to 200 NmL/min. The GHSV is calculated using the amount of fresh catalyst and is 58000 NmL/g _{cat} h.	39
10	The methane converted as a function of the catalyst bed temperature to achieve 10%, 50% and 100% converted methane, labelled T _{10%} , T _{50%} and T _{100%} , respectively. The catalyst, 2.0 wt% Pd/Al ₂ O ₃ MT was ran in reaction series as described in Table 3. The reaction number corresponds to the reaction number and consequently reaction conditions described in the table. The total molar feed flow is constant equal to 200 NmL/min. The fraction of the feed gas containing methane, oxygen and nitrogen is changed for each reaction. The GHSVs are calculated using the amount of fresh catalyst and the calculations can be found in Appendix M.	42
11	The exact weights of the 0.2 wt% Pd/Al ₂ O ₃ SP, 0.2 wt% Pd/Al ₂ O ₃ MT and 2.0 wt% Pd/Al ₂ O ₃ MT catalysts and the support used for Nitrogen Adsorption. . .	V
12	The exact weights of the 0.2 wt% Pd/Al ₂ O ₃ SP, 0.2 wt% Pd/Al ₂ O ₃ MT and 2.0 wt% Pd/Al ₂ O ₃ MT catalysts, support and boric acid (binder) used for X-Ray Fluorescence. SP and MT symbolize the palladium supported catalysts made for the Specialization Project and Master's Thesis, respectively.	V

13	The exact weights of the 0.2 wt% Pd/Al ₂ O ₃ SP, 0.2 wt% Pd/Al ₂ O ₃ MT and 2.0 wt% Pd/Al ₂ O ₃ MT catalysts used for H ₂ - and CO-chemisorption. SP and MT symbolize the palladium supported catalysts made for the Specialization Project and Master's Thesis, respectively.	VI
14	The exact weight of the 2.0 wt% Pd/Al ₂ O ₃ MT catalyst used for Thermogravimetric Analysis. MT symbolize the palladium supported catalysts made for the Master's Thesis.	VI
15	The exact weights of the 0.2 wt% Pd/Al ₂ O ₃ SP, 0.2 wt% Pd/Al ₂ O ₃ MT and 2.0 wt% Pd/Al ₂ O ₃ MT catalysts and silica carbide used for the methane oxidation testing. SP and MT symbolize the catalysts made for the Specialization Project and Master's Thesis, respectively.	VI
16	The physical-chemical properties of the 0.2 wt% Pd/Al ₂ O ₃ SP catalyst prepared during the Specialization Project during fall 2015 found by H ₂ chemisorption. Chemisorption was performed two times. The results are shown for the chemisorbed amount, only. The analysis conditions are found in Table 1.	VII
17	The observed weight% changes during TGA-measurements and the calculated mass change. The numbers correlate to the numbers in Figure 34 and thus the weight of the catalyst at that point. The weight% is equal to 100, the baseline, when the gases are switched between argon and oxygen	XVI
18	Catalyst bed temperature measurements at 350 °C for 0.2 wt% Pd/Al ₂ O ₃ catalyst.	XXII
19	Catalyst bed temperature measurements at 450 °C for 0.2 wt% Pd/Al ₂ O ₃ catalysts.	XXII
20	Catalyst bed temperature measurements for the first reaction (reference) with the second 0.2 wt% Pd/Al ₂ O ₃ catalyst with a ratio CH ₄ : O ₂ equal to 1:5. The flows of methane, oxygen and nitrogen are 4 NmL/min, 20 NmL/min and 176 NmL/min.	XXIII
21	Catalyst bed temperature measurements for the second reaction with 2.0 wt% Pd/Al ₂ O ₃ catalyst with a ratio CH ₄ : O ₂ equal to 1:10. The flows of methane, oxygen and nitrogen are 2 NmL/min, 20 NmL/min and 178 NmL/min.	XXIII
22	Catalyst bed temperature measurements for the third reaction with 2.0 wt% Pd/Al ₂ O ₃ catalyst with a ratio CH ₄ : O ₂ equal to 1:5. The flows of methane, oxygen and nitrogen are 2 NmL/min, 10 NmL/min and 188 NmL/min.	XXIV
23	Catalyst bed temperature measurements for the fourth reaction with 2.0 wt% Pd/Al ₂ O ₃ catalyst with a ratio CH ₄ : O ₂ equal to 1:5. The flows of methane, oxygen and nitrogen are 1 NmL/min, 5 NmL/min and 194 NmL/min.	XXIV

24	Catalyst bed temperature measurements for the fifth reaction with 2.0 wt% Pd/Al ₂ O ₃ catalyst with a ratio CH ₄ : O ₂ equal to 1:10. The flows of methane, oxygen and nitrogen are 1 NmL/min, 10 NmL/min and 189 NmL/min.	XXV
25	Catalyst bed temperature measurements for the sixth reaction (reference) with 2.0 wt% Pd/Al ₂ O ₃ catalyst with a ratio CH ₄ : O ₂ equal to 1:5. The flows of methane, oxygen and nitrogen are 4 NmL/min, 20 NmL/min and 176 NmL/min.	XXV
26	Catalyst bed temperature measurements for the eighth reaction with 2.0 wt% Pd/Al ₂ O ₃ catalyst with a ratio CH ₄ : O ₂ equal to 1:5. The flows of methane, oxygen and nitrogen are 4 NmL/min, 20 NmL/min and 176 NmL/min.	XXVI
27	Catalyst bed temperature measurements for the first reaction with the 2.0 wt% Pd/Al ₂ O ₃ catalyst with a ratio CH ₄ : O ₂ equal to 1:5. The flows of methane, oxygen and nitrogen are 4 NmL/min, 20 NmL/min and 176 NmL/min.	XXVI
28	Catalyst bed temperature measurements for the second reaction with 2.0 wt% Pd/Al ₂ O ₃ catalyst with a ratio CH ₄ : O ₂ equal to 1:5. The flows of methane, oxygen and nitrogen are 4 NmL/min, 20 NmL/min and 176 NmL/min.	XXVI
29	Catalyst bed temperature measurements for the third reaction with 2.0 wt% Pd/Al ₂ O ₃ catalyst with a ratio CH ₄ : O ₂ equal to 1:10. The flows of methane, oxygen and nitrogen are 2 NmL/min, 20 NmL/min and 178 NmL/min.	XXVII
30	Catalyst bed temperature measurements for the fourth reaction with 2.0 wt% Pd/Al ₂ O ₃ catalyst with a ratio CH ₄ : O ₂ equal to 1:5. The flows of methane, oxygen and nitrogen are 4 NmL/min, 20 NmL/min and 176 NmL/min.	XXVII
31	Catalyst bed temperature measurements for the fifth reaction with 2.0 wt% Pd/Al ₂ O ₃ catalyst with a ratio CH ₄ : O ₂ equal to 1:5. The flows of methane, oxygen and nitrogen are 2 NmL/min, 10 NmL/min and 188 NmL/min.	XXVII
32	Catalyst bed temperature measurements for the sixth reaction with 2.0 wt% Pd/Al ₂ O ₃ catalyst with a ratio CH ₄ : O ₂ equal to 1:5. The flows of methane, oxygen and nitrogen are 1 NmL/min, 5 NmL/min and 194 NmL/min.	XXVIII
33	Catalyst bed temperature measurements for the seventh reaction with 2.0 wt% Pd/Al ₂ O ₃ catalyst with a ratio CH ₄ : O ₂ equal to 1:10. The flows of methane, oxygen and nitrogen are 1 NmL/min, 10 NmL/min and 189 NmL/min.	XXVIII
34	Catalyst bed temperature measurements for the eighth reaction with 2.0 wt% Pd/Al ₂ O ₃ catalyst with a ratio CH ₄ : O ₂ equal to 1:5. The flows of methane, oxygen and nitrogen are 4 NmL/min, 20 NmL/min and 176 NmL/min.	XXIX
35	Catalyst bed temperature measurements for the ninth reaction with 2.0 wt% Pd/Al ₂ O ₃ catalyst with a ratio CH ₄ : O ₂ equal to 1:5. The flows of methane, oxygen and nitrogen are 0.2 NmL/min, 1 NmL/min and 198.8 NmL/min.	XXIX

- 36 Catalyst bed temperature measurements for the ninth reaction with 2.0 wt% Pd/Al₂O₃ catalyst with a ratio CH₄ : O₂ equal to 1:10. The flows of methane, oxygen and nitrogen are 0.2 NmL/min, 2 NmL/min and 197.8 NmL/min. . . . XXIX
- 37 The calculated GHSVs for each methane oxidation reaction using fresh catalyst. Catalysts made for the Specialization Project during fall 2015 and Master's Thesis during spring 2016, are marked as SP and MT, respectively. . . . XXXI
- 38 The catalytic activities for the methane oxidation reaction, using 0.2 wt% Pd/Al₂O₃ SP catalyst, at each set hold-up temperature, i.e. 200-550 °C with 50 °C intervals and GHSV equal to 59400 NmL/g_{cat}h. The real catalyst bed temperature were found by measuring the temperature throughout the catalyst bed and is 8.4 °C below the real temperature. The reaction conditions can be found in Table 3 as reaction number 1. . . . XLII
- 39 The catalytic activities for the methane oxidation reaction, using 0.2 wt% Pd/Al₂O₃ MT catalyst, at each set hold-up temperature, i.e. 250-600 °C with 50 °C intervals and GHSV equal to 58000 NmL/g_{cat}h. The real catalyst bed temperature were found by measuring the temperature throughout the catalyst bed and the measurements can be found in Appendix L. The reaction conditions can be found in Table 3 as reaction number 1. . . . XLII
- 40 The catalytic activities for the methane oxidation reaction, using 0.2 wt% Pd/Al₂O₃ MT catalyst, at each set hold-up temperature, i.e. 250-600 °C with 50 °C intervals and GHSV equal to 58000 NmL/g_{cat}h. The real catalyst bed temperature were found by measuring the temperature throughout the catalyst bed and the measurements can be found in Appendix L. The reaction conditions can be found in Table 3 as reaction number 3. . . . XLIII
- 41 The catalytic activities for the methane oxidation reaction, using 0.2 wt% Pd/Al₂O₃ MT catalyst, at each set hold-up temperature, i.e. 250-600 °C with 50 °C intervals and GHSV equal to 58000 NmL/g_{cat}h. The real catalyst bed temperature were found by measuring the temperature throughout the catalyst bed and the measurements can be found in Appendix L. The reaction conditions can be found in Table 3 as reaction number 5. . . . XLIII
- 42 The catalytic activities for the methane oxidation reaction, using 0.2 wt% Pd/Al₂O₃ MT catalyst, at each set hold-up temperature, i.e. 250-600 °C with 50 °C intervals and GHSV equal to 58000 NmL/g_{cat}h. The real catalyst bed temperature were found by measuring the temperature throughout the catalyst bed and the measurements can be found in Appendix L. The reaction conditions can be found in Table 3 as reaction number 6. . . . XLIV

- 43 The catalytic activities for the methane oxidation reaction, using 0.2 wt% Pd/Al₂O₃ MT catalyst, at each set hold-up temperature, i.e. 250-600 °C with 50 °C intervals and GHSV equal to 58000 NmL/g_{cat}h. The real catalyst bed temperature were found by measuring the temperature throughout the catalyst bed and the measurements can be found in Appendix L. The reaction conditions can be found in Table 3 as reaction number 7. XLIV
- 44 The catalytic activities for the methane oxidation reaction, using 0.2 wt% Pd/Al₂O₃ MT catalyst, at each set hold-up temperature, i.e. 250-650 °C with 50 °C intervals and GHSV equal to 58000 NmL/g_{cat}h. The real catalyst bed temperature were found by measuring the temperature throughout the catalyst bed and the measurements can be found in Appendix L. The reaction conditions can be found in Table 3 as reaction number 8. XLV
- 45 The catalytic activities for the methane oxidation reaction, using 2.0 wt% Pd/Al₂O₃ MT catalyst, at each set hold-up temperature, i.e. 200-500 °C with 50 °C intervals and GHSV equal to 58800 NmL/g_{cat}h. The real catalyst bed temperature were found by measuring the temperature throughout the catalyst bed and is 0.3 °C above the real temperature. The reaction conditions can be found in Table 3 as reaction number 1. XLV
- 46 The catalytic activities for the methane oxidation reaction, using 2.0 wt% Pd/Al₂O₃ MT catalyst, at each set hold-up temperature, i.e. 200-500 °C with 50 °C intervals and GHSV equal to 58800 NmL/g_{cat}h. The real catalyst bed temperature were found by measuring the temperature throughout the catalyst bed and the measurements can be found in Appendix L. The reaction conditions can be found in Table 3 as reaction number 2. XLV
- 47 The catalytic activities for the methane oxidation reaction, using 2.0 wt% Pd/Al₂O₃ MT catalyst, at each set hold-up temperature, i.e. 250-500 °C with 25-50 °C intervals and GHSV equal to 58800 NmL/g_{cat}h. The real catalyst bed temperature were found by measuring the temperature throughout the catalyst bed and the measurements can be found in Appendix L. The reaction conditions can be found in Table 3 as reaction number 3. XLVI
- 48 The catalytic activities for the methane oxidation reaction, using 2.0 wt% Pd/Al₂O₃ MT catalyst, at each set hold-up temperature, i.e. 250-500 °C with 25-50 °C intervals and GHSV equal to 58800 NmL/g_{cat}h. The real catalyst bed temperature were found by measuring the temperature throughout the catalyst bed and the measurements can be found in Appendix L. The reaction conditions can be found in Table 3 as reaction number 4. XLVI

- 49 The catalytic activities for the methane oxidation reaction, using 2.0 wt% Pd/Al₂O₃ MT catalyst, at each set hold-up temperature, i.e. 200-500 °C with 25-50 °C intervals and GHSV equal to 58800 NmL/g_{cat}h. The real catalyst bed temperature were found by measuring the temperature throughout the catalyst bed and the measurements can be found in Appendix L. The reaction conditions can be found in Table 3 as reaction number 5. XLVII
- 50 The catalytic activities for the methane oxidation reaction, using 2.0 wt% Pd/Al₂O₃ MT catalyst, at each set hold-up temperature, i.e. 250-600 °C with 50 °C intervals and GHSV equal to 58800 NmL/g_{cat}h. The real catalyst bed temperature were found by measuring the temperature throughout the catalyst bed and the measurements can be found in Appendix L. The reaction conditions can be found in Table 3 as reaction number 6. XLVII
- 51 The catalytic activities for the methane oxidation reaction, using 2.0 wt% Pd/Al₂O₃ MT catalyst, at each set hold-up temperature, i.e. 250-450 °C with 25-50 °C intervals and GHSV equal to 58800 NmL/g_{cat}h. The real catalyst bed temperature were found by measuring the temperature throughout the catalyst bed and the measurements can be found in Appendix L. The reaction conditions can be found in Table 3 as reaction number 7. XLVIII
- 52 The catalytic activities for the methane oxidation reaction, using 2.0 wt% Pd/Al₂O₃ MT catalyst, at each set hold-up temperature, i.e. 200-500 °C with 25-50 °C intervals and GHSV equal to 58800 NmL/g_{cat}h. The real catalyst bed temperature were found by measuring the temperature throughout the catalyst bed and the measurements can be found in Appendix L. The reaction conditions can be found in Table 3 as reaction number 8. XLVIII
- 53 The catalytic activities for the methane oxidation reaction, using 2.0 wt% Pd/Al₂O₃ MT catalyst, at each set hold-up temperature, i.e. 200-400 °C with 25-50 °C intervals and GHSV equal to 59400 NmL/g_{cat}h. The real catalyst bed temperature were found by measuring the temperature throughout the catalyst bed and the measurements can be found in Appendix L. The reaction conditions can be found in Table 3 as reaction number 9. XLVIII
- 54 The catalytic activities for the methane oxidation reaction, using 2.0 wt% Pd/Al₂O₃ MT catalyst, at each set hold-up temperature, i.e. 200-375 °C with 25-50 °C intervals and GHSV equal to 59400 NmL/g_{cat}h. The real catalyst bed temperature were found by measuring the temperature throughout the catalyst bed and the measurements can be found in Appendix L. The reaction conditions can be found in Table 3 as reaction number 10. XLIX

55 The molar flows of the gases CH₄, CO₂ and inert N₂ detected by the gas chromatograph (GC) when testing the 0.2 wt% Pd/Al₂O₃ SP catalyst for the methane oxidation reaction. Water was dried and O₂ is normally not detected by the GC. The composition of the gases in the feed was set to be 4 NmL/min, 20 NmL/min and 176 NmL/min for methane, oxygen and nitrogen, respectively, at 1 bar and GHSV equal to 59400 NmL/g_{cat}h, and the gas compositions at the reactor outlet was calculated when a 98% methane conversion was achieved at 540 °C in the catalyst bed. LI

1 Introduction

Health, environment and energy security imperatives are promoting the rapid growth of natural gas in the transportation sector.[1] In Norway as well as globally, the distribution of liquefied natural gas (LNG) is developing, which offers significant environmental advantages over gasoline and diesel. It represents an option for efficient and more environmentally friendly marine propulsion. However, the emissions from LNG consists primarily of unburned methane (CH_4) which is a greenhouse gas with 20 times the global warming potential of CO_2 . Conventional destruction of methane requires very high temperatures (up to $1000\text{ }^\circ\text{C}$) and produces noxious by-products such as NO_x . [2] NO_x and its derivatives can directly harm the environment and have health effects by reacting as acids in water, gases in the air or as a salt. [3] These can together contribute to pollution effects and is associated with acid rain.

A preferable alternative is catalytic oxidation, a process that converts unburned hydrocarbons such as methane to harmless gases by reaction on the surface of a catalyst. To improve the methane slip abatement, catalysts that can facilitate complete oxidation of CH_4 to CO_2 and H_2O at highly diluted methane concentrations and moderate temperatures are explored. Recent research by MARINTEK at SINTEF reported that the methane slip should contain small amounts of methane, such as 500-2000 ppm and the destruction ought to be below $400\text{ }^\circ\text{C}$. The catalyst should stay stable over a long term and have high activity, even in an environment containing water. [4] In a classic three-way-catalytic converter the NO_x -products react with ammonia, with aid of a catalyst and converts it into N_2 and H_2O . [5] Lower concentrations of NO_x are achieved by tuning the engine, but consequently a higher methane amount is released. New research is not able to meet both requirements on reduction. This paper will explore the opportunities of lowering methane emissions using a catalyst where supported Pd catalysts are the most active for oxidation of methane. [6]

Due to the national and international regulations that prescribe the permitted quantities of emissions, the ship building companies have to decide whether they're building ships and vessels that will use LNG fuel or not. It is hard to predict how LNG as a fuel will capture the market share in the marine transport sector, but according to CEDIGAZ' base scenario the demand could grow up to 77 million tons per year. [7] It will depend upon the fuel prices, future environmental requirements, what will be compatible with existing and future technology and the availability of natural gas. If the forecast turn out to be right, a further reduction of CH_4 emissions from LNG should be achieved with an enhanced oxidation catalyst system for improved CH_4 abatement of the exhaust gas from the high temperature burning of methane.

Catalysts for methane slip abatement need to facilitate complete oxidation and high activity at low temperatures, long-term durability and low CH_4 concentrations. [6] Numerous of catalysts have been investigated, and among them are the supported noble metals Palladium and

Platinum which are considered to usually be the most active one. There are different factors that affect the catalysts' performance, including the active phase, metal loading, support material, synthesis method, catalyst deactivation, calcination temperatures and reaction conditions. The space velocity, feed composition and the use of dry or wet feed are reaction conditions that are possible to alter. Noble metals are expensive and a catalyst with low metal loading leading to high activity and complete combustion or by using non-noble metals is needed.

A support can contribute to the catalytic activity, provide mechanical strength and to facilitate the effective dispersion of the expensive active phase, where alumina, silica and carbon are the most commonly used.[8] Alumina a commonly used for Palladium-support, due to its excellent stability.[9] It exists in various structures, but the most common are the α -, η - and γ -Al₂O₃. The γ -Al₂O₃ offers relatively big surface areas, good pore volume, relatively high thermal stability and has the ability to be shaped into mechanically stable pellets. The disadvantage of the alumina is that it undergoes a phase change at 800 °C from γ - to α -Al₂O₃, which results in a surface area loss.[2] The methane oxidation should occur below this temperature.

The main goal of this work is to synthesis palladium supported γ -Al₂O₃ catalysts, characterize them using different techniques and test them for the catalytic combustion of methane under relevant conditions. A special emphasize has been put into the variation of the feed composition to find the lowest temperature to achieve 100% conversion and deactivation of the catalyst by testing the Pd/Al₂O₃ catalysts in series of reactions under different and relevant conditions. Due to the high prices of palladium it is preferable to find cheaper alternatives giving the same high activity. The catalysts are used as references for future research of catalysts made of a palladium and other metals mix, such as nickel., or catalysts containing small or none palladium.

2 Theory

2.1 Palladium as an active metal

Noble-metal catalysts are widely used in catalytic reactions, including Palladium.[10]. The advantage of using noble metals as the active metals are their high activity, their resistance to deactivation and their ability to be regenerated.[11] A high activity of supported catalysts require large active surface areas, thus high dispersion of the active phase.[12] The small Pd-particles need a support material, to prevent sintering. In general, an increase of the palladium loading results in an increase in the catalyst activity due to the increase in active sites. Palladium is an expensive metal, and a low loading and high activity is preferable. The most typical reasons for deactivation of palladium catalysts are crystallite growth, sintering, agglomeration and carbon deposition and can lead to completely deactivation of the catalyst.[13] The methane oxidation reaction is a highly exothermic reaction, and the potential for sintering is therefore relatively high. The Palladium active phase as an oxidation catalyst is mostly identified as PdO, which is thermodynamically stable, starting from 300 °C up to at least 600 °C.[14] At higher temperatures it decomposes to Pd metal and is reported to negatively affect the activity of the methane oxidation reaction. It has been thought that the active form of Pd is in an oxidized state, i.e. PdO, but the exact configuration of the active sites is not clear so far.[15]

2.2 γ -alumina support

Inorganic materials are often used as supports, due to the fact that they are much more thermally and mechanically stable. This also applies alumina which is an amphoteric oxide of aluminium with the chemical formula Al_2O_3 . [16] The gamma form has a cubic defect spinel structure, in which the aluminium atoms occupy both the tetrahedral and octahedral sites and the oxygen atoms are arranged in a cubic close packing, as shown in Figure 1.[17] This gives Al_2O_3 a cation:anion ratio of 2:3. [9] Each unit cell contains 32 oxygen and $64/3$ Al (III) to fulfill the stoichiometry.

The γ -alumina has a surface area of 50-300 m^2/g where many particles can deposit. The mesopores is of between 5 and 15 nm and pore volumes of about 0.6 cm^3/g . The air-exposed alumina contains a monolayer of hydroxyl groups (10-15 OH/nm^2) as well as physisorbed water which may form bridges to other species.[8] Since the isoelectric point of alumina is measured to be in the range 7-9, the hydroxyl groups are amphoteric which is an advantage (especially the acidic behaviour) when a metal complex is attached to the alumina surface. In order to remove the hydroxyl groups, the alumina is dried at high temperatures, which leaves oxide anions and unsaturated aluminum ions on the surface. By treating the alumina at high temperatures (≈ 600 °C), the γ -alumina can be transformed into α - or δ - alumina. The high

thermal stability of γ -alumina can reduce the rate of Pd-sintering and inhibit the alumina to transform into other phases. The interaction with metal can stabilize the palladium particles, which is an advantageous chemical property.

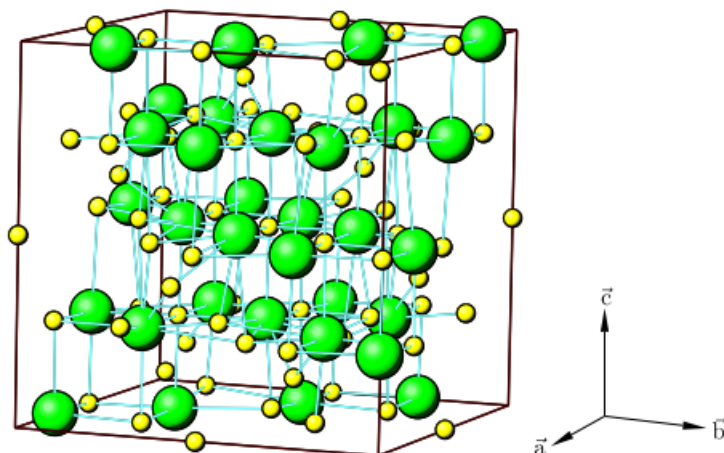
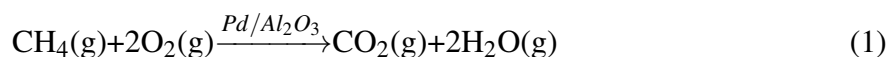


Figure 1: An illustration of the γ -alumina cubic defect spinel structure unit cell, in which the aluminium atoms occupy both the tetrahedral and octahedral sites as small, yellow spheres and the oxygen atoms are arranged in a cubic close packing as green spheres. The illustration is adapted from The University of Groningen.[17]

2.3 Methane oxidation

2.3.1 Reactions and Kinetics

Methane is a potent green house gas and is present in emissions from many sources, including the marine machinery.[2] The rapid growth of the use of natural gas (NG) offers significant advantages, however, NG emits unburned methane. It is 20 times the global warming potential of CO_2 . [14] A traditional oxidation of methane requires high temperatures and will emit noxious products. Palladium supported γ -alumina catalysts are used to facilitate complete oxidation of methane to carbon dioxide and water at lower temperatures. The catalyst need to operate at highly diluted methane concentrations. The exothermic and irreversible reaction of the complete combustion is shown below:



$$\Delta H^\circ = -803 \text{ kJ/mol} \quad (2)$$

Most kinetics studies on catalysts with excess oxygen showed that the rate law is zero order in oxygen and first order in methane.[18] Oxygen adsorbs stronger on the surface and will inhibit methane oxidation under oxidizing conditions by excluding CH_4 from the active sites. Many different mechanisms are proposed and one of the main challenges is the uncertainty

of the nature and oxidation states of the palladium surface. "Oxidation may occur on the palladium metal, on a palladium (II) oxide surface, or even on a surface partially covered with oxygen." [18]

2.3.2 Reaction Mechanisms

Several reaction mechanisms are proposed for the complete oxidation of CH₄, including Mars-van Krevelen (MvK), Langmuir-Hinshelwood (LH) and Eley-Rideal (ER) mechanism. [1] The conversion of methane is a challenging task due to the high CH₃-H bond dissociation energy (439.3 kJ/mol). [15] The direct route where the products are carbon dioxide and water is the main reaction. However, it is observed that several other reactions occur at the same time, resulting in products such as CO and H₂. The main challenge of stating the reaction mechanism of the methane oxidation is that it is a fast exothermic reaction. Consequently it is challenging to determine the rate determining step and the deactivation mechanisms that can occur. It must also be considered that even for one catalyst, the reaction may undergo different paths depending on the state of the catalyst. It is still confusion about whether palladium is oxidized (PdO) or not. [18]

The following are proposed reaction mechanisms of methane oxidation with Pd or PdO, reviewed by Chen et al. [1] According to MvK's mechanism, the CH_x species produced from the dissociation of the CH₄ react with the oxygen in PdO_x, and the rate determining step is the activation of the first C-H bond of the methane molecule. The LH mechanism which suggest that the methane oxidises through interactions between CH_x species and oxygen on the Pd surfaces. Surface reaction between dissociative adsorption of oxygen and gaseous methane is assumed in the ER mechanism.

2.4 Preparation of supported catalyst

2.4.1 Incipient Wetness Impregnation

The idea of incipient wetness impregnation is that a support is loaded with active material by exactly filling the pores of the support with a solution of the catalytically active element, after which the solvent is removed by drying. [8] The main interaction between the dissolved catalyst precursor and the surface of the support is capillary suction. [10] It is preferable that the volume of the solution is equal to the volume of the pore ($V_{PT}=V_{SOL}$). In order to determine the pore volume of the support, a test is done before the solution is introduced to the support. In the case of proper wetting no excess of solution remains outside the pore space, the so-called wetness point is reached, hence incipient wetness impregnation.

2.4.2 Drying

After the incipient wetness impregnation, the metal salts are dehydrated by being heated up in an oven up to a temperature around the boiling point of the solvent. Hydrated salts like nitrates sublime first when heated, and then decompose.[19] The precursor concentration increases as the water evaporates, until precipitation. Figure 2 illustrates the pore and particle profiles after drying at different rates.

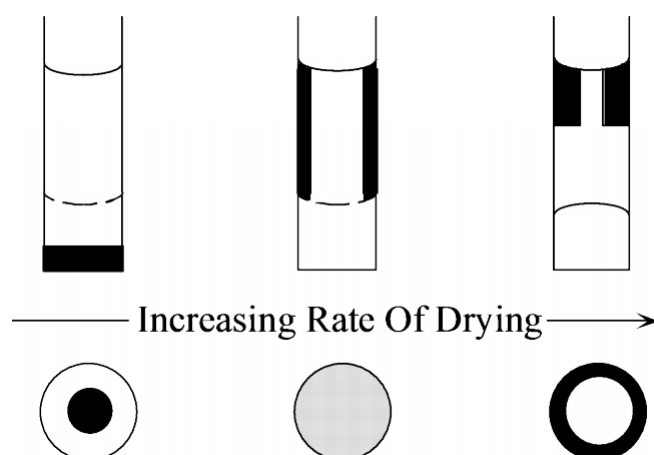


Figure 2: Pore and particle profiles after drying at different rates. The Figure is adapted from a lecture in the Specialization Course TKP4515 Catalysis and Petrochemistry fall 2015 at NTNU.

2.4.3 Calcination

Calcination is a further heat treatment in which the solid/solvent interface has been replaced by a solid/gas interface.[10] The goal of calcination is to decompose undesired salts and strip them for water or gases. [20] The calcination is usually carried out in an oxygen or inorganic containing atmosphere.

2.5 Catalyst characterization

2.5.1 Nitrogen Adsorption

In terms of finding the catalyst's specific surface area, the theory developed by Brunauer-Emmet-Teller (BET) can be applied. The BET aims to find the gas adsorption on a solid material, to determine the complete surface area of the support and metal by measuring the number of Nitrogen molecules physisorbed on the surface. The total area can be calculated using the extension of Langmuir's monolayer adsorption to multilayer adsorption by assuming that the surface is nonporous and energetically uniform, where the adsorption happens in the first layer, and the molecules in the first layer act as sites for adsorption of additional molecules,

such that a multilayer forms before the first layer is completed. [21] The BET equation is as follows:

$$\frac{p/p^0}{n_{ads}(1-p/p^0)} = \frac{1}{n_m C} + \frac{C-1}{n_m C} (p/p^0) \quad (3)$$

where p is the gas pressure [bar], p^0 is the equilibrium pressure of condensed gas [bar], n_m is the monolayer capacity, thus the volume of the first monolayer [mm^3], n_{ads} is the volume each molecule occupies [$\text{mm}^3/\text{molecule}$] and C is a parameter related with the molar energy of adsorption in the first layer.

The equation is based on the assumptions mentioned and the rates of adsorption and desorption from each layer are equal. The numbers of layers is assumed to infinite at $p/p^0=1$ and the adsorption energy is considered to be the same as the molar energy for condensation of the gas. In the first layer the molecules will adsorb on equivalent adsorption sites, but it's adsorption energy is independent of layer number two and consecutive layers.

The n_m and C values can be obtained from the slope (s) and intercept (b) if the plotting of $(p/p^0)/[n_{ads}(1-p/p^0)]$ versus p/p^0 is linear, as:

$$n_m = \frac{1}{s+b} \quad (4)$$

and

$$C = \frac{s}{b+1} \quad (5)$$

n_m can be used to find the specific surface area, A_s , using:

$$A_s = n_m a_m N_A \quad (6)$$

where a_m is the area occupied by one molecule in the monolayer and N_A is Avogadro's number.

a_m can be found by:

$$a_m = \frac{A}{m_{cat} V_m} \quad (7)$$

where m_{cat} is the mass of the catalyst, A is the total surface area and V_m is the volume of 1 mole of ideal gas, from the assumptions of standard temperature and pressure.

The pore size distribution of mesopores are obtained from adsorption and desorption isotherm branch according to Barrett, Joyner and Halenda (BJH). The pores are filled with nitrogen fluid at initial relative pressure $0.9 < p/p^0 < 0.95$ in condensed state. As the relative pressure is decreased, the pores are emptied for condensed adsorptive.[22] In order to determine the

pore size, the pore volume is found by using the Kelvin equation, which is based on classic thermodynamics.[21]

2.5.2 X-Ray Fluorescence

X-Ray Fluorescence is a spectroscopic method of material analysis of powders, bulk solids or liquid samples.[23] X-rays are generated from a excitation source (Pd-source) which excites the characteristic x-rays in the sample, i.e. fluorescent x-rays. [24] An analysing crystal receives the x-rays and sends the radiation to two different detectors, which disperse, detect, count and displays the spectrum of x-ray photons emitted by the sample.

The material gets excited with high energy (X-rays) and becomes ionized if the energy is sufficient to excite an inner electron.[25] The electron is replaced by an outer electron, and energy is released due to a decreased binding energy of the outer electron than the inner electron. The emitted radiation is termed fluorescent radiation, due to the lower energy than the primary X-rays. The resulting fluorescent x-rays can be used to identify and quantify the elements from Fluor to Uranium, due to that the emitted photon is characteristic of a transition between specific electron orbitals in a particular element. The resulting plot shows intensity (counts per second) as a function of energy (keV). The intensity of the peaks is measured in counts per second. For the trace elements, the detection limits are in the order of a few parts per million.[25]

2.5.3 Chemisorption

Chemisorption is a method to determine the dispersion of a metal in supported catalysts by using adsorption isotherms. [26] Chemisorption is the adsorption which results from chemical bond formation between the adsorbent and the adsorbate in a monolayer on the surface.[27] Adsorption isotherms are obtained by measuring the amount of gas adsorbed on a sample at increasing pressures while the catalyst is maintained at constant temperature. H₂, CO and O₂ are usually used as probe gases for chemisorption, where hydrogen and carbon monoxide are used in this thesis.

Chemisorption does not always give a realistic picture. For example the chemisorption can take place in non realistic conditions (temperature and pressure may affect the catalytic surface structure), the adsorption may take place on the carrier, promoters or other components of the catalyst, the catalytic active site may not be a completely reduced site and, most importantly, a lot of the assumptions in the Langmuir isotherm are far from reality.[28] The summary of the assumptions are obtained from HSE-lecture at NTNU during fall 2015 and are as follows:[27]

- Applied conditions that give predominantly chemisorption with full monolayer coverage

- Adsorbate that adsorbs selectively to the active component and not to any other. $A_{gas} + M_{surface} \leftrightarrow AM$ (or support)
- The surface is homogeneous and uniform
- $-\Delta H_a = \text{constant}$ (independent of coverage)
- Monolayer adsorption
- Immobile adsorption (lack of surface diffusion)

An illustration of the results obtained from a chemisorption experiment is shown in Figure 3 and illustrates how the volume adsorbed gas increases by increasing the pressure in the sample. The first isotherm shows how much CO or H₂ which are chemisorbed and physisorbed. The second isotherm is the physisorbed amount. The difference between them is the amount of gas chemisorbed.

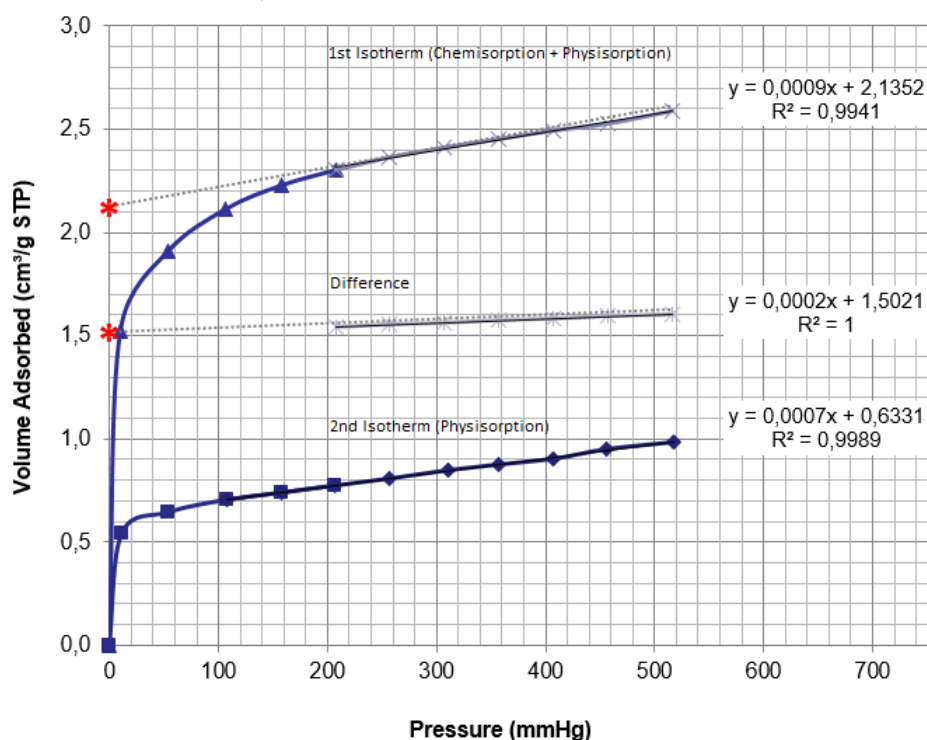


Figure 3: An illustration of chemisorption and the isotherms obtained from increasing the pressure the sample is exposed to. The highest isotherm symbolizes how the volume of gas which is chemisorbed and physisorbed. The lower isotherm is the physisorbed gas volume. The difference between the isotherms, the regression line in the middle, is the volume of gas chemisorbed. The Figure is obtained from HSE lectures at the Catalysis and Petrochemistry group during fall 2015 at NTNU held by Cristian Ledesma.[27]

The dispersion of the metal is defined as[28]:

$$D[\%] = \frac{\text{Number of surface atoms on the metal}}{\text{Total number of metal atoms in the sample}} \quad (8)$$

For calculation of the dispersion on the metal surface, the extrapolated value of volume H₂ or CO adsorbed, V_{ads} [mol/g_{cat}], can be used. The equation used to calculate the % of metal atoms exposed, i.e. dispersion, is as follows:

$$D = \frac{v_{ads} \cdot M_m \cdot F}{x_m} \quad (9)$$

where M_m is the molecular weight of the metal and x_m is the metal weight fraction in the catalyst. F is the adsorption stoichiometry, hence the number of surface atoms covered by one adsorbed molecule. Hydrogen is especially used to decide the number of surface atoms on group VIII metals. H₂ chemisorbs dissociative and it is usually assumed that the surface stoichiometry between a hydrogen atom and a metal is 1:1. For this thesis, the reaction stoichiometry is assumed as:

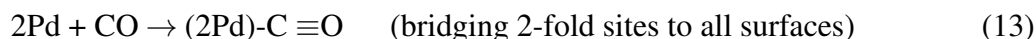


The average size of the particle, d , is:

$$d = f \cdot \frac{V_{sp}}{S_m} \quad (11)$$

where f is a factor that describes the shape of the particle, V_{sp} is the specific volume of the metal particles and S_m is the specific surface area of the metal.

CO can chemisorb in a linear form or in a bridge form, leading to stoichiometries of 1:1 or 1:2, respectively, [29], or CO can dissociate on the surface, leading to a stoichiometry equal to 2, but not necessarily. It may depend on the metal or the surface structure. The reaction stoichiometries for CO and Pd are shown below and varies with temperature, metal dispersion, metal loading and preparation:[30]



2.5.4 Temperature Programmed Reduction

Temperature Programmed Reduction (TPR) is an analysis technique to find the temperature(s) needed for the (complete) reduction of a catalyst. It is also possible to perform a pulse calibration which quantifies the H₂ uptake.

The reactor is loaded with the catalyst in its oxidized form or pre-oxidized form, and is heated at a constant rate (normally around 10 °C/min), while reduced with a reducing mixture such as hydrogen in argon. The reduction of the Palladium oxide by H₂ is described by the equation[31]:



Whether the catalyst can be reduced/oxidized or not, is decided by the thermodynamics. A reduction will proceed when the change in Gibbs free energy, ΔG , has a negative value. The following equation shows how ΔG depends on temperature and pressure[31]:

$$\Delta G = \Delta G^0 + nRT \ln \left(\frac{p_{H_2O}}{p_{H_2O,eq}} \right) \quad (15)$$

where ΔG is the change in Gibbs free energy for reduction, ΔG^0 is the same but under standard conditions (i.e. 1 atm and 25 °C), n is the stoichiometric coefficient, R the gas constant, T the temperature and p the partial pressure. The second term in Equation 15 is always negative when the catalyst is reduced by hydrogen and the water is removed efficiently. For noble metals, such as Pd, ΔG^0 is already negative at STP and reduction is thermodynamically feasible, but to achieve a complete reduction, the reaction must happen at a temperature where the kinetics is rapid enough. The opposite applies for oxidation. A phase diagram of the Pd oxide system in mixtures of H₂ and H₂O can predict the reduction process.

It is possible to measure the rate of reduction by continuously monitoring the change in the hydrogen concentration of the reducing gas mixture in effluent gas with respect to the initial percentage. The resulting reduction profile also gives the catalyst's reducibility. The area under the curve represents the total hydrogen consumption, i.e. moles of H₂ consumed per mole of palladium atoms, H₂/Pd. Peaks at lower temperatures indicates less strongly bound between oxides to the support, and vice versa. The metal oxide may be reduced in more than one step by oxidation states from +2 to 0, or surface to bulk-reduction. Where more peaks occur it is most likely reduction in several steps. The profile in Figure 4 shows that the catalyst is reduced in two steps, hence at 127 °C and 210 °C.

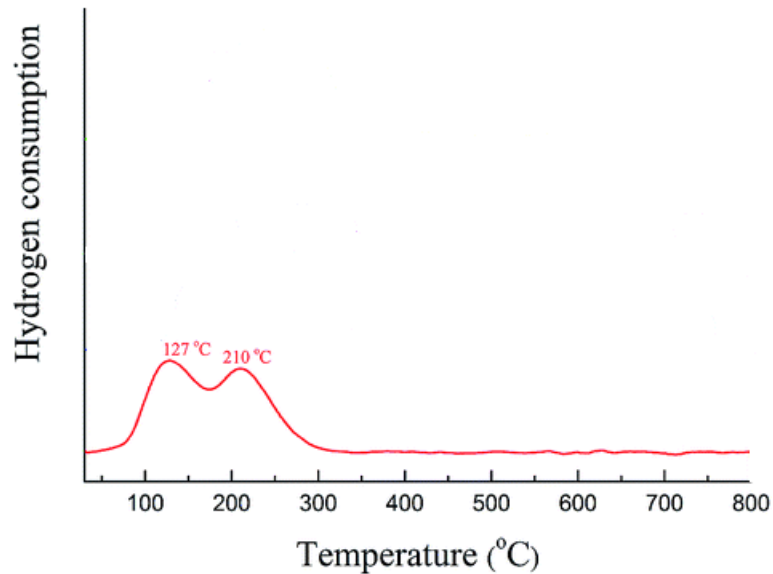


Figure 4: A TPR-profile where the hydrogen consumption of a Pd/ γ -Al₂O₃ catalyst is measured as a function of temperature (°C). The result is obtained from an article by B. Wang et al. [32].

Alumina (Aluminium Oxide) reduces to Aluminium at high temperatures using Hydrogen, as shown in Figure 5[33]. This should be considered when using temperature programmed reduction using hydrogen, even though it is normally not a huge issue.

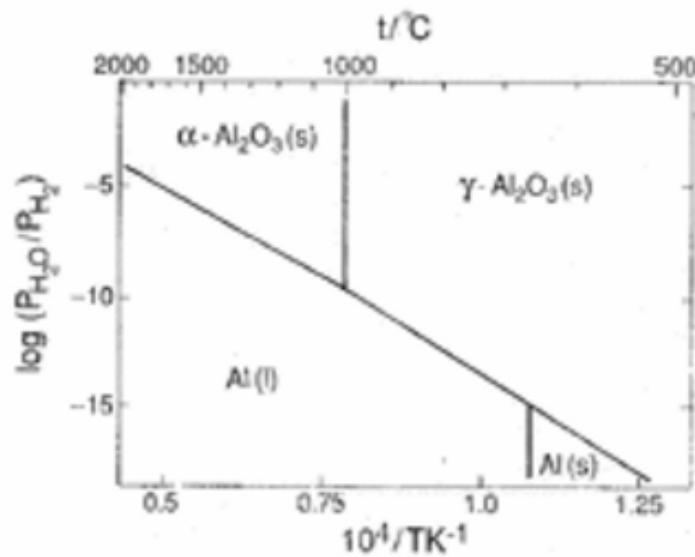


Figure 5: The equilibrium diagram for the system Al-Al₂O₃ in various pressures of H₂-H₂O at 500-2000 °C. It also shows a phase transformation of γ -alumina to α -alumina at high temperatures. By adjusting the pressure and the temperature the alumina can be reduced to liquid or solid aluminium. The Figure is adapted from *The Possible Reduction of Alumina to Aluminium Using Hydrogen*[33]

2.5.5 X-Ray Diffraction

X-Ray Diffraction (XRD) is a method for characterization of powder or microcrystalline samples to determine the crystallite size and identifying crystalline phases using x-rays.[34] X-rays scattered from the crystalline solid can constructively interfere, producing a diffracted pattern. This is based on the theory that crystalline substances act as 3-dimensional diffraction gratings for X-ray wavelengths similar to the spacing of planes in a crystal lattice.[35] Figure 6 illustrates how the crystal is made out of parallel planes of atoms, spaced a distance d apart and the angle between the incoming X-Rays and the normal to the reflecting lattice plane is θ .[8][36]

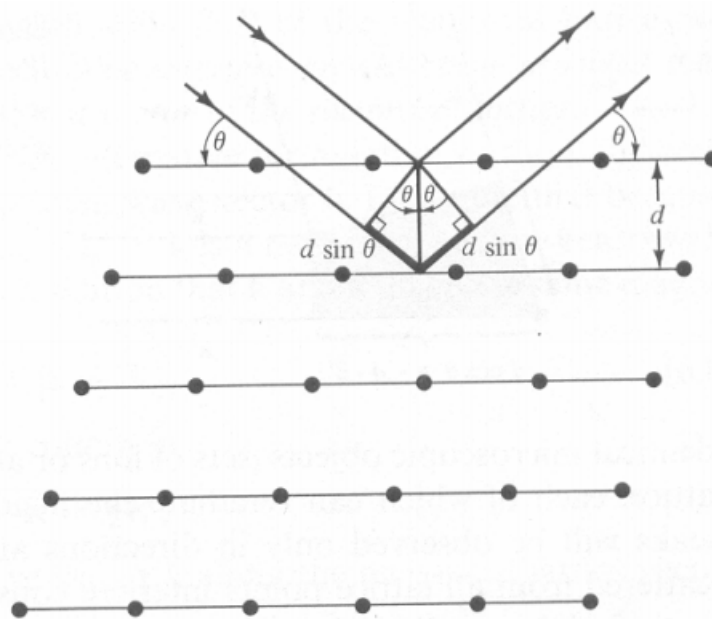


Figure 6: X-rays scattered from the crystalline solid interfere, producing a diffracted beam. The Figure is obtained from the University of Delaware.[36] λ is the wavelength of the X-rays, d is the distance between two lattice planes, θ is the angle between the incoming X-rays and the normal to the reflecting lattice plane.

The conditions for a reflected beam are given by the relation, Bragg's equation, as follows:

$$n\lambda = 2d\sin\theta; n= 1, 2,\dots \quad (16)$$

where λ is the wavelength of the X-rays, d is the distance between two lattice planes, θ is the angle between the incoming X-rays and the normal to the reflecting lattice plane and n is an integer called the order of the reflection. The lattice spacing is characteristic for a particular compound. X-ray diffraction of powder samples are much more complex due to every possible crystalline orientation is represented in the sample.[37] It is therefore assumed that the sample is randomly arranged, and each plane will be represented in the signal. To eliminate how the texturing may affect the results, the samples are often rotated. Clear or narrow peaks are

achieved for perfect crystals. For crystallite sizes below 100 nm, line broadening occurs due to incomplete destructive interference in scattering directions where the x-rays are out of phase.[8] The particle size can be determined by studying the diffraction pattern and the line broadening, and approximated by Scherrer's equation, which is as follows:

$$\tau = \frac{K\gamma}{\beta \cos \theta} \quad (17)$$

where τ , K , β , γ and θ represent the volume-weighted crystalline thickness, is a constant normally equal to 0.9, line broadening of the peak, radiation wavelength and angle of the diffraction peak, respectively. An important feature of XRD is that it can not detect particles that are either amorphous or too small and for samples with mixed compositions, the detection limit is 2% of mixed samples.[35]

2.5.6 Thermogravimetric Analysis

Thermogravimetric Analysis (TGA) is a method used to quantify the mass change while the sample is exposed to reducing or oxidizing environments at a controlled rate as a function of time and temperature.[38] By investigating the thermal stability, information about chemical reactions and/or physical changes can be found. The weight is gained when the sample is adsorbing/absorbing the gases due to oxidation, and vice versa for reduction.[39]

The TGA apparatus continuously monitors the sample weight while the furnace is heated up or cooled down. The results can be plotted as the temperature, the weight percentage and/or the heat flow as a function of time. A reference inert sample purge gas controls the sample environment. This is done so the sample only reacts to temperature when the catalyst loose or gain weight.[40]

There are some key parameters to read out of the results, including the initial temperature of decomposition or dehydration, the temperature where 50% of the sample is decomposed or dehydrated, the final sample weight and the maximum rate of decomposition or dehydration temperature. The same applies when compound is oxidized and the sample gains weight.

Prior to the analysis, it is important to know which reactions the sample undergo in contact with different gases, to better understand the result. Figure 7 shows how Palladium supported on Al_2O_3 behaves under complete reduction and oxidation.

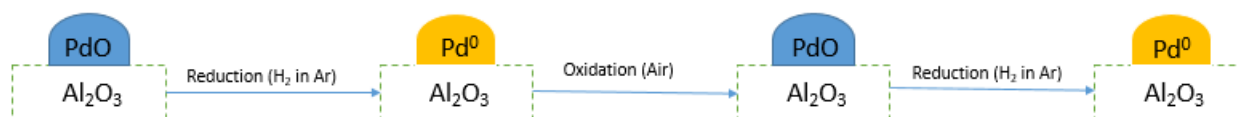


Figure 7: The procedure of oxidation and reduction of Palladium supported on Al_2O_3 under different atmospheres, including hydrogen (25% H_2 /75% Ar), argon and air (20% O_2 /80% N_2) at different temperatures. The palladium will alter between the oxidized state, PdO and the reduced state, Pd⁰.

2.6 Catalyst Testing

2.6.1 Powder vs pellets catalyst

Catalysts work best when they have a large active surface area of metal and support and are consequently usually used as pellets or powder. Pellets are mostly used in the industry. The reaction rate is proportional to the active surface area and the pellet must therefore be porous. The reactor efficiency is reduced with increasing particle diameter but the pressure drop is minimized, and vice versa. A low pressure drop minimizes the plant power costs.[41]

A fixed-bed reactor holds the catalyst in place while reactants are transported from the reactor inlet and up to the catalyst bed. Silica carbide is used in order to keep a uniform temperature profile in the catalyst bed.

2.6.2 Gas Chromatograph

Gas chromatograph(GC) is an apparatus used for obtaining information about components' molecular compositions and amounts, by separating components of mixtures (samples).[42] A block diagram showing the procedure is shown in Figure 8. The GC has a mobile phase which is the carrier gas and a stationary phase, usually an inert gas and a microscopic layer of liquid/polymer on a solid support, respectively. When a sample is prepared, an autosampler introduces the sample automatically into the inlets, in which introduces the sample into the continuous flow of carrier gas. The carrier gases used are normally nitrogen, helium and hydrogen. The stationary phase is often placed inside glass or metal tubing, called a column. Each compound will use different amounts of time through the column due to the different velocities and the time each compound uses to elute can reveal the type of compound which is present.

After the species are separated in the column, they are detected and quantified at the end of the column, and the electrical signals are generated and sent to a computer. The chromatographic detected signals can include information regarding the heights and the areas of the resolved peaks, because the detected signal of the resolved analyte is directly proportional to the concentration. The most commonly used detectors are the thermal conductivity detector (TCD) and the flame ionization detector (FID). The TCD measures the change in the thermal conductivity of a gas mixture, caused by changes in the concentration of the species it is desired to detect. [43] FID applies an electrical field between two parallel electrodes placed on both sides of a flame, to measure the ions from the combustion of organic compounds, such as hydrocarbons.[44]

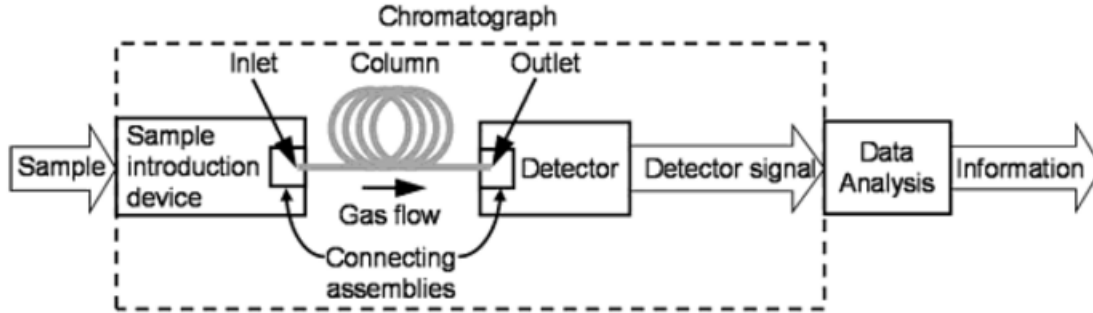


Figure 8: Block diagram of a chromatographic system, adapted from the book named Gas Chromatography[42]. It includes a sample introduction device which introduces the sample into the inlet. The gas flows through the column, before a detector detects the composition of the out flow, and sends the signal to a computer.

2.6.3 Activity and selectivity

The activity and selectivity of the catalyst can be found by running an experiment on methane oxidation using a fixed-bed reactor and analyse the measurements done by the gas chromatograph, described in section 2.6.2. The area under each peak is proportional to the amount of each component in the sample, where the data analyser analyses and computes the mol% of the flows for a specific amount of time.

The methane conversion, X_{CH_4} , can be calculated using the following equation:[28]

$$X_{CH_4}[\%] = \frac{\text{The amount of CH}_4 \text{ converted}}{\text{The amount of CH}_4 \text{ in feed}} = \frac{F_{CH_4,in} - F_{CH_4,out}}{F_{CH_4,in}} \quad (18)$$

where $F_{CH_4,in}$ and $F_{CH_4,out}$ are the molar flows before and after reaction, respectively. Conversion is a measure of how much methane that has reacted. The selectivity is the ratio of how much desired product or reactant converted that was formed compared to the undesired products, and is defined as:

$$S_i = \frac{\text{The amount of desired product}}{\text{The amount of CH}_4 \text{ converted}} = \frac{F_{i,out}}{F_{CH_4,in} - F_{CH_4,out}} \quad (19)$$

where $F_{i,out}$ is the molar flow of specie i out of the reactor. The desired product for methane oxidation is CO_2 . A selectivity of 100% is reached if all the methane has converted into the desired product, CO_2 .

2.6.4 Turnover-frequency

The rate referred to the number of catalytic sites, thus the turnover per unit time, and is known as the turnover frequency (TOF). It is found by using:

$$TOF = \frac{r \cdot M_m}{x_m \cdot D} \quad (20)$$

where r , M_m , x_m and D , are the reaction rate (mol/g_{cat}), molecular weight (g/mol), weight fraction and the dispersion, respectively. The dispersion can be found using Equation 8 in Section 2.5.3 The reaction rate is an intensive measure and a function of composition, temperature and pressure, and hard to measure in exothermic reactions, such as combustion of methane.

2.6.5 Gas Hourly Space Velocity

Space velocity is defined as the ratio of the volumetric feed flow rate to the reaction volume or the reactor's catalyst mass, as shown below:[45]

$$\text{GHSV} = \frac{\text{Volumes of feed as gas at STP/hr}}{\text{Volume of the reactor or catalyst bed or catalyst mass}} = \frac{V_0}{V \text{ or } m_{cat}} \quad (21)$$

The volumetric feed-gas flow rate, V_0 is at standard temperature and pressure, which are at 20°C and 1 atm . V is defined as the reactor volume and m_{cat} as the catalyst mass.

2.6.6 Residence Time

Residence time is the time a molecule spends in a reactive system and is shown below:[46][47]

$$\tau[s] = \frac{V}{q} = \frac{\text{System capacity to hold a substance}}{\text{Flow rate of the substance}} \quad (22)$$

where V (m^3) is the reactor volume where the catalyst would be i.e. catalyst bed and q is the flow rate of the feed into the reactor (m^3/s). τ depends upon temperature and will decrease with increased temperature due to the ideal gas law.

2.6.7 Heterogeneous Catalyst Deactivation

Most catalysts will lose their activity after use, i.e. loss of catalytic rate with time.[28] The catalyst can deactivate by chemical, thermal or/and mechanical changes caused by poisoning, coke formation and structural changes on the catalyst surface. Although palladium based catalysts have the highest known activity for methane oxidation, reaction inhibition by water and water-induced sintering can deactivate these catalysts.[48] Water may degrade Pd through sintering, where the sintering rate is dependent of the particle size. For small particles (less than 3 nm in diameter), Ostwald ripening is the most likely sintering mechanism, and for larger particles (3-10 nm), particle migration and coalescence may also occur. Ostwald ripening is a phenomena where atoms are detached from the crystallites, moves on the surface and get captured by bigger crystallites. When whole crystallites collides and grows, it is called coalescence. The movement of particles on the surface is normally the rate determining step.[28] These processes normally take place at above 500°C and accelerated by the presence of water vapor.[49]

The catalyst used in methane oxidation reaction must operate under relatively low temperatures, low concentrations of methane and high concentrations of water and carbon dioxide. Reaction inhibition by water is related to the reaction of PdO sites and H₂O, as $\text{PdO} + \text{H}_2\text{O} \rightarrow \text{Pd(OH)}_2$, resulting in inactive Pd(OH)₂-molecules, which may reduce the catalyst activity.[48]

3 Experimental

The chapter describes all the experimental work done, including synthesis, characterization and testing of the palladium γ -alumina supported catalysts for methane oxidation for low temperature combustion and lean conditions, and is described further in section 2.4, 2.5 and 2.6, respectively. Before entering the laboratory a risk evaluation was done, and is described in section 3.1.

3.1 Risk evaluation

Prior to the laboratory work, the risk of working in the laboratory with all the apparatus and chemicals was evaluated. It is necessary to identify the chemical and physical factors to avoid injuries regarding health and environment. All students and employees at NTNU are required to obey laws and regulations set by the government and NTNU, including HSE-regulations, safety data sheets, apparatus cards and "Arbeidsmiljøloven". A lab training was accomplished and a HSE-test was passed before entering the laboratory. Every laboratory and apparatus have a contact person, which can be contacted in case of any problems.

The risk evaluation included evaluation of the laboratory work and its likelihoods and consequences of potential accidents, and was done in cooperation with supervisor Professor Hilde Venvik. In order to perform the lab work as safe as possible, the suggested measures were performed if the evaluation ended up in the yellow or red fields in the matrix.

The risk assessment forms are attached in Appendix A as Figure 18 and 19. The existing safety measures were using lab coat, gloves and goggles when handling the hazardous substances. Leak tests were done for each experiment to avoid leak of the hazardous gas CO and explosive H₂-gas. No apparent dangers for human, environment or economy in conjunction with the experiments were found.

3.2 Catalyst Preparation

The catalysts used in this study consist of 0.2 and 2.0 wt% Pd supported on γ -Al₂O₃. The catalysts were prepared by a incipient wetness impregnation of Pd(NO₃)₂ × 2H₂O.[2]. The 0.2 wt% Pd/Al₂O₃ catalyst made for the Specialization Project (SP) during fall 2015 was named 0.2 wt% Pd/Al₂O₃ SP, and the two catalysts made for the Master's Thesis (MT) during spring 2016 were named 0.2 wt% Pd/Al₂O₃ MT and 2.0 wt% Pd/Al₂O₃ MT.

The support, γ -alumina, was calcined in a high temperature furnace for six hours at 600 °C and a heating rate of 5 °C/min. It was then fractionated to particle size 75-150 μ m using sieves of size 75, 150 and 250 μ m.

5 g of the calcined support was weighed out and de-ionized water was added using a pipette

until the incipient wetness point was found. The saturated support was weighed again, the amount of water used was noted and the amount of water needed for 10 g of support was calculated. This is shown in Appendix C. The amount of $\text{Pd}(\text{NO}_3)_2 \times \text{H}_2\text{O}$ that were used were 0.0433 g to prepare the 0.2 wt% palladium supported catalysts and 0.3032 g for 2.0 wt%. The calculations are shown in Appendix B.

10 g of the support and the dissolved salt were then mixed in a ceramic bowl, dried for three hours at 120 °C, while mixing every half an hour for the first hour and then every hour. The temperature is chosen due to the boiling point of water.

The dried supported catalyst was calcined in air using a calcination reactor. The reactor was filled with the catalyst using a funnel, and then placed in the calcination apparatus. The temperature was raised to 500 °C at 1 atm for two hours at a rate of 5 °C/min with air-gas.

3.3 Catalyst Characterization

The catalysts were characterized using different techniques, including Nitrogen Adsorption, X-Ray Fluorescence, Hydrogen and Carbon Monoxide Chemisorption, Temperature Programmed Reduction, X-Ray Diffraction and Thermogravimetric Analysis. The descriptions are found in section 2.5.

3.3.1 Nitrogen Adsorption

The Nitrogen Adsorption experiments were performed using the Micromeritics Tri Star 3000 Surface Area and Porosity Analyzer. The purpose was to find the total surface area of the support and the metal, and the pore volumes and sizes.

About 0.1 g of the catalysts or the support were placed in a sample tube. The exact weights of the 0.2 wt% and 2.0 wt% palladium supported catalysts and support can be found in Table 11 in Appendix D.1. They were first placed in a cooling station for degassing for one hour with vacuum, and then placed in the heating station in 200 °C until the pressure in the degas unit was below 100 mTorr. Liquid Nitrogen was filled in the dewar, the sample tubes installed and the analyse were done overnight.

3.3.2 X-Ray Fluorescence

Material analyzes of the alumina, 0.2 and 2.0 wt% palladium supported catalysts were made using the Wavelength Dispersive X-Ray Fluorescence (WDXRF) Supermini200 analyser. About 0.2 g of the catalysts were weighed out and mixed in a mortar with about 2.8 g boric acid as a binder. The exact weights of the 0.2 wt% and 2.0 wt% palladium supported catalysts, support and boric acid can be found in Table 12 in Appendix D.2. The homogeneous mixtures were placed in a pellet die and later in a press machine to make pellets. The final pellets were placed

in the sample retainers, covered with propylene films and covered with the sample holders.

The Pulse Height Analyzer (PHA) was adjusted before analysis in order to calibrate the detector. Then the sample holders with the pellets were positioned, and information such as type of binder, sample weights and binder weights were typed in the software, before the analysis was started.

3.3.3 Chemisorption

In order to find the dispersions of the catalysts a hydrogen and carbon monoxide chemisorption were performed, using Chemisorption ASAP 2020 (SINTEF). A piece of quartz wool was placed in the sample tube and a sample of about 0.15 g catalyst were weighed out and poured into the sample tube and a portion of quartz wool was placed on top of it, before it was weighed and dried for one hour at 120 °C. The exact weights of the 0.2 wt% and 2.0 wt% palladium supported catalysts can be found in Table 13 in Appendix D.3.

The tube was installed into the apparatus with clean O-rings and gloves to avoid contamination. The sample was evacuated to approximate vacuum followed by a leak test until the pressure change was less than 50 μ mHg/min.

The thermocouple was attached, the furnace placed around the sample tube and the system was isolated. During the Specialization Project, two analyses were performed on the 0.2 Pd/Al₂O₃ wt% SP catalyst using hydrogen. The analysis conditions used for hydrogen chemisorption are found in Table 1. For the Master's Thesis, two carbon monoxide analyses were performed for each of the three catalysts. The analyse conditions using carbon monoxide as the adsorptive gas are shown in Table 2.

Table 1: The analyse conditions using Chemisorption ASAP 2020 (SINTEF) at NTNU. The adsorptive was hydrogen, flows of hydrogen (H₂) and helium (He) were used and the sample was evacuated with vacuum. The analyses were performed on 0.2 wt% palladium supported catalyst SP.

Task	Gas	Temperature [°C]	Rate [°C/min]	Time [min]
Flow	He	200	10	10
Evacuation		100	10	10
Flow	H ₂	400	10	30
Evacuation		400	10	30
Evacuation		35	10	120
Leak Test		35	10	
Evacuation		35	10	10
Analysis	H ₂	35	10	

Table 2: The analyse conditions using Chemisorption ASAP 2020 (SINTEF) at NTNU. The adsorptive was carbon monoxide, flows of hydrogen (H₂) and helium (He) were used and the sample was evacuated with vacuum. The analyses were performed on the 0.2 wt% Pd/Al₂O₃ SP and 0.2 wt% and 2.0 wt% palladium supported catalysts MT.

Task	Gas	Temperature [°C]	Rate [°C/min]	Time [min]
Flow	He	200	10	10
Evacuation		100	10	10
Flow	H ₂	400	10	30
Evacuation		400	10	30
Evacuation		35	10	30
Leak Test		35	10	
Evacuation		35	10	10
Analysis	CO	35	10	

3.3.4 X-Ray Diffraction

An apparatus called DaVinci1 at the Department of Materials Science and Engineering at NTNU was used to do the X-Ray Diffraction analysis. Samples (0.2 and 2.0 wt% palladium supported catalysts and alumina) were prepared in sample holders. The parameters scan time, angle range and divergence slit were set, and chosen as 30 minutes, 10-75° and V6, respectively. V6 means that it keeps a constant six mm of sample illuminated at all angles. Kristin Høydalsvik, the lab responsible, loaded the samples into DaVinci1.

3.3.5 Thermogravimetric Analysis

The Thermogravimetric Analysis was performed with a NETZSCH temperature controller, DCU PFEIFER vacuum controller, STA 449C JUPITER, pump and power unit, and in JULABO F257MC water bath and PFEIFER turbo pump. Three correction files were made, first reduction, then oxidation and lastly reduction with an empty crucible. The reduction correction files were made using argon (Ar) and hydrogen (25% H₂/75% Ar) at a rate of 5°C/min and temperatures between 30-350 °C. The oxidation correction file was made using air (20% O₂/80% N₂) within 30-700 °C and the same temperature rate as the reduction. The hold-times varied between 0-30 minutes. Later a sample of about 0.10-0.20 mg of the 2.0 wt% Pd/Al₂O₃ SP catalyst was placed in the crucible and run with the same parameters as the correction files. The exact weights of the catalyst can be found in Table 14 in Appendix D.4. An illustration of the temperature profile with the exposed gases can be seen in Figure 9.

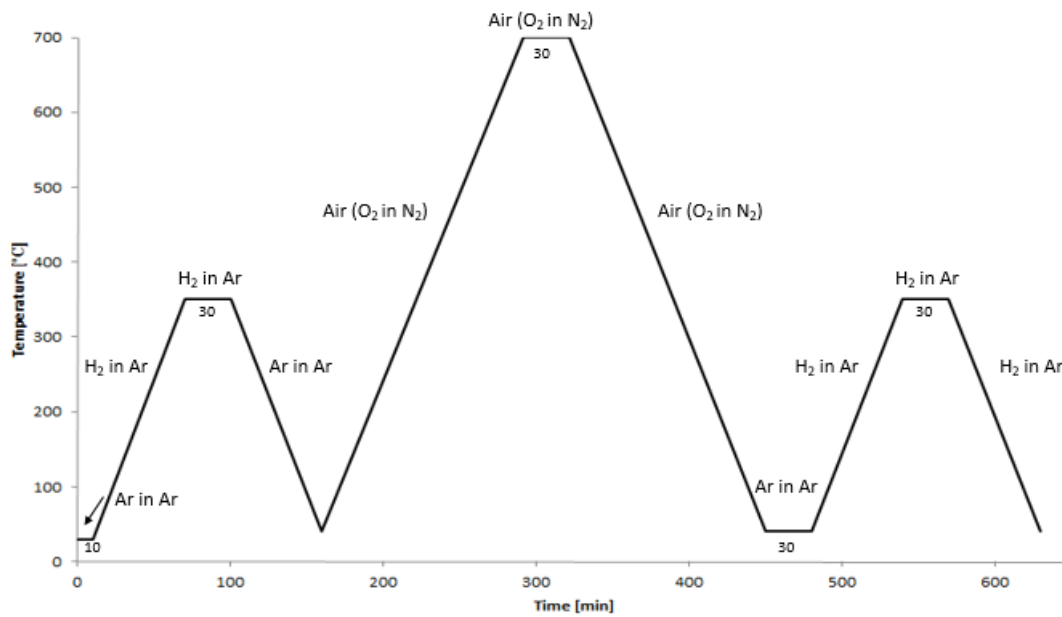


Figure 9: An illustration of the temperature profile as a function of time(min) of the TGA with the exposed gases and the hold-time (minutes) shown below the curve. The curve is divided in isothermal and dynamic parts, where the rate is 5°C/min in the dynamic parts. The gases are hydrogen (25% H₂/75% Ar), argon (Ar) and Air (20% O₂/80% N₂).

3.4 Activity Measurements

The methane oxidation testing was ran in a setup prepared by Research Scientist Jia Yang and build by Professor Hilde Venvik, and is equipped with mass flow and temperature controllers, connections to feed gases and analysis apparatus. Figure 10 shows the flow diagram of the process. The experiments were performed outside the concentration explosion limits for methane which are 5-15 percent per volume for methane in air.[50] A sketch of the reactor can be found in Appendix J and the heights and radii of the catalyst bed were measured to be 2 cm and 0.5 cm, respectively. Setpoints (% open valves) that were implemented in the labview window were found using calibration data from calibrations of the mass flow controllers. The analysis of the feed amount and composition was done using Agilent 3000 Micro Gas Chromatograph and column type porous layer open tubular column, where the stationary phase is molsieve (HP-AL/M) and the carrier gas used is helium. HP-PLOT Q column was used for detection of CO₂. Each analysis required approximately 7 analysis of the feed and product flows for each temperature hold-up time.

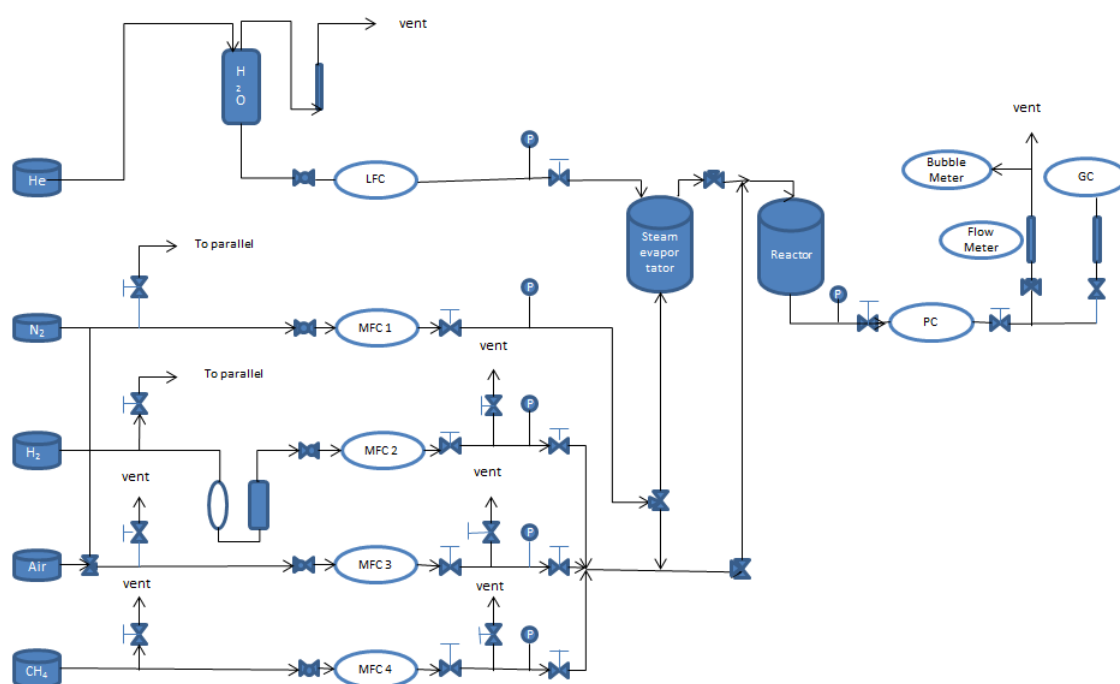


Figure 10: The flow diagram of the methane oxidation process, where MFC and PC are controllers of the mass flows, level and pressure, respectively. The GC is the gas chromatography. The inlet gases used for this work are nitrogen, air and methane and the flows are opened by control valves. Several vents are present to release the reactants, products and by-products if required.

To achieve the wanted flows, set points for the flows of CH₄, O₂ (synthetic air) and N₂ were calculated using the MFC calibration data from Jia Yang. The calculations can be found in Appendix K.

To minimize the pressure drop and the friction between the flow of the reactants and the

catalyst particles, pellets of sizes 250-500 μm were made of the newest 0.2 wt% and 2 wt% Pd/Al₂O₃ MT catalysts using a pellet die, pressure machine and sieves. Powder was used for the 0.2 wt% Pd/Al₂O₃ SP catalyst.

A mix of a sample of the catalyst (about 0.2 g) and silicon carbide (about 2.0 g) was loaded into the quartz reactor, the reactor was placed in the furnace with a thermocouple inside (same height as the catalyst bed), the gas inlet and outlet were connected and then a leak test with hydrogen (20 NmL/min, 2.8%) in N₂ (100 NmL/min, 15.1%) was performed. The exact weights of the 0.2 wt% and 2.0 wt% palladium supported catalysts can be found in Table 15 in Appendix D.5. The sample was reduced with H₂ in N₂ from 20 °C up to 350 °C with a rate five °C/min, the temperature was kept constant for 120 minutes before it was reduced to 200 °C.

To analyse the catalyst behaviour and methane oxidation under oxygen rich and very-rich environment, the compositions of the reactant feed consisting of methane, oxygen and nitrogen (CH₄/O₂(synthetic air)/N₂) are varied from CH₄:O₂-ratio equal to 1:5 and 1:10. The total molar feed flow was constant equal to 200 NmL/min for each run. The reference reaction was ran with a CH₄:O₂-ratio equal to 1:5, flows of methane, oxygen and nitrogen equal to 4, 20 and 176 NmL/min, respectively, and MFC set points equal to 24.5%, 91.4% and 15.2%. The 0.2 wt% Pd/Al₂O₃ SP catalyst was tested under reference conditions, only. The reference reaction is reaction #1 in Table 3. The 2.0 wt% Pd/Al₂O₃ MT is ran in series under different conditions as shown in Table 3 as reaction #1 to #8. The 0.2 wt% Pd/Al₂O₃ MT catalyst was tested in the order reaction #1, #3, #5, #6, #7 and #8 as explained in Table 3.

To achieve lower methane concentrations, a gas bottle with 5% CH₄ in N₂ was installed. It was assumed that the MFC gas correction factors for nitrogen and methane, which are 1 and 0.72, respectively, could be used to correct the MFC calibration data in Appendix K.[51] The calculations can be found in Appendix K and the analysis conditions for reaction number 9 and 10 can be found in Table 3.4 below. The 2.0 wt% Pd/Al₂O₃ MT catalyst was tested under conditions described in reaction number 9 and 10 in Table 3.4.

Table 3: The feed flow compositions for reactions with different reaction conditions. The compositions differ with a CH₄:O₂-ratio equal to 1:5 and 1:10, i.e. rich and very rich oxygen environment. The reactions were ran from around 200 to around 650 °C, depending on the activity, with temperature intervals of 25 to 50 °C, rate at five °C/min and hold-up times of 20 to 30 minutes. The total feed flow were held constant at 200 NmL/min, where the composition of methane, oxygen and nitrogen were varied and consequently the set points. The calculations of the MFC set points to achieve the desired feed flows can be found in Appendix K.

Reaction no.	CH ₄ :O ₂	Flows [Nml/min]			Fraction, F _i /F _{tot} CH ₄ /O ₂ /N ₂	Set points [%] CH ₄ /air/N ₂
		F _{CH₄}	F _{O₂}	F _{N₂}		
1	1:5	4	20	176	2%/10%/88%	24.5/91.4/15.2
2	1:5	4	20	176	2%/10%/88%	24.5/91.4/15.2
3	1:10	2	20	178	1%/10%/89%	12.3/91.8/15.4
4	1:5	4	20	176	2%/10%/88%	24.5/91.4/15.2
5	1:5	2	10	188	1%/5%/94%	12.3/45.8/21.9
6	1:5	1	5	194	0.5%/2.5%/97%	6.15/22.7/25.3
7	1:10	1	10	189	0.5%/5%/94.5%	6.15/45.8/22.1
8	1:5	4	20	176	2%/10%/88%	24.5/91.4/15.2
9	1:5	0.2	1	198.8	0.1%/0.5%/99.4%	17.7/4.3/27.7
10	1:10	0.2	2	197.8	0.1%/1%/98.9%	17.7/8.92/27.0

The temperature profile was set from around 200 to around 650 °C, depending on the activity of the catalyst, with temperature intervals of 25 to 50 °C, rate at 5 °/min and hold-up times of 20 to 30 minutes, as shown below:

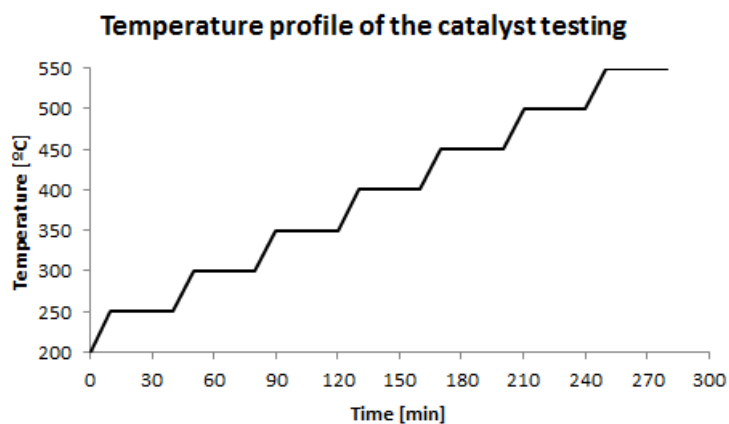


Figure 11: An illustration of the temperature profile of the catalyst testing, with 25 to 50 °C intervals, hold-up times of 20 to 30 minutes and a rate of 5 °C/min.

In order to find the actual temperature in the catalyst bed, the temperatures were recorded at set-point temperatures 350 °C and 450 °C, by noting the temperatures along the catalyst bed to make temperature profiles. The described procedure was done for the 0.2 wt% Pd/Al₂O₃ SP catalyst. The temperature measurements are shown in Appendix L. For the other catalysts, temperature measurements were performed every 25 or 50 °C across the catalyst bed. The measurements can be found in Tables 20, 21, 22, 23, 24 and 25, 27, 28, 29, 30, 31, 32, 33, 34,

35 and 36 in Appendix L, for the 0.2 wt% and 2.0 wt% Pd/Al₂O₃ MT catalysts, respectively.

The system was then stepped down in the same manner as shown in Figure 11, from around 600 to 250 °C, and the flows were switched off in the order CH₄, air and lastly N₂ (which flows for five minutes to remove air from the system). The reactor was then cooled down to around 25 °C.

The GHSVs were calculated using Equation 21 and the calculations can be found in Appendix M. They were found to be 59400 NmL/g_{cat}h, 58000 NmL/g_{cat}h, 58800 NmL/g_{cat}h and 59400 NmL/g_{cat}h for the 0.2 wt% Pd/Al₂O₃ SP, 0.2 wt% Pd/Al₂O₃ MT and the 2.0 wt% Pd/Al₂O₃ MT catalysts tested with the initial methane gas bottle and the diluted methane gas bottle, respectively.

4 Results and discussion

The results have been divided into two sections. Results obtained from the characterization and activity measurements of the catalysts, and can be found in Section 4.1 and 4.2, respectively. The 0.2 wt% Pd/Al₂O₃ SP was made using incipient wetness impregnation method for the Specialization Project and are also included in this work. The 0.2 wt% Pd/Al₂O₃ MT and 2.0 wt% Pd/Al₂O₃ MT catalysts were prepared using the same synthesis method and were made for my Master's Thesis at NTNU spring 2016.

4.1 Catalyst Characterization

The catalysts were characterized using Nitrogen Adsorption, H₂- and CO-chemisorption, X-Ray Fluorescence, X-Ray Diffraction and Thermogravimetric Analysis.

4.1.1 Nitrogen Adsorption

The Nitrogen Adsorption method is described in Section 2.5.1, and the properties found using BET of the alumina, 0.2 wt% Pd/Al₂O₃ SP, 0.2 wt% Pd/Al₂O₃ MT and 2.0 wt% Pd/Al₂O₃ MT catalysts are summed up in Table 4. The loss of BET area and pore volume, compared to alumina, of the 0.2 wt% Pd/Al₂O₃ catalysts can possibly be attributed to the deposition of Pd species in the pores, but it is not significant. When the loading of Pd is increased to 2.0 wt%, the surface area and pore volume decreased significantly compared to the 0.2 Pd wt% catalysts and γ -alumina, which may be due to the blockage of inner pores by palladium and especially small ones. The pore diameter confirms that the support is of mesoporous material as mentioned in Section 2.2.

The pore volume distributions, showing the volume adsorbed N₂ or the pore volume as a function of the pore size, can be found in Appendix F. The preferred catalyst is having small pore volume and diameter, and high surface area but high dispersion. Too big pores may reduce the mechanical strength of the alumina, but the mass transport of reactants flowing through the catalyst may be reduced by too tight and long pores. By studying the distributions for alumina, 0.2 wt% Pd/Al₂O₃ SP, 0.2 Pd/Al₂O₃ MT and 2.0 wt% Pd/Al₂O₃ MT catalysts in Figures 20, 21, 22, and 23, respectively, it is possible to see where the majority of the volume is. The catalysts exhibited broad distributions, indicating that they are in all type of sizes. The catalyst with high loading shows a greater volume of smaller pores.

The results obtained from the adsorption and desorption isotherm differ from each other. The adsorption isotherm is supposed to give a more realistic picture, due to that evaporation along the desorption branch can not occur if the pathway is blocked by other filled pores, but an empty pore during adsorption can be filled.[52] It was only possible to obtain the desorption

isotherms from the experiments performed during spring 2016.

Table 4: The physical-chemical properties of the prepared 0.2 wt% Pd/Al₂O₃ SP, 0.2 wt% Pd/Al₂O₃ MT and 2.0 wt% Pd/Al₂O₃ MT catalysts found by Nitrogen Adsorption using BET and BJH. Catalyst SP and MT are performed during fall 2015 for the Specialization Project and for the Master's Thesis during spring 2016, respectively. The results are shown for desorption and adsorption isotherms, respectively. Where one number is presented, the number is obtained from the desorption isotherm.

Catalyst	Surface area [m ² /g]	Pore volume [cm ³ /g]	Pore diameter [nm]
0.2 wt% Pd/Al ₂ O ₃ SP	146	0.66-0.67	13-16
0.2 wt% Pd/Al ₂ O ₃ MT	144	0.66	14
2.0 wt% Pd/Al ₂ O ₃ MT	130	0.59	13
Al ₂ O ₃	152	0.68-0.68	13-16

4.1.2 Chemisorption

Chemisorption experiments were performed using hydrogen and carbon monoxide gas, and the results are shown in Table 5 and 6, respectively.

During the Specialization Project fall 2015, only hydrogen chemisorption was performed and the analysis conditions and results can be found in Table 1 and 5, respectively. Dispersion, a measure indicative of the percentage of exposed palladium atoms, increased with increasing evacuation time, resulting in smaller crystals and a higher metal surface area. As explained in Section 2.5.3 and shown in Figure 3, the first dispersion represents the total adsorbed amount of adsorption gas (physisorbed and chemisorbed) and the second the difference between the isotherms, i.e. the amount of gas chemisorbed. The chemisorbed results showed negative/low values for the dispersion, as shown in Table 16 in Appendix E and could possibly be explained in terms of more gas is physisorbed on the surface than chemisorbed. This results in negative/low values may be due to hydrogen not being strongly bound to the surface. A solution could be to increase the evacuation period. Other theories are that the catalyst is not completely reduced when starting the chemisorption or there is a leakage in the system. According to Shin et al., hydrogen can dissolve in Pd and diffuse through palladium.[53] Hydrogen is adsorbed on the palladium surface at low pressures, but at high pressures adsorbed in the bulk, which can give lower dispersion results.

As mentioned, a proposed solution is to increase the evacuation time. A longer time to remove the air in the sample the more correct picture of the dispersion may be found. When residue air is present in the sample, less hydrogen is chemisorbed to the surface and the dispersion can show lower values than in reality indicating that the hydrogen is physisorbed. When the second isotherm is made, showing that more hydrogen is removed than the quantity physisorbed. When the second isotherm is made, showing that more hydrogen is removed than the quantity physisorbed, and give low/negative "difference" dispersion.

Table 5: The physical-chemical properties of the 0.2 wt% Pd/Al₂O₃ SP catalyst prepared during the Specialization Project during fall 2015 found by H₂ chemisorption. Chemisorption was performed two times. The results are shown for the total adsorbed amount. The analysis conditions are found in Table 1.

Experiment no.	Dispersion [%]	Crystallite Size [nm]	Metal surface area [m²_{metal}/g_{cat}]
1	65	1.7	0.58
2	70	1.6	0.62

As mentioned, it is discussed whether hydrogen is dissolved in palladium or not [53], therefore the chemisorption experiments performed during the Master's Thesis were done using only carbon monoxide and the results can be found in Table 6. The analysis conditions are described in Table 2. Two individual chemisorption experiments with the same analysis conditions were performed for each catalyst, i.e. the 0.2 wt% Pd/Al₂O₃ SP, the 0.2 wt% Pd/Al₂O₃ MT and 2.0 wt% Pd/Al₂O₃ MT catalysts, and as shown in Table 6 the total metal dispersion varied from 16% to 26%, 46% to 54% and 17% to 26% for the catalysts, respectively. The results indicate that the palladium atoms are well dispersed on the γ -alumina support and that the dispersion increased with decreasing loading. It may be explained by a lower loading of palladium and consequently fewer atoms are easier to disperse than many active metal atoms.

The chemisorption experiments were performed in the same period of time using fresh catalyst and no one used the same apparatus in between these experiments, to minimize the uncertainties of the experiments. Despite that, clear deviations are observed in the repeated experiments, i.e. the two 0.2 wt% catalysts which can be explained by uncertainties during the catalyst preparations. More experience when preparing the catalyst the second time can give more accurate results. The relatively high dispersions can be explained in terms of the preparation method used. When the catalysts are prepared using the impregnation method instead of the bulk preparation method, more active metal is deposited on the support surface instead of trapped within the bulk matrix. The dispersion results indicate that the impregnation method was a good preparation method to make the active sites available on the support surface.[30]

By comparing the dispersion data obtained from H₂- vs CO-chemisorption it is trustworthy to believe that the CO results show the most realistic picture of the dispersion, due to the negative and very high dispersion using H₂. However, there are some errors associated with using CO, because, as mentioned in Section 2.5.3, the CO can chemisorb in various forms, that can introduce errors to the reliability of the data.[30]

Table 6: The physical-chemical properties of prepared 0.2 wt% Pd/Al₂O₃ SP, 0.2 wt% Pd/Al₂O₃ MT and 2.0 wt% Pd/Al₂O₃ MT catalysts found by CO chemisorption. Chemisorption were performed two times for each catalyst for repetition of the experiments. The results are shown for the total adsorbed amount. The analysis conditions are found in Table 2.

Catalyst	Experiment no.	Dispersion [%]	Crystallite Size [nm]	Metal surface area [m²_{metal}/g_{cat}]
0.2 wt% Pd/Al₂O₃ SP	1	26	4.3	2.3
	2	16	6.8	0.15
0.2 wt% Pd/Al₂O₃ MT	1	54	2.1	0.48
	2	46	2.4	0.41
2.0 wt% Pd/Al₂O₃ MT	1	26	4.3	2.3
	2	17	6.8	1.5

4.1.3 X-Ray Fluorescence

The detected compounds found using XRF and their intensity versus 2θ can be found in Figure 24, 25, 26, 27, 28, 29, 30, 31, 32 and 33 in Appendix G. The summary of the results obtained can be found in Table 7, where the compounds with lower detected weight% than 0.1 have been excluded. The XRF-apparatus was newly calibrated in front of the experiments to reduce the uncertainties regarding the apparatus and wrong XRF-references. Here the pure HBO_3 (binder) is used as reference. Alumina was detected, so was palladium and oxygen which were detected as palladium oxide. The amount of pure palladium in the catalysts was calculated to be 0.11%, 0.28% and 1.70% for the 0.2 wt% $\text{Pd}/\text{Al}_2\text{O}_3$ SP, 0.2 wt% $\text{Pd}/\text{Al}_2\text{O}_3$ MT and 2.0 wt% $\text{Pd}/\text{Al}_2\text{O}_3$ MT catalysts, respectively, based on the amount of PdO detected. The calculations can be found in Appendix H. The weight% were supposed to be 0.2 and 2.0, but the losses and gains may be attributed to the catalyst pellets not being homogeneous mixtures. The results confirm that the preparation conditions including the heating temperatures for drying and calcination have been sufficient to remove organic compounds and the nitrate from the starting salt, as described in Section 2.4.

Table 7: The mass% of the compounds detected of the 0.2 wt% $\text{Pd}/\text{Al}_2\text{O}_3$ SP, 0.2 wt% $\text{Pd}/\text{Al}_2\text{O}_3$ MT, 2.0 wt% $\text{Pd}/\text{Al}_2\text{O}_3$ MT catalysts, alumina and the binder (HBO_3) using X-Ray Fluorescence. The intensity is measured in kilo counts per second(kcps). The mass% of pure Pd is calculated based on the mass% of PdO. The calculations can be found in Appendix H.

Catalyst	Compound	Mass%	Intensity [kcps]
0.2 wt% $\text{Pd}/\text{Al}_2\text{O}_3$ SP	Al_2O_3	99.9	8.61
	PdO	0.124	0.0211
	Pd (calculated)	0.110	
0.2 wt% $\text{Pd}/\text{Al}_2\text{O}_3$ MT	Al_2O_3	99.7	8.35
	PdO	0.319	0.0307
	Pd (calculated)	0.280	
2.0 wt% $\text{Pd}/\text{Al}_2\text{O}_3$ MT	Al_2O_3	98.1	6.08
	PdO	1.90	0.234
	Pd (calculated)	1.70	
Alumina	Al_2O_3	100	9.45
HBO_3 (binder)	K_2O	99.0	0.182
	SiO_2	1.01	0.0111

4.1.4 X-Ray Diffraction

The X-ray diffraction patterns for all four samples, including the alumina support, the 0.2 wt% Pd/Al₂O₃ SP, 0.2 wt% Pd/Al₂O₃ MT and 2.0 wt% Pd/Al₂O₃ catalysts are shown in Figure 12. The results from the XRD of alumina and the Pd/Al₂O₃ catalysts are fairly similar and indicate that the catalysts contain too small amounts of palladium or that the particles are too small for palladium to obtain a diffraction peaks. The relative heights matched the crystal reflections for γ -alumina. As γ -alumina is semi-amorphous, the resulting peaks are broad.[?]

By heat treatment, γ -alumina can be transformed into different alumina phases, i.e. θ -, α -, η - and δ -Al₂O₃, as mentioned in Section 2.2 and 2.5.4. With reference to previous work, i.e. Rane et. al [54], θ , η and δ phases were excluded when fitting the resulting patterns with the characteristic patterns for Al₂O₃. According to Rane et. al the γ -alumina will transform into the other phases with heat treatment above 800 °C. The alumina prepared for this work was only heated up to 600 °C. α -alumina was not detected either, and conclusively the alumina probably did not undergo a phase change.[54]

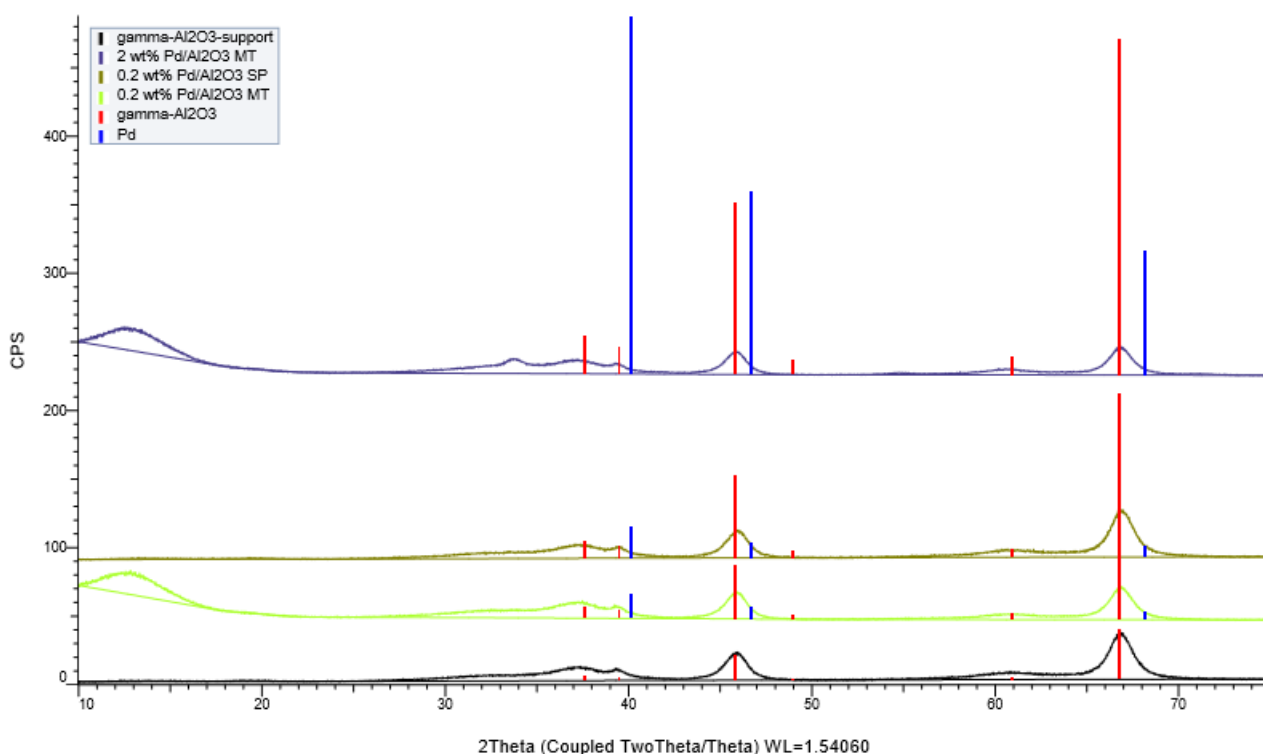


Figure 12: The XRD patterns for the alumina support (black line), 2 wt% Pd/Al₂O₃ MT catalyst (purple line), the 0.2 wt% SP catalyst (dark green line) and 0.2 wt% MT catalyst (light green line). The lines marked red and blue are crystal reflections for γ -Al₂O₃ and palladium, respectively. The graph is shown as counts per minute (CPS) as a function of 2θ . The Y Offset is adjusted to fit all the results in the same plot by position the objects above or below the baseline.

4.1.5 Thermogravimetric Analysis

A Thermogravimetric Analysis of the 2.0 wt% Pd/Al₂O₃ MT catalyst was performed and the results can be found in Figure 13. The blue and the red curves represent the weight% and temperature changes as a function of time when the catalyst is exposed to reducing and oxidizing environments, as explained in Section 2.5.6 and illustrated in Figures 7 and 9. The palladium will alter between being oxidized, PdO, and the reduced state, Pd⁰. The three "temperature sections" represent first the reducing, then the oxidizing and lastly the reducing atmosphere, using hydrogen in argon, oxygen in nitrogen and hydrogen in argon, respectively. It is noteworthy that each time the gases are switched, it starts on a new baseline, which is where the weight% is equal to 100.

The drop in the weight% in the first part where the catalyst is heated up to 350 °C strongly suggests that the palladium is reduced from bulk-palladium oxide to palladium. By assuming that the weight loss is attributed to oxygen, the amount of oxygen removed by reduction is 1.70 mg. The calculations can be found in Appendix I in Table 17. A TPR experiment performed by B. Wang et al. as shown in Figure 4, shows that palladium supported on γ -alumina reduces at 127 °C and 210 °C, which may explain the reduction temperatures from the TGA-measurements.

When introducing the catalyst to the inert argon gas, the catalyst weight increases. This may be due to contaminated gas or leakage in the system, where the catalysts may be exposed to oxygen.

As the temperature is raised to 700 °C and the catalyst is introduced to air, the weight of the catalyst is stable. The catalyst may be fully oxidized before injecting the oxygen in the system. It may be explained by the temperature decrease between the reducing/oxidizing "sessions".

The weight of the catalyst is decreasing when introducing it to hydrogen and temperature increase the second time. The weight loss of oxygen is calculated to be 1.40 mg after the second reduction. The oxygen amount is almost the same as the oxygen loss in the first reduction under the same conditions. The results strongly suggest that the palladium is initially oxidized and is reduced at temperature increase up to 350 °C with hydrogen as the reducing gas.

The XRF results showed that the catalyst most likely contained palladium oxide or palladium and oxygen, and therefore a reduction was performed first to remove the oxygen from the palladium. A preliminary conclusion of the TGA results can be that the palladium is most likely carrying a significant amount of oxygen, due to the loss of mass when introducing the catalyst to a reducing environment. As mentioned in Section 2.1, at temperatures starting from 300 °C and up to 600 °C, the palladium can be identified as PdO.

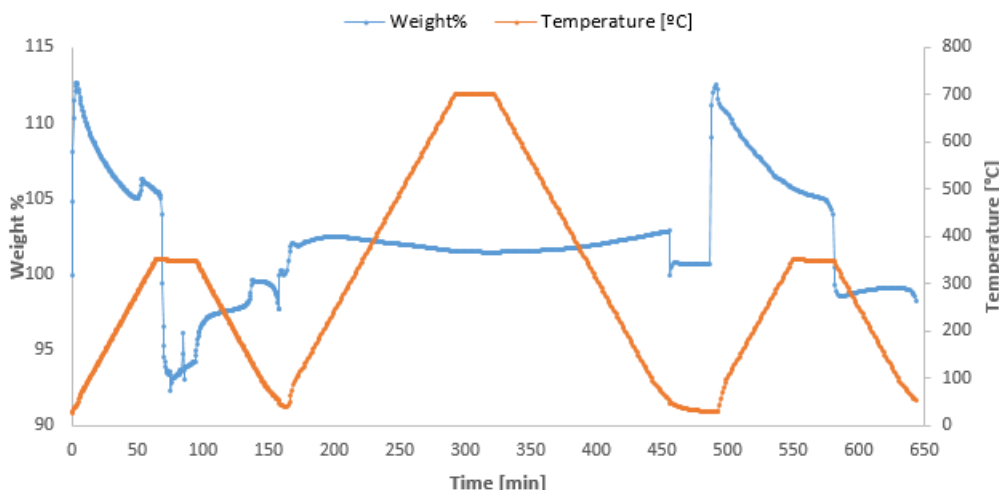


Figure 13: TGA measurement of 2.0 wt% Palladium supported Al_2O_3 catalyst. The blue and red line are the change in weight% of the catalyst and the temperature as a function of time, respectively. The procedure of oxidation and reduction of Palladium supported on Al_2O_3 under different atmospheres, including hydrogen (25% H_2 /75% Ar), argon and air (20% O_2 /80% N_2) at different temperatures. An illustration can be found in Section 2.5.6 in Figure 7. The catalyst is reduced for three hours up to 350 °C, oxidized for five hours up to 700 °C and lastly reduced for three hours up to 350 °C. The palladium will alter between being an oxygen-carrier, PdO , and the reduced state, Pd^0 . It starts on the baseline equal to 100 wt% each time the gases are switched.

4.2 Activity Measurements

The catalysts were loaded in the reactor and the catalytic activity was studied by altering the reaction conditions such as feed composition of methane, oxygen and nitrogen and monitoring the gaseous products by GC. The molar feed flow was held constant at 200 NmL/min for each reaction. The extent of deactivation was found by running the reactions in series without replacing the catalyst and comparing the $T_{100\%}$, because the reaction is extremely exothermic and irreversible. The testing results of the 0.2 wt% Pd/ Al_2O_3 SP, 0.2 wt% Pd/ Al_2O_3 MT and 2.0 wt% Pd/ Al_2O_3 MT catalysts are presented in Table 8, 9 and 10, respectively. There are no mass flow limitations in the system and therefore the use of powder or pellets will not affect the results. No pressure drop was observed in any of the experiments. The combustion curves, i.e. the catalytic activities of the 0.2 wt% Pd/ Al_2O_3 SP, 0.2 wt% Pd/ Al_2O_3 MT and 2.0 wt% Pd/ Al_2O_3 MT catalysts as a function of the reactor bed temperature, can be found in Appendix N.1, N.2 and N.3, respectively. The conversion calculations are found in Appendix O. The temperatures where the catalysts achieved 10%, 50% and 100% methane conversion labelled as $T_{10\%}$, $T_{50\%}$ and $T_{100\%}$, respectively, and are summarized in Table 8, 9, and 10. Where a 10% methane conversion is achieved it is referred to as the ignition temperature and $T_{50\%}$ as the light-off temperature. The 0.2 wt% Pd/ Al_2O_3 MT catalyst was made for checking the validation of the results by repeating the experiments.

To test the presence of temperature gradients in the catalyst bed, measurements across the bed were performed for each hold-up temperature. The temperature was not uniform and therefore the average of the three measurements was used, i.e. 0 cm, 1 cm and 2 cm into the bed. Figure 14 shows the temperature profile of measurements performed when testing the 2.0 wt% Pd/Al₂O₃ at setpoint temperatures 250 to 500 °C and at reference conditions, including a total molar flow of 200 NmL/min with composition of methane, oxygen and nitrogen equal to 2%, 10% and 88%, respectively. All the temperatures measurements of the catalyst bed for each run can be found in Appendix L. It can be seen that there is general higher temperature in the middle of the catalyst bed, i.e. 1 cm, and consequently the bed is not uniform. Also, there are observed some deviations between the setpoint temperatures and the measured temperatures, indicating that the temperatures in the catalyst are lower than the system measures. This is unfortunate for the control of the reaction conditions such as the temperature.

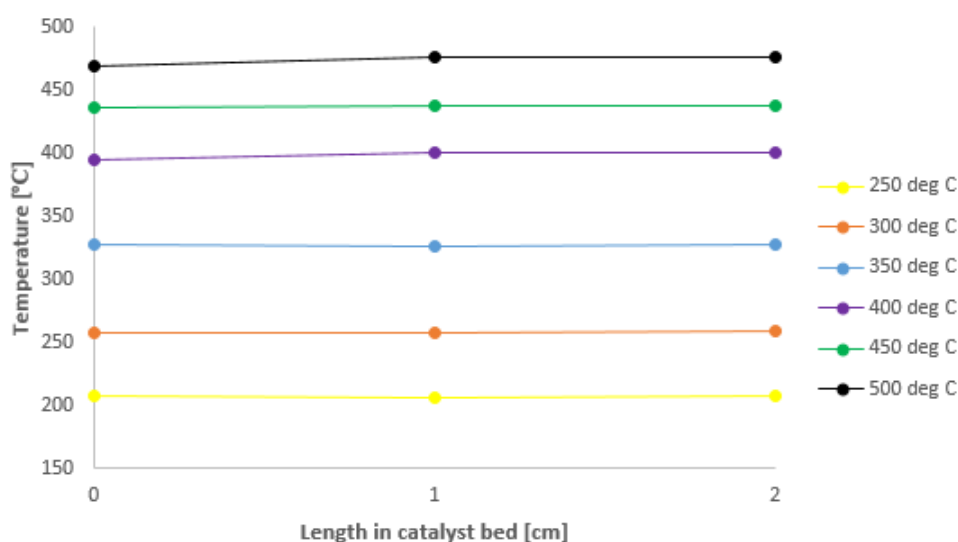


Figure 14: The temperature profile of the 2.0 wt% Pd/Al₂O₃ MT catalyst at each setpoint hold-up temperature when testing the catalyst for methane oxidation using a total molar flow equal to 200 NmL/min and gas feed composition of methane, oxygen and nitrogen equal to 2%, 10% and 88%, respectively. The setpoint temperatures were every 50 °C from 250 to 500 °C. The catalyst bed was 2 cm in height and the measurements were performed at axial length across the catalyst bed equal to 0 cm, 1 cm and 2 cm.

The GC did not detect any CO and it is assumed that the combustion was almost complete, apart from the 2% methane that was not converted into water and carbon dioxide. To ensure that the best accuracy was obtained, the flows of each component in the reaction were calculated based on 98% methane conversion as shown in Appendix P and the results in Table 55. The calculated results were compared to the component flows detected by the GC. It was found that the calculated and the actual flows (detected by the GC) were in agreement and conclusively it is reasonable to believe that the GC is extremely sensitive hence gives reasonable data. The selectivity of CO₂ is set to be almost 100% because no other products were detected.

The catalytic activity of the 0.2 wt% Pd/Al₂O₃ SP catalyst by increasing the temperature in the catalyst bed, can be found in Figure 15. As seen, it takes time before the reaction is initiated, i.e. T_{10%} equal to 325 °C, but as the temperature arises it goes quickly before maximum conversion is achieved. A well-controlled laboratory reactor would have given coincided heating and cooling curves. That is not observed here, due to temperature dissipation in the system and the reaction rate increases rapidly after ignition as the reaction is strongly exothermic. As the reactor is cooled, the system is not able to remove heat quickly enough. Dissipation is a contributor for controlling the temperature.

As seen from the results in Table 8 and Figure 15, the 0.2 wt% Pd/Al₂O₃ SP catalyst did only achieve 98% methane conversion, because the reaction was stopped at 550 °C. By increasing the catalyst bed temperature further for the 0.2 wt% Pd/Al₂O₃ MT, T_{100%} was 541 °C, as seen in Table 9. Conclusively, the temperature raise was not high enough for the first catalyst. Since the 0.2 wt% Pd/Al₂O₃ MT catalyst achieved 100% methane conversion, it is said to show higher activity, and it may be due to the greater palladium loading, 0.28 wt%, observed using XRF. Consequently, the catalyst has higher palladium loading and therefore showed greater dispersion and thus more available active sites. These observations indicate that additional and repeated experiments always should be performed.

The XRF and TGA results indicate that the catalysts contained a considerable amount of oxygen, also at temperatures above 300 °C. It confirms what Gèlin et. al claim, where PdO is stable in an oxidized state from temperatures from 300 to 800 °C, which are within the temperature intervals these catalysts are tested.[14] It is assumed, based on the results, that the temperature, the hold-time and the reducing environment the catalysts were exposed to before starting the methane oxidation reaction, were good enough to reduce the oxygen-carrying palladium to palladium. The palladium is most likely oxidized when the catalysts are exposed to the reactants.

Table 8: The methane converted as a function of the catalyst bed temperature to achieve 10%, 50% and 100% converted methane, labelled T_{10%}, T_{50%} and T_{100%}, respectively. The 0.2 wt% Pd/Al₂O₃ SP catalyst was only tested under the reference conditions described in Section 3.4. The reaction number corresponds to the reaction number and consequently reaction conditions described in the table. The fraction of the feed gas containing methane, oxygen and nitrogen is changed for each reaction and the total molar feed flow is 200 NmL/min. The GHSV is calculated using the amount of fresh catalyst and is 59400 NmL/g_{cat} h.

Catalyst	Reaction no.	Fraction, F_i/F_{tot} CH₄/O₂/N₂	T_{10%} [°C]	T_{50%} [°C]	T_{100%} [°C]
0.2 wt% Pd/Al ₂ O ₃ SP	1	2%/10%/88%	325	430	535*

* The temperature when 98% of the methane has converted, T_{98%}.

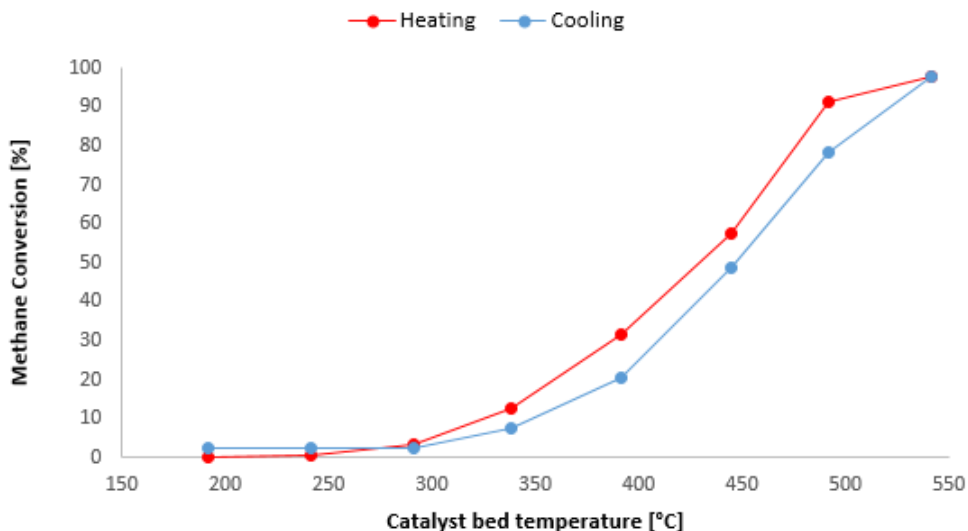


Figure 15: The methane converted (%) in the catalytic combustion of methane over the 0.2 wt% Pd/Al₂O₃ SP catalyst as a function of the catalyst bed temperature (°C) with a GHSV equal to 59400 NmL/g_{cat}h. The temperature was ramped for 5°C/min and the temperature was held for 30 minutes every 50 °C. The total molar flow is 200 NmL/min and the flow reactant feed CH₄/O₂/N₂ is 4/20/176 (2%/10%/88%) NmL/min. The red curve symbolizes when the reaction was heated up to 550 °C and the blue curve when it was cooled from 550 to 250 °C.

As explained in Section 2.6.7, deactivation of the catalyst can contribute to loss of active sites and consequently decrease in catalytic activity. The results of running the reactions in series using the same 0.2 wt% Pd/Al₂O₃ MT catalyst can be found in Table 9. When comparing the catalyst bed temperatures needed to achieve 10%, 50% and 100% methane conversion for a reaction tested under reference conditions, i.e. reaction no. 1 and 8, it is evident that the catalyst has lost activity. The first and last run achieved 100% combustion of methane at 541 °C and 624 °C, respectively. One theory is that the loss of active sites are due to palladium atoms migrate and collide with bigger crystallites, making bigger crystallites and fewer active sites. Another theory is that palladium is mostly active and thermodynamically stable as PdO, starting from 300 °C and up to 600 °C.[14] The results obtained in the present work are hence in agreement with other literature studies and evidenced that the Pd metal is reported to negatively affect the activity. It is discussed that palladium store a considerable amount of oxygen which contribute to increase activity towards combustion of methane.

An article by Carlsson et al. [18] on the influence of the gas composition changes on the methane conversion, suggested that lean conditions are beneficial and results in more active sites due to palladium crystallites undergo bulk oxidation. This is in line with the present observations where the A/F (Air/Fuel) ratio was altered between 5 and 10. The reactions ran under very oxygen rich conditions showed 100% methane conversion at lower catalyst bed temperatures, T_{100%}, than the A/F ratio equal to 5. In addition, it was observed that lowering the methane feed concentrations, in which is preferable according to MARINTEK, also lowered

the $T_{100\%}$. Although the data in Table 9 cannot be compared directly because they are run under different conditions, they do show that reaction number 3 with a $\text{CH}_4/\text{O}_2/\text{N}_2$ equal to 1%/10%/89% has the lowest $T_{100\%}$ equal to 539 °C. Reaction number 7, with a $\text{CH}_4/\text{O}_2/\text{N}_2$ equal to 0.5%/5%/94.5%, also showed low catalyst bed temperature, i.e. 549 °C, despite the catalyst was used four times in advance. Reaction number 3 and 7 both proceeded under lean-burn i.e. A/F ratio equal to 10 at low methane feed concentrations. The trend can also be seen in Figure 16. The ignition temperatures, $T_{100\%}$, are fairly similar but the light-off temperatures seem to be more dependent on the reaction conditions. The reactions ran with A/F-ratio equal to 10 and lower methane feed composition have lower $T_{50\%}$ and consequently steeper curves.

Table 9: The methane converted as a function of the catalyst bed temperature to achieve 10%, 50% and 100% converted methane, labelled $T_{10\%}$, $T_{50\%}$ and $T_{100\%}$, respectively. The catalyst, 0.2 wt% Pd/Al₂O₃ MT was ran in reaction series as described in Table 3. The reaction number corresponds to the reaction number and consequently reaction conditions described in the table. The fraction of the feed gas containing methane, oxygen and nitrogen is changed for each reaction and the total molar feed flow was kept constant equal to 200 NmL/min. The GHSV is calculated using the amount of fresh catalyst and is 58000 NmL/g_{cat}h.

Catalyst	Reaction no.	Fraction, F_i/F_{tot} $\text{CH}_4/\text{O}_2/\text{N}_2$	$T_{10\%}$ [°C]	$T_{50\%}$ [°C]	$T_{100\%}$ [°C]
0.2 wt% Pd/Al ₂ O ₃ MT	1	2%/10%/88%	299	382	541
	3	1%/10%/89%	324	409	539
	5	1%/5%/94%	356	425	567
	6	0.5%/2.5%/97%	323	386	551
	7	0.5%/5%/94.5%	359	438	549
	8	2%/10%/88%	378	470	624

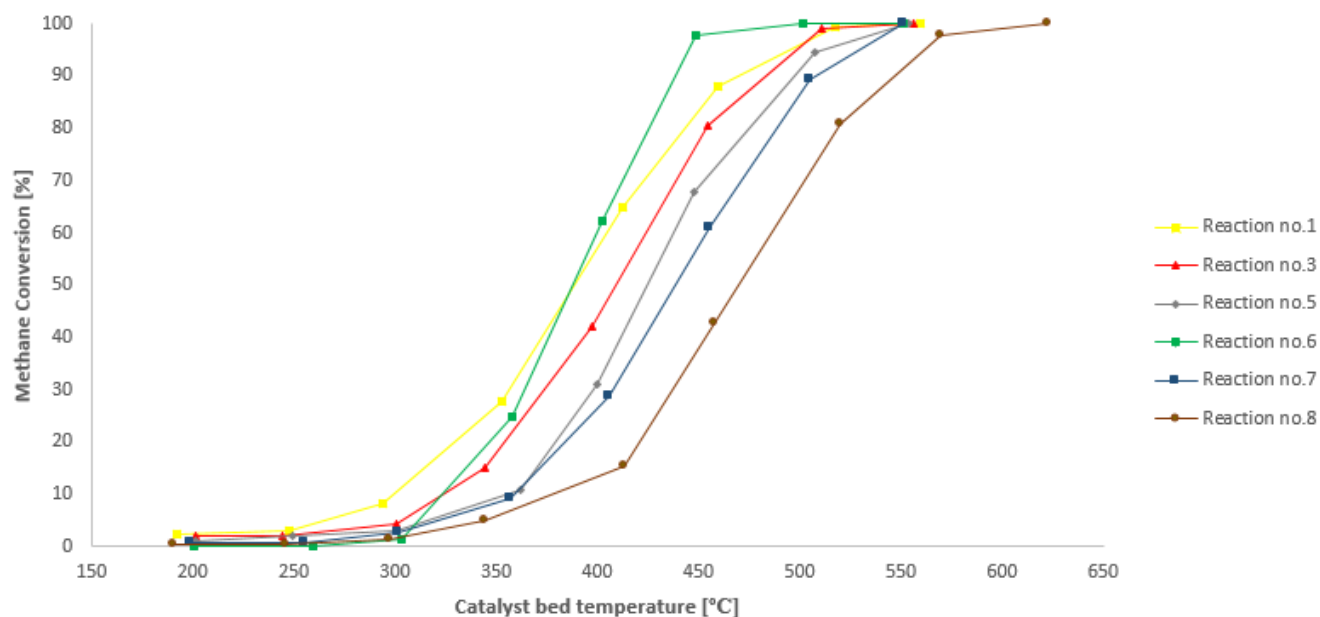


Figure 16: The methane converted (%) in the catalytic combustion of methane over the 0.2 wt% Pd/Al₂O₃ MT catalyst as a function of the catalyst bed temperature (°C) with a GHSV equal to 58000 NmL/g_{cat}h. The temperature was ramped for 5°C/min and the temperature was held for 20-30 minutes every 50 °C.

In order to study how the loading may affect the catalyst activity, a catalyst with 2.0 wt% palladium supported on alumina was prepared. The 2.0 wt% Pd/Al₂O₃ MT catalyst was studied for combustion of methane by alter the feed gas composition and deactivation by running the reactions in series. The catalyst was tested in series of reactions, i.e. reaction number 1 to 8 as described in Table 3. The results can be found in Table 10. In general, the temperatures were lower and all reactions achieved 100% methane conversion. Reaction number 1 achieved 100% conversion at 437 °C which is significantly lower than for the 0.2 wt% Pd/Al₂O₃ MT catalyst under the same conditions. It is most likely a consequence of more active sites being present on the catalyst surface. The results from the chemisorption experiments revealed that the metal surface area was significantly bigger and that the palladium was greatly dispersed on the support.

In order to study the catalyst deactivation, the 2.0 wt% Pd/Al₂O₃ MT catalyst was used when running the reaction under the same (reference) conditions, i.e. reaction number 1 and 2 in Table 10. An increase in T_{100%} by three degrees from reaction number 1 (437°C) to number 2 (440°C) indicates that the catalyst is slightly deactivated. It may be explained by a loss of catalytic area caused by such as water-induced sintering, despite Argyle et al. [49] suggest that sintering happens above 500 °C. The phenomena is probably more applicable explaining the deactivation occurring when using the catalysts with a 0.2 wt% palladium loading, due to the T_{100%} being above 500 degrees.

The ignition temperature is significantly higher for reaction number 2, which is not favourable.

The lower temperature, the lower the energy consumption in the methane slip abatement is needed.

The A/F ratio was adjusted hence the methane gas feed was decreased to achieve as low methane concentration as possible to meet the recommendations from MARINTEK at SINTEF of having methane slip containing small amounts of methane, such as 500-2000 ppm. By lowering the inlet methane concentration and increasing the A/F ratio to 10, the $T_{100\%}$ decreased significantly. The data in Table 10 cannot directly be compared due to that the reactions are run in series, but it is remarkable that by adjusting the O_2/CH_4 ratio from 5 to 10 in reaction number 2 and 3, the $T_{100\%}$ decreased by 22 degrees, using a spent catalyst. Throughout the catalytic run it is observed that the $T_{100\%}$ decreases as the methane inlet flow decreases and the lowest temperature where 100% of the methane is converted at 397 °C. That is 40 °C lower than the first reaction where a fresh catalyst was used. Conclusively, by increasing the A/F ratio to 10 and run the reaction in lean-burn i.e. $CH_4/O_2/N_2$ fraction equal to 0.5%/5%/94.5%, compared to the reference conditions that is equal to 2%/10%/88%, lower methane combustion temperatures are achieved, which is preferable. The results are in line with what Carlsson et al.[18] reported on the effect of oxygen to Pd/Al₂O₃ in a methane oxidation reaction, as described in an earlier section.

Due to limitations of the MFCs, a gas bottle containing diluted methane (5% in N₂) was installed to achieve lower methane inlet concentrations. A fresh 2.0 wt% Pd/Al₂O₃ MT catalyst was placed in the reactor, resulting in a $T_{100\%}$ equal to 340 °C when the gas inlet composition $CH_4/O_2/N_2$ was equal to 0.1%/0.5%/98.9% (reaction number 9 in Table 10). Upon further oxygen excess by increasing the A/F ratio from 5 to 10 (reaction number 10), the catalyst's activity increases and 100% conversion of methane was achieved at 317 °C (marked red in the table). The results suggest that the palladium particles are more active in an oxygen rich environment, i.e. lean burn and it may correspond to bulk oxidation of the Pd particles becoming more active.

Table 10: The methane converted as a function of the catalyst bed temperature to achieve 10%, 50% and 100% converted methane, labelled $T_{10\%}$, $T_{50\%}$ and $T_{100\%}$, respectively. The catalyst, 2.0 wt% Pd/Al₂O₃ MT was ran in reaction series as described in Table 3. The reaction number corresponds to the reaction number and consequently reaction conditions described in the table. The total molar feed flow is constant equal to 200 NmL/min. The fraction of the feed gas containing methane, oxygen and nitrogen is changed for each reaction. The GHSVs are calculated using the amount of fresh catalyst and the calculations can be found in Appendix M.

Catalyst	Reaction no.	Fraction, F_i/F_{tot} CH₄/O₂/N₂	GHSV [NmL/g_{cat}h]	T_{10%} [°C]	T_{50%} [°C]	T_{100%} [°C]
2.0 wt% Pd/Al ₂ O ₃ MT	1	2%/10%/88%	58800	302	362	437
	2	2%/10%/88%		363	326	440
	3	1%/10%/89%		271	327	418
	4	2%/10%/88%		259	327	436
	5	1%/5%/94%		288	336	420
	6	0.5%/2.5%/97%		299	388	401
	7	0.5%/5%/94.5%		277	324	397
	8	2%/10%/88%		250	320	469
2.0 wt% Pd/Al ₂ O ₃ MT	9	0.1%/0.5%/99.4%	59400	269	304	340
	10	0.1%/1%/98.9%		224	276	317

The combustion curves when testing the 2.0 wt% Pd/Al₂O₃ MT catalyst can be found in Figure 17. The ignition and light-off temperatures of the reactions ran with an A/F-ratio equal to 10 are much lower and consequently the curves are much steeper. Also, the reactions achieve 100% methane conversion at much lower temperatures. As the reactions are ran in series, it is clearly that the steepness of the curves decreases as the catalyst are tested under different conditions. The resulting heating and cooling curves for each reaction can be found in Appendix N.3. The catalyst's ignition temperature should be close to the temperature of the outlet of the burned LNG in the marine machinery and minimal pressure drop.[56] To get even more correct conversion data more temperature measurements should be done at shorter temperature intervals. The analysis time with temperature measurements for each reaction took one to two days and therefore measurements thought to be within the most critical phases were prioritized to analyse. It was needed to be present at the lab to measure the actual temperature throughout the catalyst bed.

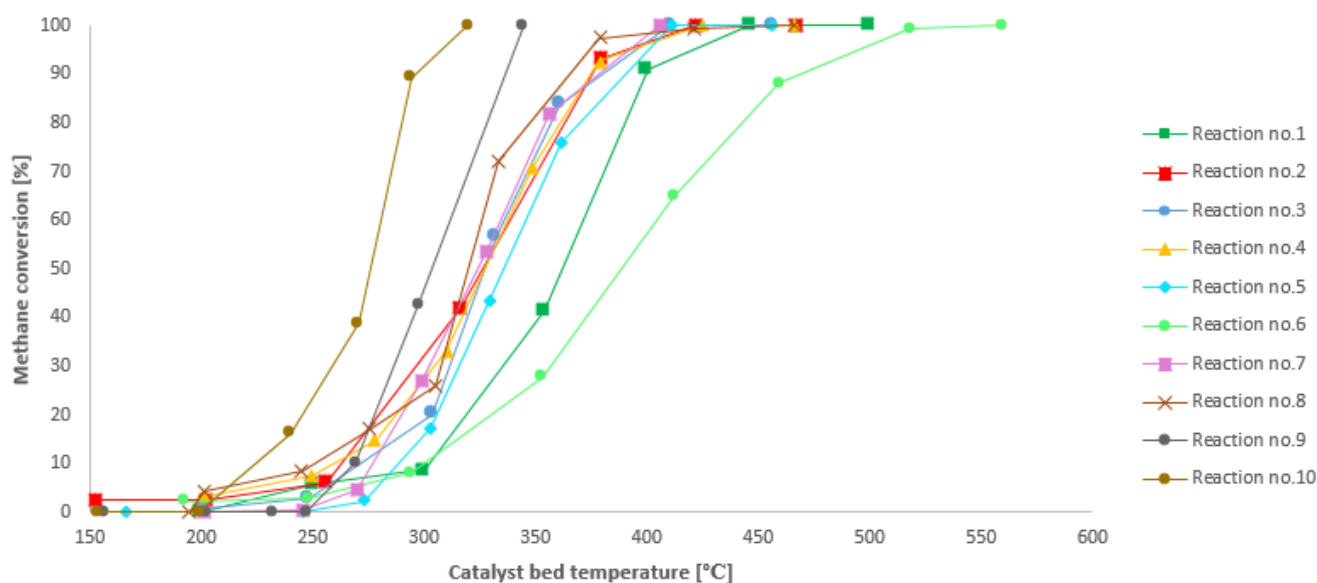


Figure 17: The methane converted (%) in the catalytic combustion of methane over the 0.2 wt% Pd/Al₂O₃ MT catalyst as a function of the catalyst bed temperature (°C) with a GHSV equal to 58800 NmL/g_{cat}·h for reaction number 1 to 8 and 59400 NmL/g_{cat}·h for reaction number 9 and 10, as described in Table 3. The temperature was ramped for 5°C/min and the temperature was held for 20-30 minutes every 50 °C.

As mentioned, the GC is thought to give reasonable data, and no CO is detected in any of the runs when testing the Pd/Al₂O₃ catalysts and 100% of the methane was converted in each reaction, i.e. the amount of methane into the reactor is equal to the amount of carbon dioxide out of the reactor, the selectivity of CO₂ is 100% for each reaction.

An increase in metal loading increases the number of active sites, thus the activity, if the active sites are available. The results show a clearly increase in activity when increasing the loading. The T_{100%} has decreased from 624 °C to 317 °C for the reaction with the lowest to the reaction with the highest activity, respectively, when increasing the loading. The obtained data reveal that the 2.0 wt% Pd/Al₂O₃ MT catalyst has the highest activity for combustion of methane when comparing it to the catalysts with lower loading, i.e. 0.2 wt% Pd/Al₂O₃. The results obtained when testing the 2.0 wt% Pd/Al₂O₃ MT catalyst was good and it performed well below the temperature limit MARINTEK has recommended.[4] However, the costs of using a loading of 2.0 instead of 0.2 wt% palladium have to be considered. Palladium is an expensive metal and increasing the loading increases the expenses. The benefits and drawbacks of increasing the loading must be measured against each other, such as the benefits of increasing the loading gives higher activity but the life-time of the catalyst is limited as the catalyst is deactivated when running the reactions in series. An economic evaluation is not included in this work. The purpose of this work is to evaluate the catalysts that consist of pure metal, where the results are later being used as reference to further analyses using palladium based catalysts mixed with other metals, such as nickel, or catalysts containing small or no amount of

palladium.

Sintering is a possible explanation for the activity loss when running the reactions in series. Several techniques could reveal the extent of the sintering, such as chemisorption, Transmission Electron Microscope (TEM) and X-Ray Powder Diffraction (XRDP). TEM could be used on the spent catalyst to get visual pictures of the dispersion of the active metal on the support surface. An increase in the particle size could indicate sintering and chemisorption experiments or comprehensive X-Ray Powder Diffraction (XRDP) of the used catalysts could reveal that. A comparison of the decrease in dispersion of the spent catalyst due to sintering and the observed deactivation, could give indication of other deactivation mechanisms co-exist.

The catalysts used for this thesis are mixed with SiC, making it harder to analyse the spent catalysts. An idea could be to run the reactions using only the catalysts. Also, a XRD analysis should be performed on the spent catalyst to find out if the activity loss could be prescribed to a phase transformation from γ -alumina to α or δ , as described in Section 2.2 and 2.5.4.

The reaction mechanisms and the reaction rates are not included in this work, and consequently the turnover frequency is not calculated. The turnover frequency could have given an indication of the catalyst activity. The reaction rates must be measured under correct conditions.

5 Conclusions

The main objective of the study was to investigate whether catalytic oxidation of methane using palladium supported catalysts is a good alternative to oxidise the methane exhaust from the high-temperature burning of methane, which produces noxious by-products, to improve the methane slip abatement. The engines working today can achieve very low NO_x -emissions, but the exhaust gas will contain small amounts of methane. The catalysts used should have great activity at appropriate reaction conditions, such as low temperature and low inlet methane concentrations. The expensive catalysts are meant to be used as references to cheaper palladium based catalysts using a mix of other metals, such as nickel, or catalysts containing small or none palladium.

Three catalysts, 0.2 wt% Pd/ Al_2O_3 SP, 0.2 wt% Pd/ Al_2O_3 MT and 2.0 wt% Pd/ Al_2O_3 MT, were made using the incipient wetness impregnation and characterized using Nitrogen Adsorption, X-Ray Fluorescence, Chemisorption with H_2 and CO, X-Ray Diffraction and Thermogravimetric Analysis. Their catalytic activities were also tested for methane oxidation by altering the reaction conditions such as feed composition and making catalysts with different loadings. The extent of deactivation was also studied by letting the reactions run in series without replacing the catalyst.

The BET showed a decreasing BET areas and pore volumes of the supported catalysts, compared to alumina. It also showed that the particles are of mesoporous material. Chemisorption experiments were performed using hydrogen and carbon monoxide gas. The results from the H_2 -chemisorption suggests that hydrogen is not being strongly bound to the surface and that hydrogen can dissolve in Pd and diffuse through palladium. It is discussed whether hydrogen dissolves in palladium or not, and it promoted doing chemisorption using CO. The dispersion of palladium atoms on the γ -alumina increased with decreasing palladium loading. The relatively high dispersion results can be a cause of impregnation method being good enough to deposit active metal on the surface. It is also concluded that CO-chemisorption gives more reliable results.

The XRD and XRF experiments did not show any impurities, indicating that the preparation conditions were good enough to remove organic and nitrate compounds.

The activities were compared by the temperature where 100% methane was converted, $T_{100\%}$, because the reaction is extremely exothermic and irreversible. Low temperatures are favourable. By running the reaction under reference conditions with a total molar feed flow constant equal to 200 NmL/min and a methane/oxygen/nitrogen feed composition equal to 2%/10%/88%, the catalysts achieved 100% conversion at 535 °C (only 98% conversion), 541 °C and 437 °C for the 0.2 wt% Pd/ Al_2O_3 SP, 0.2 wt% Pd/ Al_2O_3 MT and 2.0 wt% Pd/ Al_2O_3 MT catalyst, respectively. In general, the catalyst with the highest loading performed the best

with an A/F-ratio equal to 10 and low inlet methane concentration. A constant total feed flow equal to 200 NmL/min and feed composition equal to 0.1%/1%/98.9% under oxygen rich environment and a used catalyst, $T_{100\%}$ was equal to 317 °C. The methane concentration is within the concentration limits recommended by MARINTEK, i.e. 500-2000 ppm. The TGA results strongly suggest that the palladium is carrying a lot of oxygen and will especially in an oxygen rich environment contribute to an increased activity. It is suggested that the bulk-oxygen become more active under these conditions. All the catalysts made for the Master's Thesis achieved 100% conversion and selectivity at relatively low temperatures. The ignition temperatures, $T_{10\%}$, are low, which is favourable to save energy in the process. The temperature should almost be at the same temperatures as the outlet temperature of the high temperature burning of methane in the marine machinery.

The activity loss due to catalyst deactivation can be observed by the increasing temperatures when running the reactions in series. In general, the temperature increases for each run, indicating that the catalyst is deactivated and the observed activity loss may be related to sintering of palladium crystallites.

6 Suggestions for further work

The cause of the deactivation when running the reactions in series can be investigated further by studying the spent catalyst. Sintering can be one explanation of it. Several techniques could reveal the extent of the sintering, such as chemisorption, Transmission Electron Microscopy and X-Ray Powder Diffraction. Chemisorption experiments of the spent catalyst could have given data on the dispersion change. A decrease in dispersion and increase in particle size could indicate sintering. Also, using TEM to get visual pictures and XRDP to see if the support has undergone a phase transformation, could also reveal the reasons for deactivation. A comparison of the decrease in dispersion of the spent catalyst due to sintering and the observed deactivation, could give indication of other deactivation mechanisms co-exist. There are still work to overcome when it comes to pressure drop. The experiments were performed using a mix of the catalyst and SiC, making it hard to analyse the spent catalysts. Also, Temperature Programmed Reduction experiments could be performed to reveal the reduction temperature of PdO, which could be used to explain the catalyst activity. The TPR-apparatus was mostly broken and therefore not available for experiments during the spring 2016.

The uncertainty in whether the hydrogen dissolves in palladium or not promotes to do TEM analysis to get visual pictures of the dispersions and compare it to the chemisorption results. Having reliable chemisorption data is important when evaluating the preparation method and if it is good enough to disperse the active sites on the support.

The results showed increasing activity by increasing the palladium loading. Catalysts with higher loadings can be prepared to achieve 100% methane conversion at lower temperatures. However, by increasing the loading and the expensive palladium the costs also increase and it must be evaluated against the cons. Experiments using catalysts with promoters, such as alkaline metals, could be performed to increase the activity with lower palladium loading or a mix with cheaper metals. These results can be used as reference catalysts.

Other feed conditions, such as using wet feed, can experimentally reveal the sensitivity of the catalyst towards water. Also, altering the space velocities by adding more catalyst to the reactor bed or additional study on the catalyst effect of feed compositions, can be performed. A repetition of the experiments should also be done, to strengthen the reliability of the results.

Sintering has been postulated as a cause of deactivation and a long-term deactivation experiment should be done to study the catalysts' activities over a long period of time. A such experiment could give a better understanding on the catalysts' behaviours during methane oxidation on an industrial level. The activity loss due to catalyst deactivation is observed, still, the cause and the mechanism are not clear and further studies are necessary to reveal it.

References

- [1] J. Chen, H. Arandiyana, X. Gao, J. Li. *Recent Advances in Catalysts for Methane Combustion*. Springer Science & Business Media, New York, 2015.
- [2] L.S. Escandòn, S. Ordòñez, A. Vega, F. V. Díez. *Oxidation of methane over palladium catalysts: effect of the support*. Chemosphere, Vol. 58, pages 9-17, 2005.
- [3] U.S. Environmental Protection Agency. *Technical Bulletin- Nitrogen Oxides(NO_x), why and how they are controlled*. U.S. EPA, 1999.
- [4] Inside information from the Norwegian Marine Technology Research Institute (MARINTEK) part of the SINTEF Group.
- [5] J.A.Z. Pieterse, R.W. van den Brink, S. Boonevald, H. Top, J.E. Westing, F. Vollink, K. Hoving. *Selective catalytic reduction of NO_x in real exhaust gas of gas engines using unburned gas*. Chemical Engineering Journal, 2005.
- [6] L. Guzzi, A. Erdòhelyi. *Catalysis for Alternative energy Generation*. Springer Science & Business Media, 2012.
- [7] C. L. Fevre, M. Madden, N. White. *LNG in Transportation*. CEDIGAZ, 2014.
- [8] I. Chorkendorff, J. W. Niemantsverdriet. *Concepts of Modern Catalysis and Kinetics*. Wiley-VCH, Weinheim, 2007.
- [9] J. Bolstad. *Process Intensification of the Fischer- Tropsch Synthesis*. NTNU, 2014.
- [10] Krijn P. de Jong. *Synthesis of Solid Catalysts*. Wiley-VCH, Weinheim, 2009.
- [11] Specialization Course TKP 4515 Catalysis and Petrochemistry fall 2015 at NTNU held by Professor Hilde Venvik in Catalytic Combustion.
- [12] M.L. Toebes, J.A. van Dillen, K.P. de Jong. *Synthesis of supported palladium catalysts*. Journal of Molecular Catalysis A: Chemical, Vol. 173, pages 75-98, 2001.
- [13] P. Albers, J. Pietsch, S. Parker. *Poisoning and deactivation of palladium catalysts*. Journal of Molecular Catalysis A: Vol. 173, pages 275-286, 2001.
- [14] P. Gèlin. *Catalytic complete oxidation of methane at low temperatures*. Topsøe Catalysis Forum, 2009.

- [15] B.C. Enger, R. Lødeng, A. Holmen. *A review of catalytic partial oxidation of methane to synthesis gas with emphasis on reaction mechanisms over transition metal catalysts*. Applied Catalysis A: General, Vol. 346, pages 1-27, 2008.
- [16] N.J. Schoenfeldt. *Synthesis and Characterization of Gamma-alumina Supported Manganese Oxides Prepared by Grafting and Impregnation for Applications in Heterogeneous Catalysis*. Proquest LLC, 2009.
- [17] University of Groningen. *γ-alumina unit cell*. [Internet]. Available from: <http://www.rug.nl/research/portal/files/9818571/appendix.pdf> (page 106)(read November 5. 2015)
- [18] P.A. Carlsson, E. Fridell, M. Skoglundh. *Methane oxidation over Pt/Al₂O₃ and Pd/Al₂O₃ catalysts under transient conditions*. Catalysts Letters, Vol. 115, 2007.
- [19] K.H. Stern. *High Temperature Properties and Decomposition of Inorganic Salts Part 3. Nitrates and Nitrites*. Electrochemistry Branch, Naval Research Laboratory, Washington D.C. 20390.
- [20] Norwegian language encyclopedia *Definition of Calcination*. [Internet]. Available from: <https://snl.no/kalsinering> (read October 10. 2015)
- [21] J. L. Figueiredo, M. M. Pereira, J. Faria. *Catalysis from Theory to Application*, pages 89-93. COIMBRA, 2008.
- [22] J.M. Thomas, W.J. Thomas. *Principles and Practice of Heterogeneous Catalysis*, page 300. Wiley-VCH, Weinheim, 2014.
- [23] XRF Procedure written June 29. 2015 by Cristian Ledesma at the Department of Chemical Engineering an NTNU.
- [24] R. Jenkins. *Quantitative X-Ray Spectrometry*. CRC Press, 1995.
- [25] SERC-the Science Education Resource Center at Carleton College. *X-Ray Fluorescence*. [Internet]. Available from: http://serc.carleton.edu/research_education/geochemsheets/techniques/XRF.html (read October 22. 2015)
- [26] Z. Paàl, P.G. Menon. *Hydrogen effects in Catalysis: Fundamentals and Practical Application*. Marcel Dekker, Inc, New York, 1988.
- [27] HSE lectures in the course TKP 4510 Catalysis and Petrochemistry at the Norwegian University of Science and Technology fall 2015.

- [28] Anders Holmen. *Heterogen Katalyse*. Institutt for kjemisk prosess teknologi, NTNU, 2002.
- [29] J. B. Butt, E. E. Petersen *Activation, Deactivation, and Poisoning of Catalysts*. Academic Press, Inc., 1988.
- [30] National Programme on Technology Enhanced Learning- A project funded by MHRD, Government of India. *CO-chemisorption*. [Internet]. Available from: <http://nptel.ac.in/courses/103103026/14> (read May 9. 2016)
- [31] J.W. Niemantsverdriet. *Spectroscopy in Catalysis: An Introduction, pages 9-19*. John Wiley & Sons, 2008.
- [32] B. Wang, L. Si, Y. Yuan, Y. Li, L. Chen, X. Yan. *Reductive cyclization of 2-nitro-2'-hydroxy-5'-methylazobenzene to benzotriazole over K-doped Pd/Al₂O₃*. Royal Society Using Hydrogen, Springer, 2000.
- [33] O. Braaten, A. Kjekshus, H. Kvande. *The Possible Reduction of Alumina to Aluminum Using Hydrogen*. Springer, 2000.
- [34] A. Saha, 2008. Synthesis and Characterization of Grafted Vanadium and Co-grafted Vanadium/zirconium Mixed Oxides on Gamma-alumina Surface.
- [35] SERC-the Science Education Resource Center at Carleton College *X-Ray Diffraction*. [Internet]. Available from: http://serc.carleton.edu/research_education/geochemsheets/techniques/SXD.html (read October 19. 2015)
- [36] University of Delaware *Illustration of X-Ray Diffraction, page 2*. [Internet]. Available from: <http://www.physics.udel.edu/~yji/PHYS624/Chapter3.pdf> (read February 23. 2016)
- [37] Wikipedia- The Free Encyclopedia. *Powder X-Ray Diffraction*. [Internet]. Available from: https://en.wikipedia.org/wiki/Powder_diffraction (read May 28. 2016)
- [38] B.H. Stuart. *Polymer Analysis, pages 201-206*. John Wiley & Sons, 2002.
- [39] R. Chen, S.W.S. McKeever. *Theory of Thermoluminescence and Related Phenomena, page 375*. World Scientific, 1997.
- [40] Perkin Elmer- For the Better. *TGA apparatus*. [Internet]. Available from: http://www.perkinelmer.com/CMSResources/Images/44-74556GDE_TGABeginnersGuide.pdf (read November 4. 2015)

- [41] H. Silla. *Chemical Process Engineering- Design and Economics*, page 348. CRC Press, 2003.
- [42] C.F. Poole. *Gas Chromatography*. Elsevier, 2012.
- [43] W. Boyes. *Instrumentation Reference Book*. Butterworth-Heinemann, 2009.
- [44] G. Guiochon, C.L. Guillemin. *Quantitative Gas Chromatography for Laboratory Analyses and On-Line Process Control*. Elsevier, 1988.
- [45] J.R. Couper, W. R. Penney, J.R. Fair. *Chemical Process Equipment revised 2E: Selection and Design*, page 581. Gulf Professional Publishing, 2009.
- [46] E.B. Nauman. *Chemical Reactor Design, Optimization and Scaleup*, page 535. Wiley Publications, 2008.
- [47] Wikipedia- The Free Encyclopedia. *Residence Time*. [Internet]. Available from: https://en.wikipedia.org/wiki/Residence_time (read May 5. 2016)
- [48] R. Gholami, M. Alyani, K.J. Smith. *Deactivation of Pd Catalysts by Water during Low Temperature Methane Oxidation Relevant to Natural Gas Vehicle Converters*. MDPI- Multidisciplinary Digital Publishing Institute, 2015.
- [49] M.D.Argyle, C.H. Bartholomew. *Heterogeneous Catalyst Deactivation and Regeneration*. MDPI- Multidisciplinary Digital Publishing Insitute, 2015.
- [50] Matheson-The Gas ProfessionalsTM. *Lower and Upper Explosive Limits for Flammable Gases and Vapors*. [Internet]. Available from: [https://www.mathesongas.com/pdfs/products/Lower-\(LEL\)-&-Upper-\(UEL\)-Explosive-Limits-.pdf](https://www.mathesongas.com/pdfs/products/Lower-(LEL)-&-Upper-(UEL)-Explosive-Limits-.pdf) (March 31. 2016)
- [51] Seniro Scientist Rune Lødeng (SINTEF). *MFC gas correction factors*.
- [52] Y. H. Tan, J.A. Davis, K. Fujikawa, N.V. Ganesh, A.V. Demchenko, K.J. Stine. *Surface area and pore size characteristics of nanoporous gold subjected to thermal, mechanical, or surface modification studied using gas adsorption isotherms, cyclic voltammetry, thermogravimetric analysis, and scanning electron microscopy*. J Mater Chem pages 6733-6745, 2012.
- [53] E. W. Shin, S.II Cho, J. H. Kang, W.J. Kim, J.D. Parkm S.H. Moon. *Palladium-hydrogen interaction on supported palladium catalysts of different metal dispersions*. Korean Journal of Chemical Engineering, Vol. 17, Issue 4, p 468-472, 2000.

- [54] S. Rane, Ø. Borg, J. Yang, E. Rytter, A. Holmen. *Effect of alumina phases on hydrocarbon selectivity in Fischer-Tropsch synthesis*. Appl. Catal. A Vol. 388, pages 160-167, 2010.
- [55] p. McKinney. *The Adsorption of Gases on Palladium Oxide*. Journal of the American Chemical Society, 1933.
- [?] Lectures in the use of the XRD-apparatus held by Kristin Høydalsvik at the Department of Materials Science and Engineering at NTNU.
- [56] G. Zhu. *Kinetics of Complete Methane Oxidation on Palladium Model Catalysts*. Doctoral Thesis, Worcester Polytechnic Institute, 2004.
- [57] NIST Chemistry WebBook *Physical Properties*. [Internet]. Available from: webbook.nist.gov/

A Risk assessment

15.09.2015 Side 1 av 2

M:\Prosjekt\Risk assesment- Final.xlsx

NTNU		Hazardous activity identification process		Prepared by		Date			
				HSE section		HMSRV2501		22.03.2011	
				Approved by		Page		Replaces	
HSE				The Rector		01.12.2006			

Unit: (Institute) Department for Chemical Engine **Date:** 07.09.2015

Line manager: (responsible supervisor) Hilde Venvik

Participants in the identification process (incl. function): Hilde Venvik (supervisor), Rune Lødeng (co-supervisor), Jia Yang (PhD stipendiat), Helene Sandvik

Short description of the main activity/main process: Synthesis of supported Palladium catalyst


Signatures: *Hilde Venvik*

ID nr.	Activity/process	Responsible person	Existing documentation	Existing safety measures	Laws, regulations etc.	Comment
1	Assembling/ use of flammable gas CH ₄ , H ₂	Hilde Venvik	safety data sheet no number (C4H10O) YPX078A (CH ₄)	Leak testing, goggles, gloves, lab coat, local- and room gas detector	HSE-regulations, Arbeidsmiljøloven	Changing of gas bottles is done within the working hours and has to be done by the staff.
2	Use of high temperature calcination furnace	Hilde Venvik	Apparatus card	Sensors and control systems for the temperature, gloves, maintenance, goggles, lab coat	HSE-regulations, Arbeidsmiljøloven	
3	Assembling/ use of inert and non-toxic gases. N ₂ , Ar, He, CO ₂	Hilde Venvik	safety data sheet.	Leak testing, goggles	HSE-regulations, Arbeidsmiljøloven	Changing of gas bottles is done within the working hours and has to be done by the staff.
4	Assembling/use of toxic salt Pd(NO ₃) ₂	Hilde Venvik	safety data sheet. No number	Leak testing, goggles, gloves, lab coat, dust mask	HSE-regulations, Arbeidsmiljøloven	Dust mask
5	Cleaning of equipment acetone/ethanol	Hilde Venvik	safety data sheet. No number	goggles, gloves, lab coat	HSE-regulations, Arbeidsmiljøloven	
6	Use of gamma-alumina	Hilde Venvik	safety data sheet.	goggles, gloves, lab coat, dust mask	HSE-regulations, Arbeidsmiljøloven	Be careful not to breath in the powder.

Figure 18: The risk evaluation due to the experimental work done, including synthesis, characterization and testing of the catalysts for methane oxidation under application relevant conditions.

NTNU	Risk assessment			Prepared by	Number	Date
				HSE section	HMSRV2603	04.02.2011
HMS /KS				Approved by	Page	Replaces
				The Rector		09.02.2010



Unit: *(Institute)* _____
Line manager: *(responsible supervisor)* Hilde Venvik
Participants in the identification process (incl. function): Hilde Venvik (supervisor), Rune Lødeng (co-supervisor), Jia Yang (PhD supervisor, student, co-supervisor, others)
Risk assessment of: Synthesis of supported Palladium catalyst
Signaturer: 

ID nr.	Activity from the identification process form	Potential undesirable incident/strain	Likelihood: (1-5)	Consequence:			Risk value (human)	Comments/status Suggested measures
				Human (A-E)	Environment (A-E)	Economy/material (A-E)		
1	Assembling/ use of flammable gas CH ₄ , H ₂	1) leakage 2) fire	1) 3 2) 1	1) A 2) D	1) A 2) D	1) A 2) D	1) A3 2) D1	
2	Use of high temperature calcination furnace	1) skin burned 2) fire	1) 3 2) 1	1) A 2) D	1) A 2) D	1) A 2) D	1) A3 2) D1	
3	Assembling/ use of inert and non-toxic gases. N ₂ , Ar, He, CO ₂	1) leakage 2) explosion	1) 3 2) 1	1) B 2) E	1) A 2) D	1) A 2) E	1) A3 2) E1	
4	Assembling/use of toxic salt Pd(NO ₃) ₂	1) Spill 2) sensitization 3) burns	1) 3 2) 3 3) 2	1) B 2) A 3) A	1) D 2) A 3) A	1) A 2) A 3) A	1) B3 2) A3 3) A2	Dust mask
5	Cleaning of equipment acetone/ethanol	1) Spill 2) fire	1) 4 2) 1	1) A 2) D	1) A 2) D	1) A 2) D	1) A4 2) D1	
6	Use of gamma-alumina	1) spill	1) 3	1) A	1) D	1) A	1) A3	Dust mask

Figure 19: The risk evaluation due to the experimental work done, including synthesis, characterization and testing of the catalysts for methane oxidation under application relevant conditions and the likelihoods and consequences of potential accidents.

B Calculation of amount of $\text{Pd}(\text{NO}_3)_2 \times \text{H}_2\text{O}$ used

Two catalysts with 0.2 weight% palladium supported on 10 g of alumina were made. The following calculations are made to find the mass of $\text{Pd}(\text{NO}_3)_2 \cdot 2\text{H}_2\text{O}$ to use in the preparation of the catalysts. The molecular weight of $\text{Pd}(\text{NO}_3)_2 \cdot 2\text{H}_2\text{O}$ and Pd are 230.43 g/mol and 106.4 g/mol, respectively.[57] The amount of palladium is:

$$\frac{0.2 \text{ g Pd}}{100 \text{ g Al}_2\text{O}_3} \cdot 10 \text{ g Al}_2\text{O}_3 = 0.02 \text{ g Pd} \quad (23)$$

The number of moles of palladium is as follows:

$$n(\text{Pd}) = \frac{m(\text{Pd})}{Mm(\text{Pd})} = \frac{0.02 \text{ g}}{106.4 \text{ g/mol}} = 1.88 \cdot 10^{-4} \text{ moles} \quad (24)$$

The stoichiometric relationship between Pd and $\text{Pd}(\text{NO}_3)_2 \cdot 2\text{H}_2\text{O}$ is 1:1, and therefore the number of moles of palladium equals the number of moles of the salt, thus the amount of salt needed is:

$$m(\text{Pd}(\text{NO}_3)_2 \cdot 2\text{H}_2\text{O}) = 230.43 \text{ g/mol} \cdot 1.88 \cdot 10^{-4} \text{ moles} = 0.0433 \text{ g} \quad (25)$$

A catalyst with 2.0 weight% palladium supported on 7 g of alumina was also made. The following calculations was made to find the mass of $\text{Pd}(\text{NO}_3)_2 \cdot 2\text{H}_2\text{O}$ to use in the preparation of the catalyst. The amount of palladium is:

$$\frac{2.0 \text{ g Pd}}{100 \text{ g Al}_2\text{O}_3} \cdot 7 \text{ g Al}_2\text{O}_3 = 0.14 \text{ g Pd} \quad (26)$$

$$n(\text{Pd}) = \frac{m(\text{Pd})}{Mm(\text{Pd})} = \frac{0.14 \text{ g}}{106.4 \text{ g/mol}} = 1.32 \cdot 10^{-3} \text{ moles} \quad (27)$$

By using the same stoichiometric approach as above, the amount of salt needed is 0.3032 g.

C Calculation of the amount of water needed

The amount of water needed for the incipient wetness impregnation preparation is found by dripping water to 5 g of support, until it was saturated. The weight of the support was measured before and after wetness, to find the weight of water needed. The water weight was found to be:

$$11.0250 \text{ g} - 4.9964 \text{ g} = 6.0286 \text{ g} \quad (28)$$

The relationship between the water and support weight is found to be:

$$\frac{6.0286 \text{ g water}}{4.9964 \text{ g support}} = 1.2066 \text{ g water/g support} \quad (29)$$

The amount of water needed for 10 g of support:

$$10 \text{ g support} \cdot 1.2066 \text{ g water/g support} = 12.0659 \text{ g water} \quad (30)$$

The amount of water needed for 7 g of support is 8.4462 g water.

D Exact catalyst mass used for the experiments

The exact catalyst mass used for the experiments using the following techniques: Nitrogen Adsorption, X-Ray Fluorescence, Chemisorption with H₂ and CO, Temperature Programmed Reduction and Thermogravimetric Analysis. The exact compound weights used for testing the catalysts in methane oxidation reaction can be found in Table D.5.

D.1 Nitrogen Adsorption

Table 11: The exact weights of the 0.2 wt% Pd/Al₂O₃ SP, 0.2 wt% Pd/Al₂O₃ MT and 2.0 wt% Pd/Al₂O₃ MT catalysts and the support used for Nitrogen Adsorption.

Catalyst	Experiment no.	Mass [g]
0.2 wt% Pd/Al ₂ O ₃ SP	1	0.0902
0.2 wt% Pd/Al ₂ O ₃ MT	1	0.0850
	2	0.0747
2.0 wt% Pd/Al ₂ O ₃ MT	1	0.0928
	2	0.0756
Al ₂ O ₃	1	0.0760

D.2 X-Ray Fluorescence

Table 12: The exact weights of the 0.2 wt% Pd/Al₂O₃ SP, 0.2 wt% Pd/Al₂O₃ MT and 2.0 wt% Pd/Al₂O₃ MT catalysts, support and boric acid (binder) used for X-Ray Fluorescence. SP and MT symbolize the palladium supported catalysts made for the Specialization Project and Master's Thesis, respectively.

Catalyst	Mass of catalyst [g]	Mass of boric acid [g]	Total mass [g]
0.2 wt% Pd/Al ₂ O ₃ SP	0.1994	2.7932	2.993
0.2 wt% Pd/Al ₂ O ₃ MT	0.2122	2.7970	3.009
2.0 wt% Pd/Al ₂ O ₃ MT	0.1932	2.8355	3.029
Al ₂ O ₃	0.2174	2.8559	3.073

D.3 Chemisorption

Table 13: The exact weights of the 0.2 wt% Pd/Al₂O₃ SP, 0.2 wt% Pd/Al₂O₃ MT and 2.0 wt% Pd/Al₂O₃ MT catalysts used for H₂- and CO-chemisorption. SP and MT symbolize the palladium supported catalysts made for the Specialization Project and Master's Thesis, respectively.

Catalyst	Experiment no.	Mass of catalyst used for H ₂ [g]	Mass of catalyst used for CO [g]
0.2 wt% Pd/Al ₂ O ₃ SP	1	0.1473	0.1385
	2	0.1443	0.1450
0.2 wt% Pd/Al ₂ O ₃ MT	1		0.1433
	2		0.1515
2.0 wt% Pd/Al ₂ O ₃ MT	1		0.1647
	2		0.1396

D.4 Thermogravimetric Analysis

Table 14: The exact weight of the 2.0 wt% Pd/Al₂O₃ MT catalyst used for Thermogravimetric Analysis. MT symbolize the palladium supported catalysts made for the Master's Thesis.

Catalyst	Mass of catalyst [mg]
2.0 wt% Pd/Al ₂ O ₃ MT	19.7

D.5 Catalyst Testing

Table 15: The exact weights of the 0.2 wt% Pd/Al₂O₃ SP, 0.2 wt% Pd/Al₂O₃ MT and 2.0 wt% Pd/Al₂O₃ MT catalysts and silica carbide used for the methane oxidation testing. SP and MT symbolize the catalysts made for the Specialization Project and Master's Thesis, respectively.

Catalyst	Experiment no.	Mass of catalyst used [g]	Mass of silica carbide used [g]
0.2 wt% Pd/Al ₂ O ₃ SP	1	0.2020	1.9924
0.2 wt% Pd/Al ₂ O ₃ MT	1	0.2070	1.9803
2.0 wt% Pd/Al ₂ O ₃ MT	1	0.2040	2.0014
	2	0.2021	1.9931

E H₂-Chemisorption results using the 2nd isotherm

The results of the H₂-chemisorption shown using the amount of gas chemisorbed, only.

Table 16: The physical-chemical properties of the 0.2 wt% Pd/Al₂O₃ SP catalyst prepared during the Specialization Project during fall 2015 found by H₂ chemisorption. Chemisorption was performed two times. The results are shown for the chemisorbed amount, only. The analysis conditions are found in Table 1.

Experiment no.	Dispersion [%]	Crystallite Size [nm]	Metal surface area [m²_{metal}/g_{cat}]
1	-14	-8.2	-0.12
2	23	4.8	0.21

F Pore Size Distribution

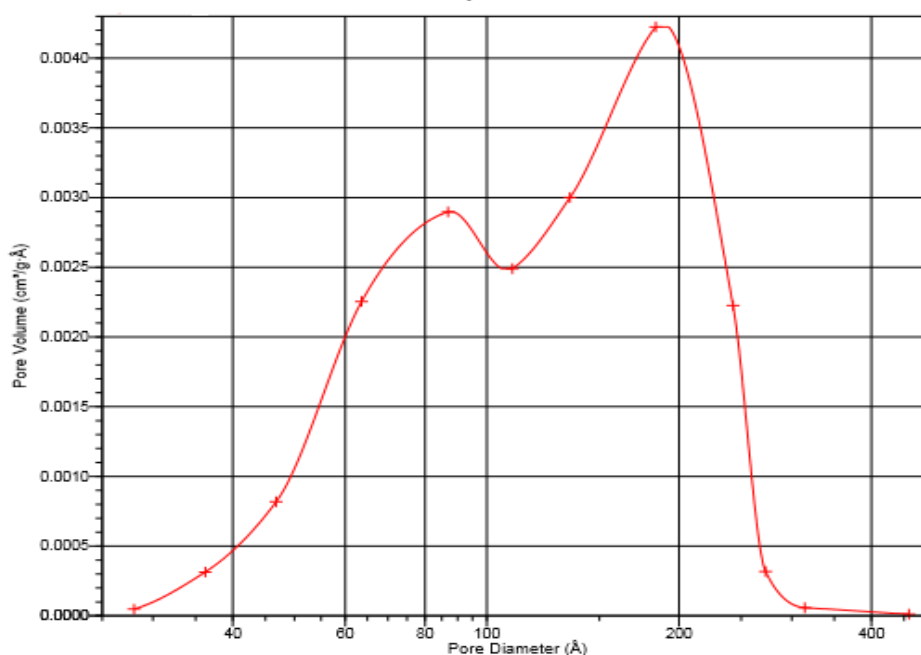


Figure 20: The pore volume ($\text{cm}^3/\text{g} \cdot \text{\AA}$) distribution as a function of the pore size (\AA) for alumina based on desorption branch using BJH model. The pore diameter is given in a logarithmic scale.

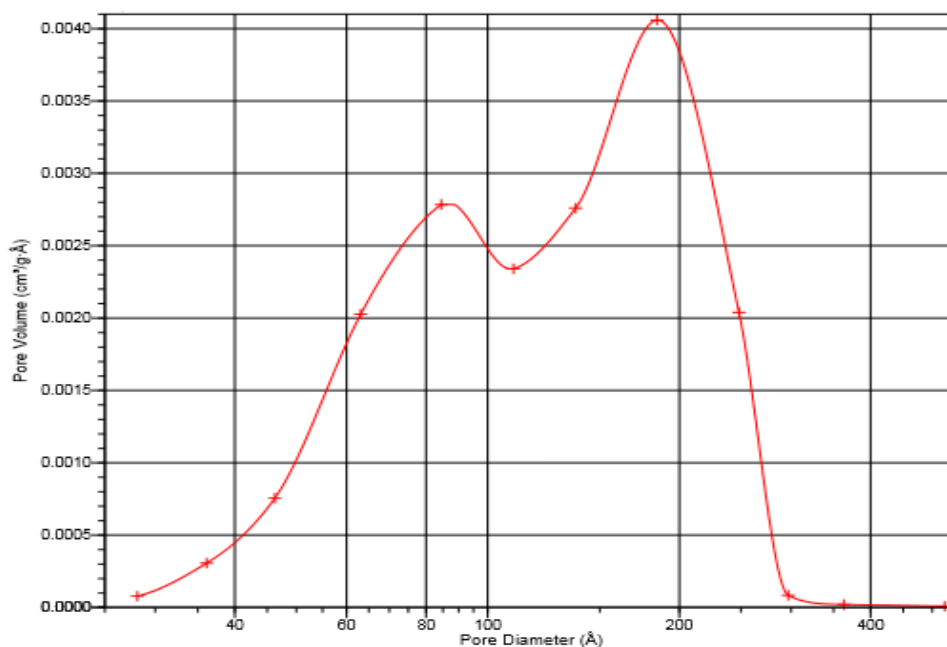


Figure 21: The pore volume ($\text{cm}^3/\text{g} \cdot \text{\AA}$) distribution as a function of the pore size (\AA) for the 0.2 wt% Pd/ Al_2O_3 SP catalyst based on desorption branch using BJH model. The pore diameter is given in a logarithmic scale.

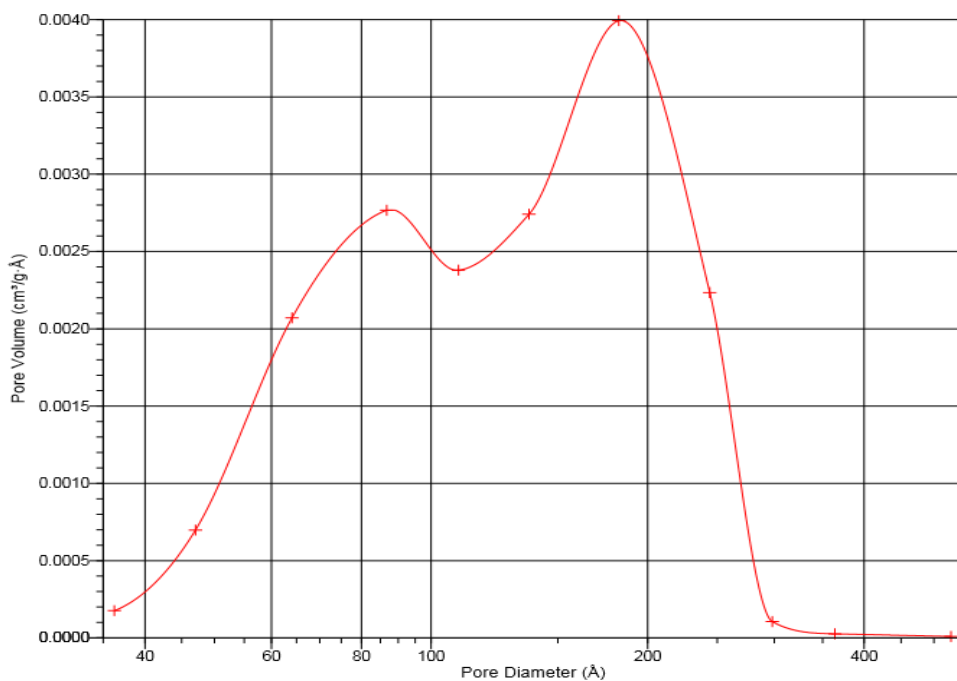


Figure 22: The pore volume ($\text{cm}^3/\text{g} \cdot \text{\AA}$) distribution as a function of the pore size (\AA) for the 0.2 wt% Pd/ Al_2O_3 MT catalyst based on desorption branch using BJH model. The pore diameter is given in a logarithmic scale.

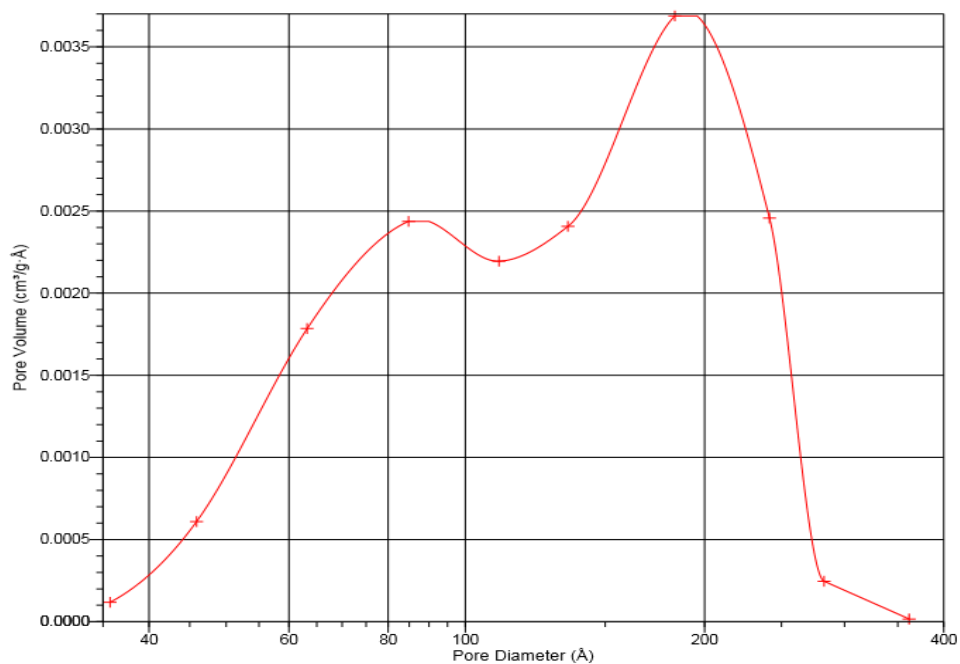


Figure 23: The pore volume ($\text{cm}^3/\text{g} \cdot \text{\AA}$) distribution as a function of the pore size (\AA) for the 2.0 wt% Pd/ Al_2O_3 MT catalyst based on desorption branch using BJH model. The pore diameter is given in a logarithmic scale.

G XRF-results

The results obtained using the X-Ray Fluorescence technique on the alumina sample, HBO₃-binder and the two 0.2 wt% and 2.0 wt% Pd/Al₂O₃ catalysts.

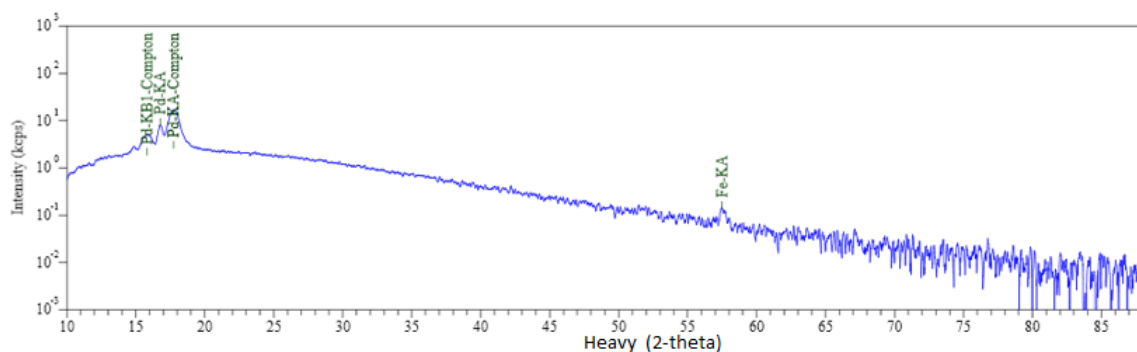


Figure 24: The intensity (kcps)(blue line) measured as a function of 2θ up to $2\theta=88$ for 0.2 wt% Pd/Al₂O₃ SP, where palladium and alumina compounds were detected (green writing). Palladium compounds were detected around around 15-20 2θ . Iron compound was detected around 2θ equal to 57.

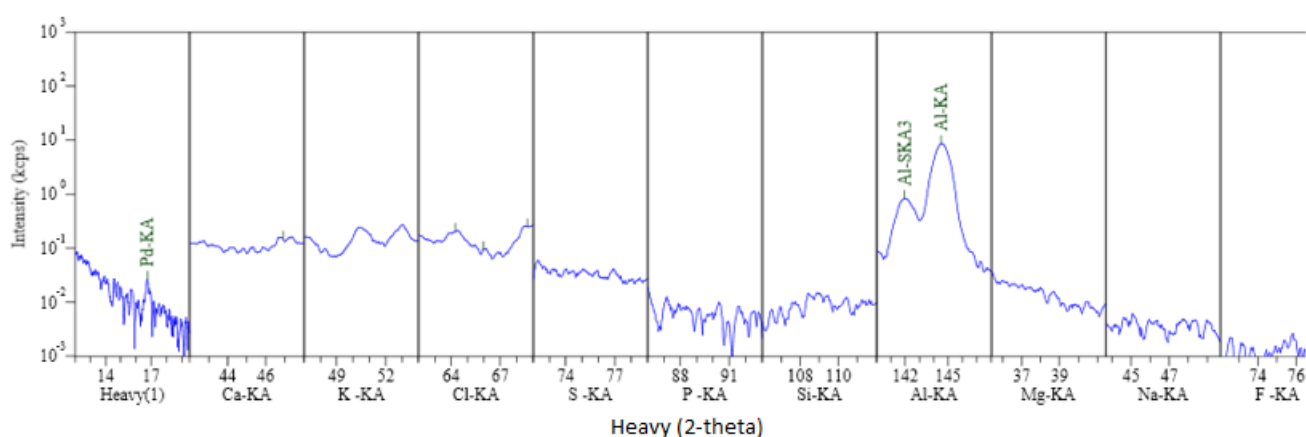


Figure 25: The intensity (kcps)(blue line) of 0.2 wt% Pd/Al₂O₃ SP as a function of 2θ , where the results are not continuous, but only showed for the most common compounds. The XRF detected palladium and alumina. There are no traces of calcium, potassium, chlorine, sulfur, phosphorus, silicon, magnesium, sodium or fluorine.

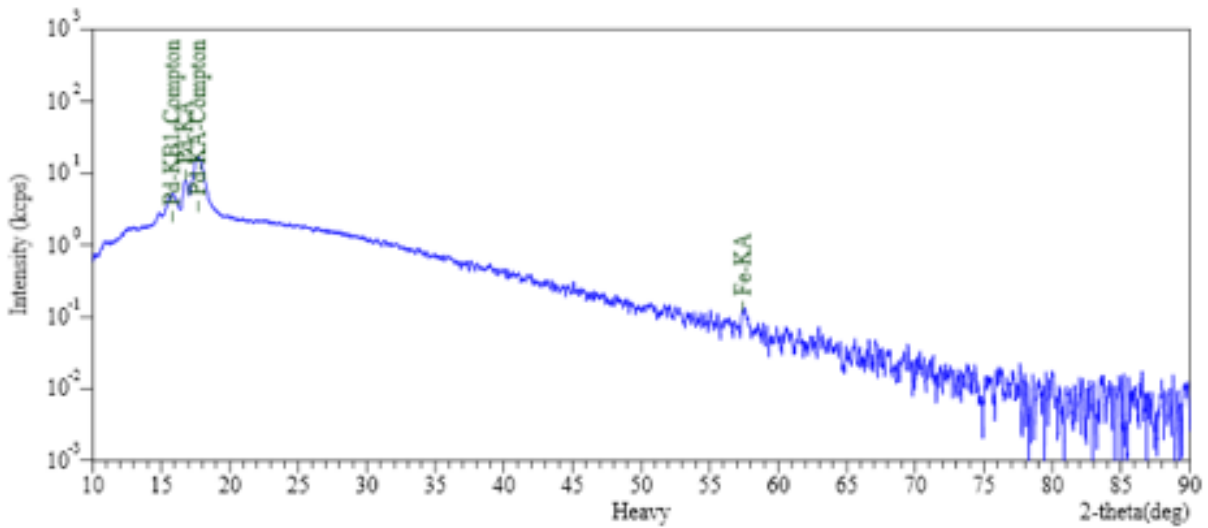


Figure 26: The intensity (kcps)(blue line) measured as a function of 2θ up to $2\theta=88$ for the second made 0.2 wt% Pd/Al₂O₃ MT, where palladium and alumina compounds were detected (green writing) and traces of silica, sulfur and silver. Palladium compounds were detected around around 15-20 2θ . Iron compound was detected around 2θ equal to 57.

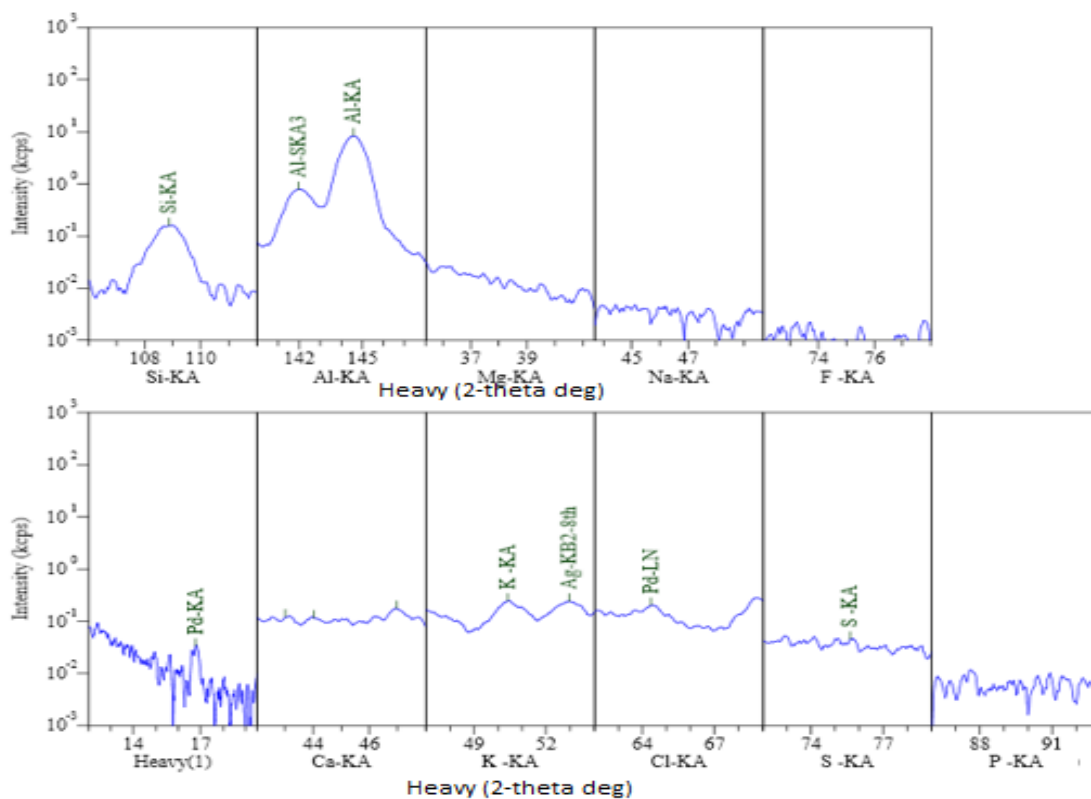


Figure 27: The intensity (kcps)(blue line) of the second made 0.2 wt% Pd/Al₂O₃ MT as a function of 2θ , where the results are not continuous, but only showed for the most common compounds. The XRF detected palladium and alumina. There were also detected traces of silicon, potassium, silver and sulfur. There are no traces of calcium, chlorine, phosphorus, magnesium, sodium or fluorine.

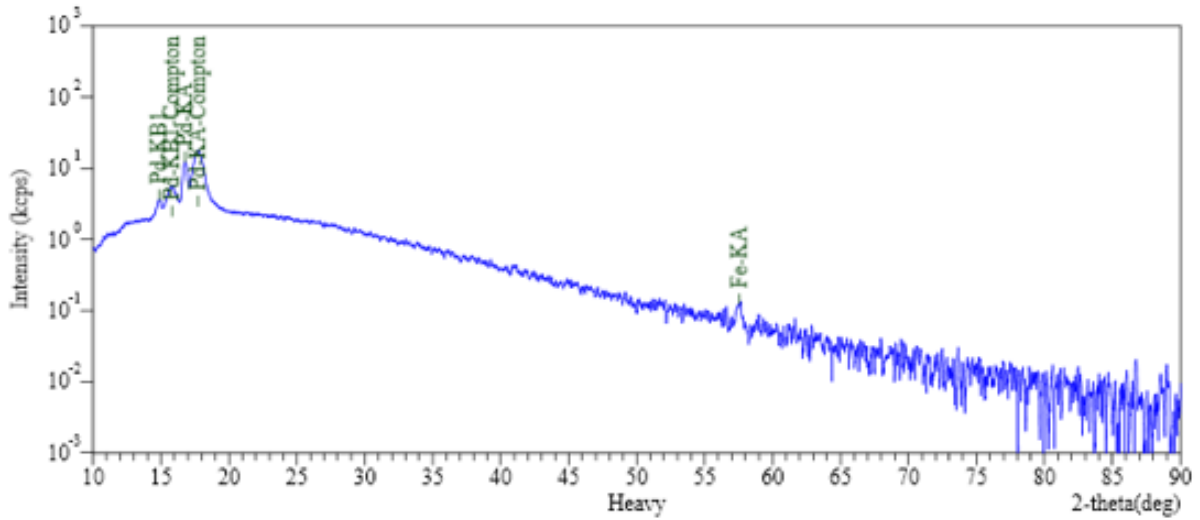


Figure 28: The intensity (kcps)(blue line) measured as a function of 2θ up to $2\theta=88$ for 2.0 wt% Pd/Al₂O₃ MT, where palladium and iron were detected (green writing). Palladium compounds were detected around around 15-20 2θ and iron compounds were detected around 2θ equal to 57.

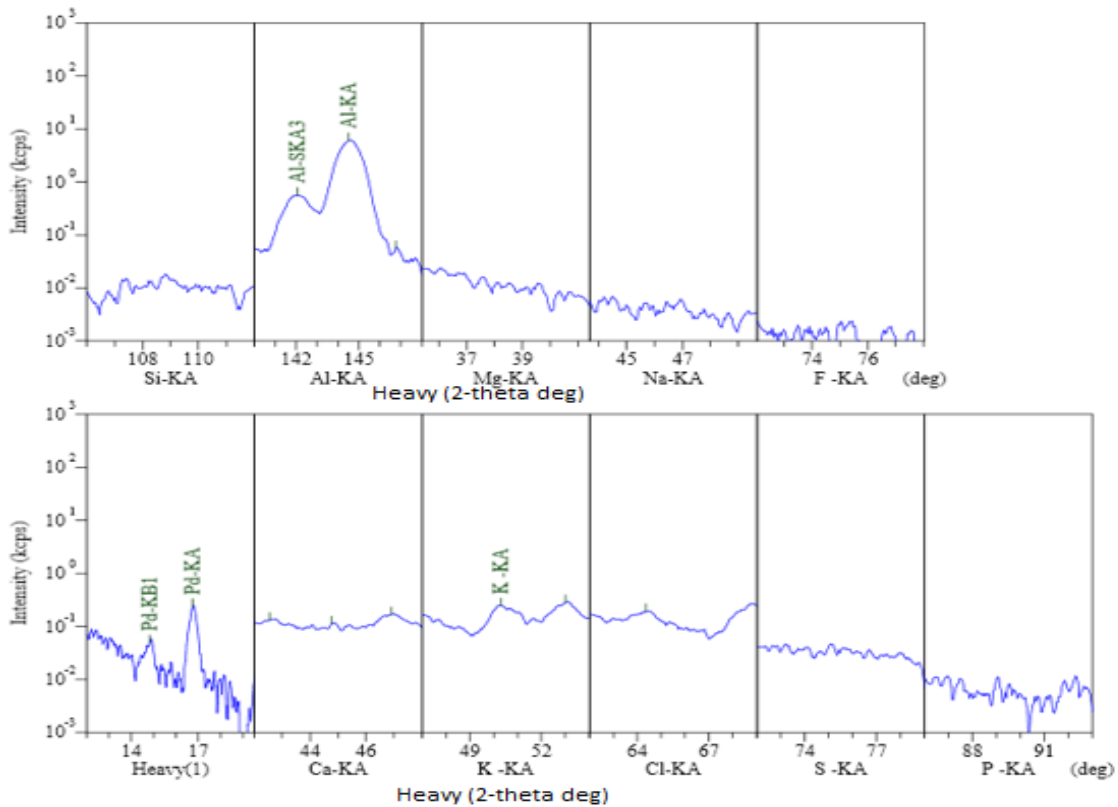


Figure 29: The intensity (kcps)(blue line) of 2.0 wt% Pd/Al₂O₃ MT as a function of 2θ , where the results are not continuous, but only showed for the most common compounds. The XRF detected palladium and alumina, and traces of potassium. There are no traces of calcium, chlorine, sulfur, phosphorus, silicon, magnesium, sodium or fluorine.

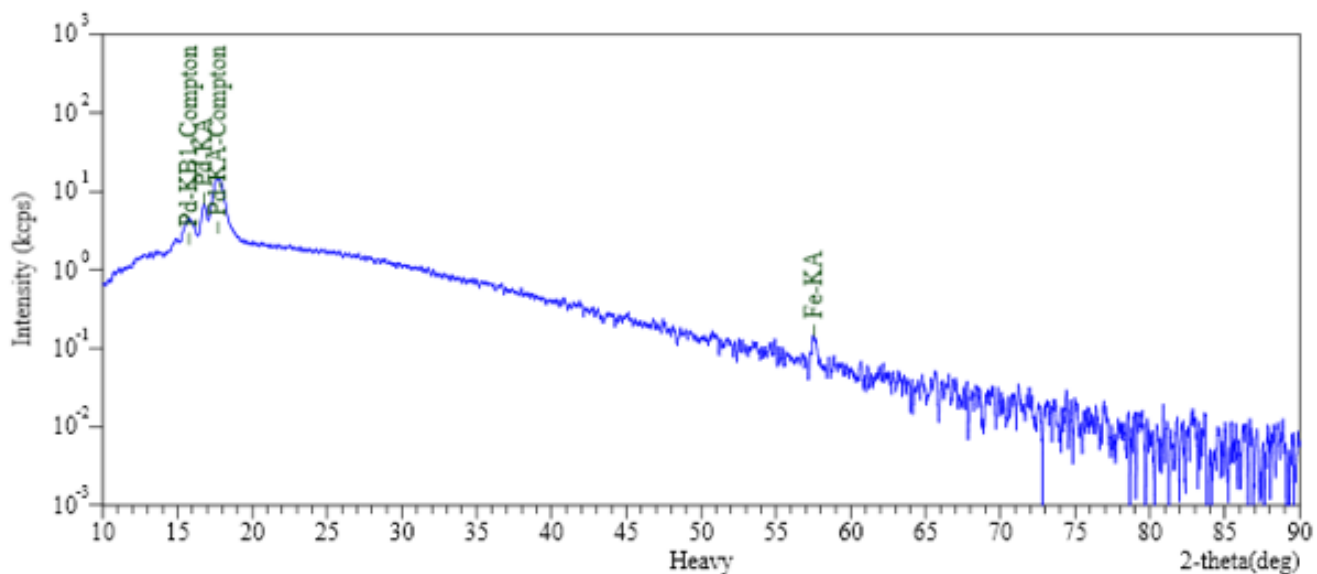


Figure 30: The intensity (kcps)(blue line) measured as a function of 2θ up to $2\theta=88$ for alumina, where palladium compounds were detected (green writing). Palladium compounds were detected around 15-20 2θ . Iron compound was detected around 2θ equal to 57.

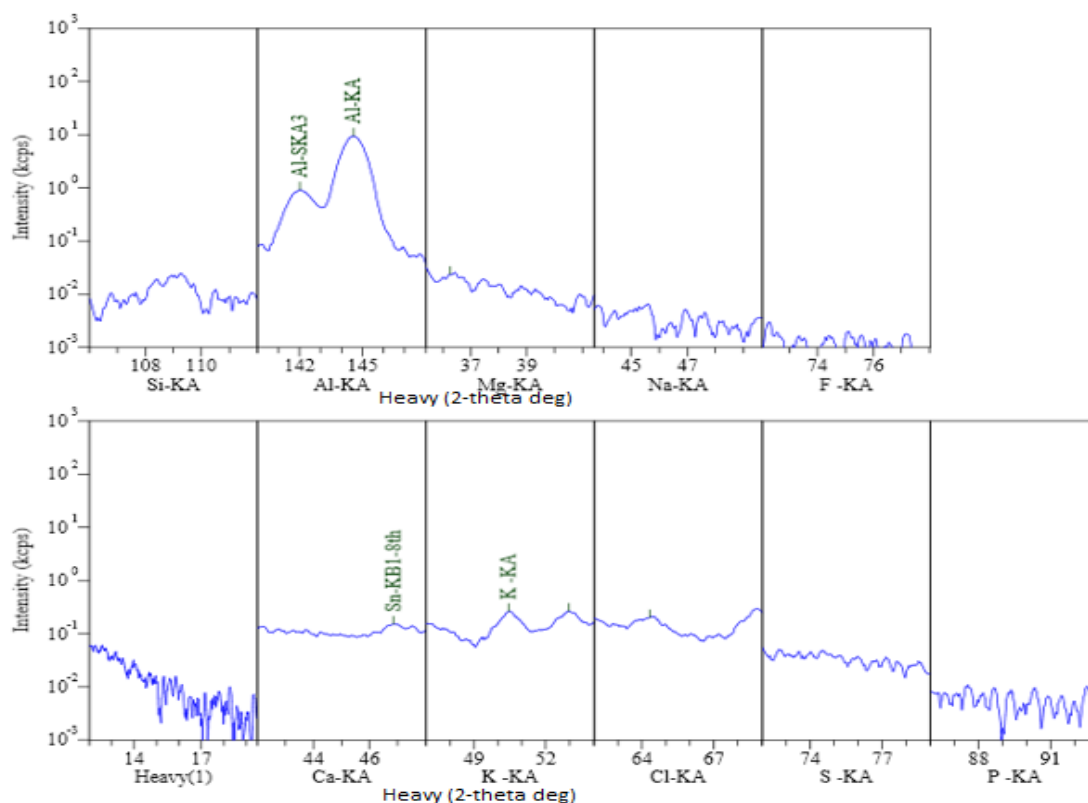


Figure 31: The intensity (kcps)(blue line) of alumina as a function of 2θ , where the results are not continuous, but only showed for the most common compounds. The XRF detected alumina, and traces of potassium and tin. There are no traces of calcium, chlorine, sulfur, phosphorus, silicon, magnesium, sodium or fluorine.

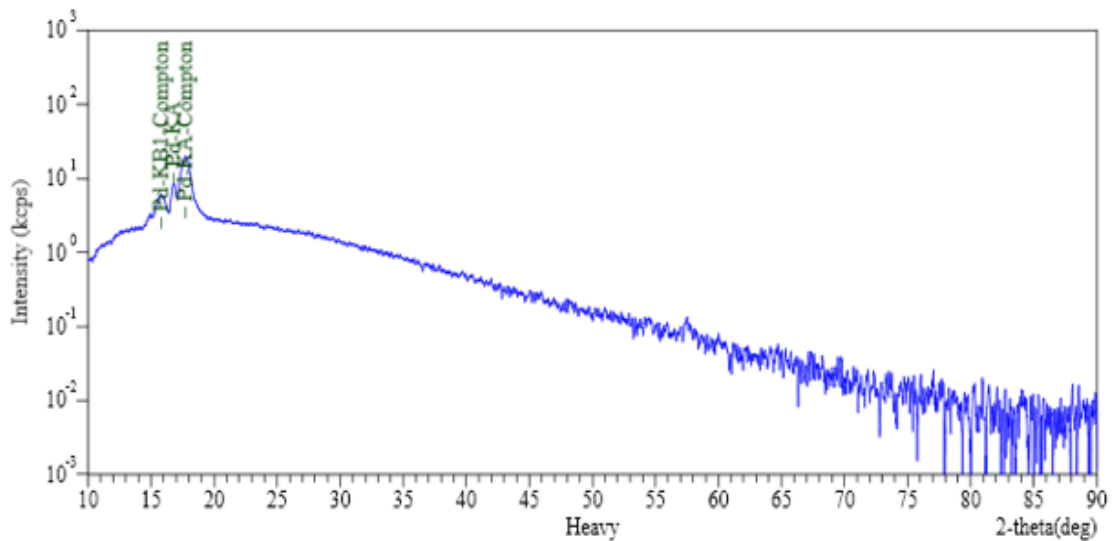


Figure 32: The intensity (kcps)(blue line) measured as a function of 2θ up to $2\theta=88$ for the binder (HBO_3), where palladium compounds were detected (green writing). Palladium compounds were detected around 15-20 2θ .

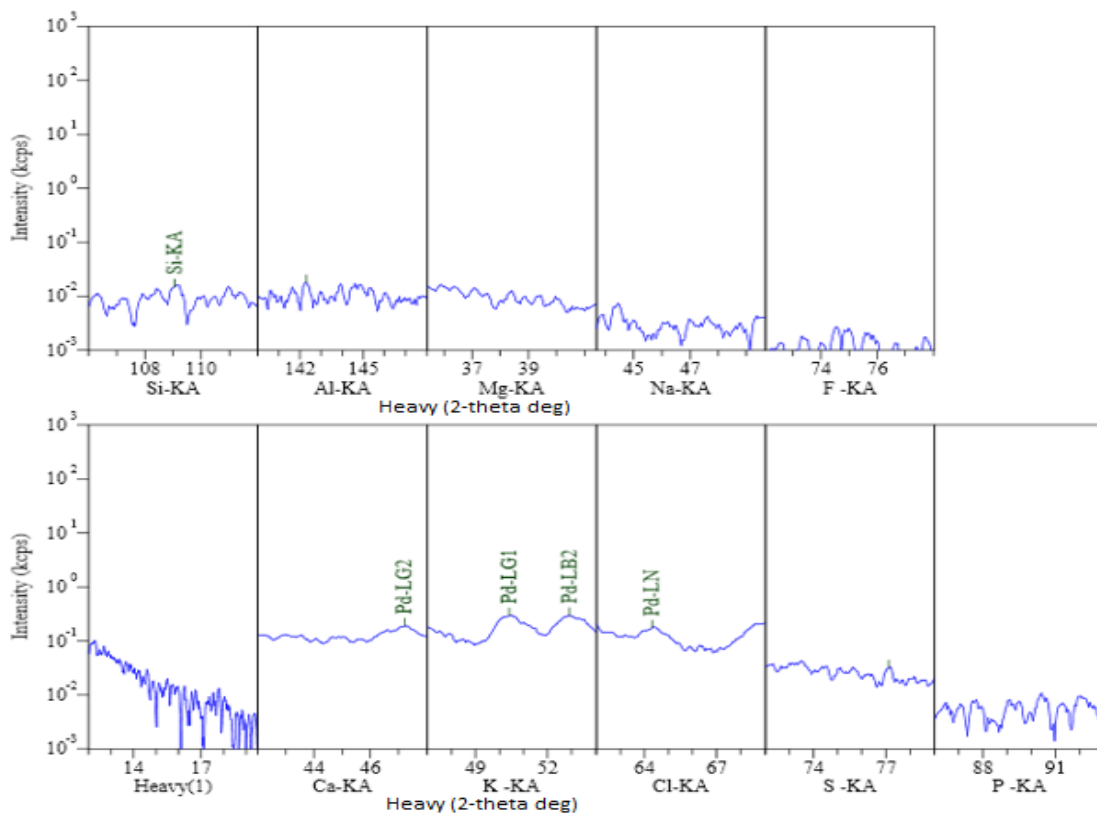


Figure 33: The intensity (kcps)(blue line of the binder (HBO_3)) as a function of 2θ , where the results are not continuous, but only showed for the most common compounds. The XRF detected palladium and silicon. There are no traces of calcium, potassium, chlorine, sulfur, phosphorus, magnesium, sodium or fluorine.

H Weight% of Palladium in the XRF-results

The weight% of PdO can be found in Table 7, and are found to be 0.124, 0.319 and 1.90 for the 0.2 wt% Pd/Al₂O₃ SP, the 0.2 wt% Pd/Al₂O₃ MT, and 2.0 wt% Pd/Al₂O₃ MT catalysts, respectively. The weight of the samples are found in Table D.2 in Appendix , and are 2.993 g, 3.009 g and 3.029 g for the 0.2 wt% Pd/Al₂O₃ SP, the 0.2 wt% Pd/Al₂O₃ MT, and 2.0 wt% Pd/Al₂O₃ MT catalysts, respectively. The weight% of Pd in the 0.2 wt% Pd/Al₂O₃ SP is calculated below, by using 122.4 and 106.4 g/mol as the molecular weights for PdO and Pd, respectively[57]:

$$0.124 \frac{\text{g PdO}}{\text{g sample}} \cdot 2.993 \text{ g sample} = 0.371 \text{ g PdO} \quad (31)$$

The number of moles PdO:

$$n_{PdO} = \frac{0.371 \text{ g PdO}}{122.4 \text{ g/mol}} = 0.00303 \text{ mol PdO} \quad (32)$$

The stoichiometric relationship between PdO and Pd is 1:1, and therefore the number of moles of PdO equals the number of moles Pd in the sample. The weight of Pd in the sample is:

$$m_{Pd} = 0.00301 \text{ mol Pd} \cdot 106.4 \text{ g Pd/mol Pd} = 0.323 \text{ g Pd} \quad (33)$$

The weight% of Pd in the sample is then:

$$Wt\%_{Pd} = \frac{0.323 \text{ g Pd}}{2.993 \text{ g sample}} = 0.11 \quad (34)$$

The same approach are used for the 0.2 wt% Pd/Al₂O₃ MT and 2.0 wt% Pd/Al₂O₃ MT catalysts and the weight% of Pd in the samples are 0.28 and 1.7, respectively.

I TGA-measurements: weight changes

The resulting mass changes during the TGA-experiments are found in Table 17. The calculations are based on the resulting weight% changes during gas switches or temperature changes as seen in Figure 13. It is assumed that the palladium catalyst is fully oxidized, i.e. PdO, at 2), 6) and 7) in Figure 34, and completely reduced at 4), 11) and 12). Consequently, the mass change is attributed to loss or gain of oxygen. The results are found by using:

$$m(\text{Pd or PdO}) = m_0 \cdot \frac{100 \pm (\text{wt}\%_0 - \text{wt}\%_1)}{100} \quad (35)$$

where m , m_0 , m_1 , $\text{wt}\%_0$ and $\text{wt}\%_1$, are the catalyst mass, catalyst mass before and after temperature or gas switch and the weight% before and after the temperature or gas switch

Table 17: The observed weight% changes during TGA-measurements and the calculated mass change. The numbers correlate to the numbers in Figure 34 and thus the weight of the catalyst at that point. The weight% is equal to 100, the baseline, when the gases are switched between argon and oxygen

Number	Weight%	Weight% change [mg]	Catalyst weight
1	100		19.7
2	113	+13.0	22.2
3	105	-8.00	20.5
4	96.0	-9.00	18.7
5	98.0	+2.00	19.0
baseline	100		19.0
6	102	+2.00	19.3
7	102	-	19.3
8	102	-	19.3
baseline	100		19.3
9	113	+8.00	21.7
10	108	+5.00	20.7
11	106	-7.00	20.3
12	98.0	-8.00	18.7

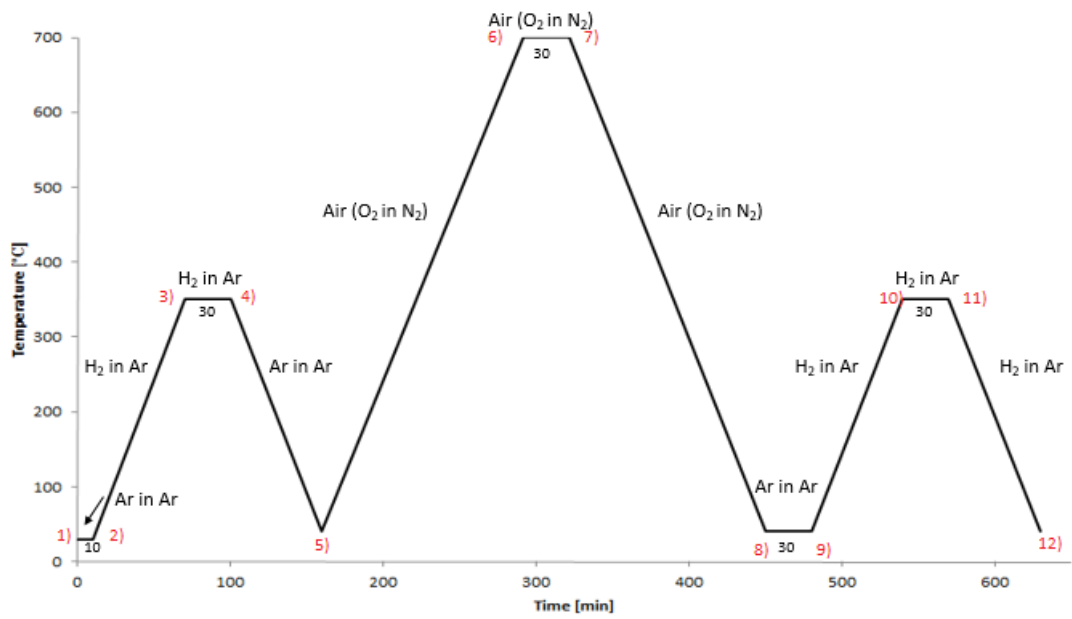


Figure 34: An illustration of the temperature profile as a function of time of the TGA with exposed gases and hold-up times. The red numbers illustrate the reaction conditions where the data for mass change are calculated from.

J Sketch of the methane oxidation reactor

A sketch by Jia Yang of the reactor used for methane oxidation is shown in Figure 35.

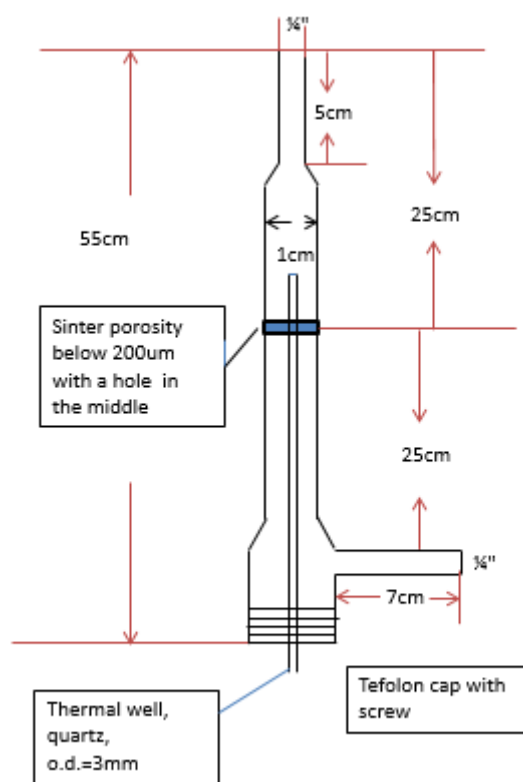


Figure 35: A sketch of the reactor with dimensions which is used when 0.2 and 2.0 wt% palladium supported catalysts are tested during methane oxidation.

K MFC calibration data

The setpoints that were calculated were based on MFC calibrations that Jia Yang performed. The calibration curves showed the flow of gas as a function of the % setpoint of the mass flow controller. The curves are shown in the Figures below:

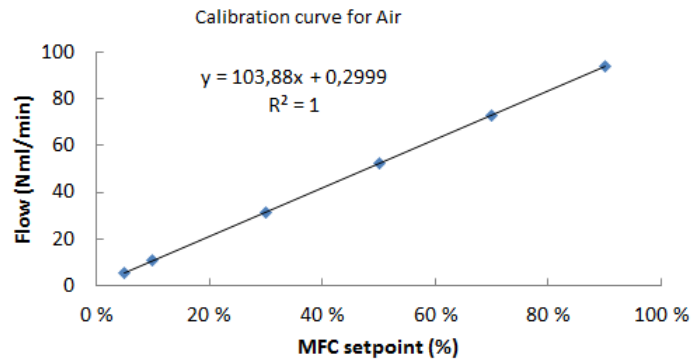


Figure 36: The calibration curve of the air flow as a function of the % setpoint of the mass flow controller, where the trend line equation is shown.

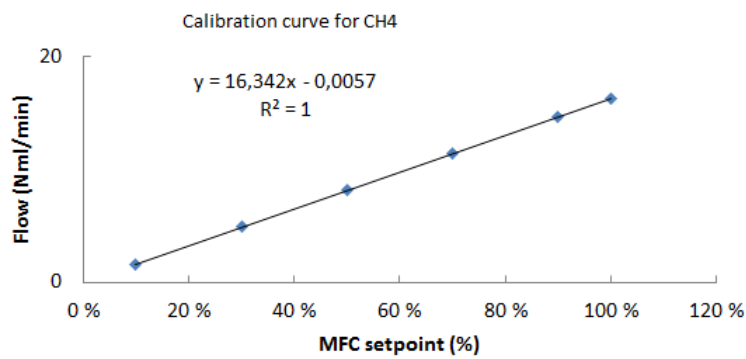


Figure 37: The calibration curve of the Methane flow as a function of the % setpoint of the mass flow controller, where the trend line equation is shown.

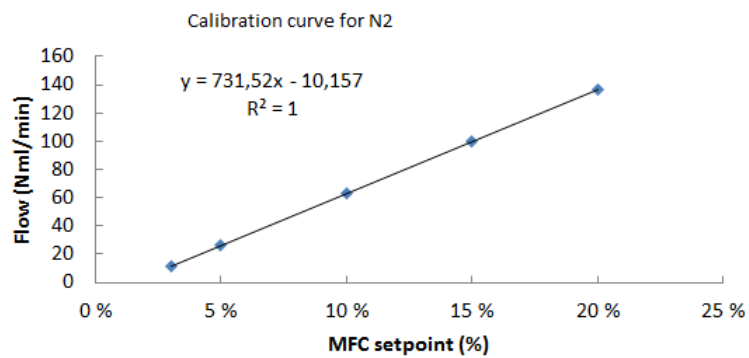


Figure 38: The calibration curve of the Nitrogen flow as a function of the % setpoint of the mass flow controller, where the trend line equation is shown.

It was necessary to find the setpoints to obtain the appropriate flow used in each reaction. The reference reaction, i.e. reaction number 1 in Table 3, using a flow with CH₄/O₂(synthetic air)/N₂=4/20/176 NmL/min (2%/10%/88%) for the total flow of 200 NmL/min. The flows were substituted into the trend line equations of the calibration curve. The methane flow were found by:

$$2\% \cdot 200 \text{ NmL/min} = 4 \text{ NmL/min} \quad (36)$$

which give a setpoint of 24.5%.

For synthetic air, the flow is:

$$10\% \cdot 200 \text{ NmL/min} = 20 \text{ NmL/min} \quad (37)$$

but the air contains 21% O₂ and 79 % N₂, and therefore:

$$1 \text{ O}_2 = \frac{1}{0.21} \text{ Air} \quad (38)$$

and

$$20 \text{ O}_2 = \frac{20}{0.21} \text{ Air} = 95.2 \text{ NmL/min} \quad (39)$$

which give a setpoint of 91.4%.

The rest is Nitrogen:

$$(200 - 4 - 95.2) \text{ NmL/min} = 100.8 \text{ NmL/min} \quad (40)$$

which give a setpoint of 15.2%. The same approach was obtained when finding the setpoints for molar flows of CH₄/O₂(synthetic air)/N₂ equal to 2/20/178, 2/10/188, 1/5/194 and 1/10/189 NmL/min. The resulting setpoints can be found in Table 3 in Section 3.4. The same calibration data was used when using 5% CH₄ in N₂, only MFC gas correction factors of 1 and 0.72 for nitrogen and methane, respectively, were used. 0.2 NmL/min of pure methane is achieved with a 4 NmL/min of diluted methane due to the 5% CH₄/95% N₂. The calculations are shown below:

$$\frac{0.2 \text{ NmL/min pure CH}_4}{X \text{ NmL/min diluted CH}_4} = 0.05 \text{ pure CH}_4/\text{diluted CH}_4 \quad (41)$$

where X is the diluted methane flow and is found to be 4 NmL/min. A N₂ calibrated controller which gives 100 NmL/min at a set point will give 72 NmL/min CH₄ at the same value. The opposite will apply for the opposite incident. The MFC is calibrated with respect to methane and the flow which is implemented into the calibration data is:

$$4 \text{ NmL diluted CH}_2 \cdot 0.72 = 2.88 \text{ NmL/min} \quad (42)$$

The resulting setpoint for the methane MFC is 17.7%. A CH₄:O₂ ratio equal to 1:5 results in a oxygen flow of 1 NmL/min and air flow of 4.78 NmL/min which give a setpoint for the air MFC equal to 4.31%. The nitrogen flow is equal to 192.34 NmL/min and the MFC setpoint is 27.7%. The same approach is applied for a CH₄:O₂ ratio equal to 1:10 and a methane flow of 0.2 NmL/min. The results can be found in Table 3 in Section 3.4.

L Temperature measurements in the catalyst bed

Temperature profiles of the catalysts were performed during the testing. Temperature measurements performed during testing of the 0.2 wt% Pd/Al₂O₃ SP catalyst at 350 and 450 °C can be found in Table 18 and 19. The catalyst bed is 2 cm in height and 0.5 cm in width.

Table 18: Catalyst bed temperature measurements at 350 °C for 0.2 wt% Pd/Al₂O₃ catalyst.

Distance from top of the catalyst bed [cm]	Temperature [°C]
	0.2 wt% Pd/Al₂O₃
0	336.3
1	338.0
2	340.3
3	338.9
Average T	338.4

Table 19: Catalyst bed temperature measurements at 450 °C for 0.2 wt% Pd/Al₂O₃ catalysts.

Distance from top of the catalyst bed [cm]	Temperature [°C]
	0.2 wt% Pd/Al₂O₃
0	435.2
1	440.9
2	451.9
3	451.4
Average T	444.9

The temperatures in the 0.2 wt% Pd/Al₂O₃ SP catalyst bed at the theoretical temperatures 200, 250, 300, 400 and 550 °C were found using the difference between the theoretical and the average catalyst bed temperature.

$$338.4^{\circ}\text{C} - 350.0^{\circ}\text{C} = -11.6^{\circ}\text{C} \quad (43)$$

$$444.9^{\circ}\text{C} - 450.0 = -5.1^{\circ}\text{C} \quad (44)$$

Equation 43 and 44 were used to find the average difference from the real catalyst bed temperature at 250 and 550 °C. As shown below:

$$\frac{-11.6^{\circ}\text{C} + (-5.1)^{\circ}\text{C}}{2} = -8.4^{\circ}\text{C} \quad (45)$$

The real catalyst bed temperature is 8.4 °C below the set temperature for the 0.2 wt% palladium supported catalyst.

The temperature profiles were measured for each temperature interval for the second 0.2 wt% and 2.0 wt% Pd/Al₂O₃ MT catalysts and the measurements can be found in Tables 20, 21, 22, 23, 24 and 25, 27, 28, 29, 30, 31, 32, 33, 34, 35 and 36.

Table 20: Catalyst bed temperature measurements for the first reaction (reference) with the second 0.2 wt% Pd/Al₂O₃ catalyst with a ratio CH₄ : O₂ equal to 1:5. The flows of methane, oxygen and nitrogen are 4 NmL/min, 20 NmL/min and 176 NmL/min.

Set Temp. [°C]	Distance from top of catalyst bed [cm]	Real Temp. [°C]			
		0	1	2	Average
250		197.1	192.2	192.1	192.1
300		253.9	249.1	241.1	248.0
350		300.9	293.9	287.4	294.1
400		360.9	355.1	342.5	352.8
450		428.8	412.1	395.4	412.1
500		467.1	462.0	448.5	459.2
550		540.9	515.6	496.7	517.7
600		582.7	554.7	542.2	559.9

Table 21: Catalyst bed temperature measurements for the second reaction with 2.0 wt% Pd/Al₂O₃ catalyst with a ratio CH₄ : O₂ equal to 1:10. The flows of methane, oxygen and nitrogen are 2 NmL/min, 20 NmL/min and 178 NmL/min.

Set Temp. [°C]	Distance from top of catalyst bed [cm]	Real Temp. [°C]			
		0	1	2	Average
250		205.6	201.3	196.6	201.2
300		248.5	243.3	240.9	244.2
350		303.4	301.2	296.7	300.4
400		349.3	344.5	340.0	344.6
450		402.7	398.7	391.1	397.5
500		460.6	455.5	447.2	454.4
550		515.3	510.4	506.4	510.7
600		565.8.3	553.6	548.7	556.0

Table 22: Catalyst bed temperature measurements for the third reaction with 2.0 wt% Pd/Al₂O₃ catalyst with a ratio CH₄ : O₂ equal to 1:5. The flows of methane, oxygen and nitrogen are 2 NmL/min, 10 NmL/min and 188 NmL/min.

Set Temp. [°C]	Distance from top of catalyst bed [cm]	Real Temp. [°C]			
		0	1	2	Average
250		206.7	200.3	197.4	201.5
300		256.0	249.7	241.4	249.0
350		304.0	301.3	296.4	300.6
400		366.0	361.2	358.9	362.0
450		407.8	401.3	389.9	399.7
500		455.0	450.0	438.6	447.9
550		513.6	506.3	501.7	507.2
600		560.9	552.4	548.7	554.0

Table 23: Catalyst bed temperature measurements for the fourth reaction with 2.0 wt% Pd/Al₂O₃ catalyst with a ratio CH₄ : O₂ equal to 1:5. The flows of methane, oxygen and nitrogen are 1 NmL/min, 5 NmL/min and 194 NmL/min.

Set Temp. [°C]	Distance from top of catalyst bed [cm]	Real Temp. [°C]			
		0	1	2	Average
250		203.2	201.1	197.6	200.6
300		268.3	260.4	249.7	259.5
350		307.4	302.9	298.1	302.8
400		367.0	354.8	350.7	357.5
450		407.8	401.3	398.1	402.4
500		456.4	450.1	439.9	448.8
550		504.0	501.3	499.2	501.5
600		557.4	549.2	546.6	551.1

Table 24: Catalyst bed temperature measurements for the fifth reaction with 2.0 wt% Pd/Al₂O₃ catalyst with a ratio CH₄ : O₂ equal to 1:10. The flows of methane, oxygen and nitrogen are 1 NmL/min, 10 NmL/min and 189 NmL/min.

Set Temp. [°C]	Distance from top of catalyst bed [cm]	Real Temp. [°C]			
		0	1	2	Average
250		201.7	199.0	196.4	199.0
300		258.9	256.3	251.3	255.5
350		304.0	300.6	298.7	301.1
400		362.1	357.4	352.2	357.2
450		409.0	406.4	401.7	405.7
500		459.8	457.0	449.3	455.4
550		507.6	505.0	501.2	504.6
600		555.7	550.0	547.3	551.0

Table 25: Catalyst bed temperature measurements for the sixth reaction (reference) with 2.0 wt% Pd/Al₂O₃ catalyst with a ratio CH₄ : O₂ equal to 1:5. The flows of methane, oxygen and nitrogen are 4 NmL/min, 20 NmL/min and 176 NmL/min.

Set Temp. [°C]	Distance from top of catalyst bed [cm]	Real Temp. [°C]			
		0	1	2	Average
250		195.1	191.1	186.2	190.8
300		249.1	244.8	243.1	245.7
350		298.9	297.6	294.3	296.9
400		348.8	343.6	341.0	344.5
450		424.0	416.3	398.9	413.1
500		461.4	458.7	454.0	458.0
550		526.2	518.3	514.9	519.8
600		577.7	568.0	564.4	570.0
650		630.3	622.7	615.0	622.7

Table 26: Catalyst bed temperature measurements for the eighth reaction with 2.0 wt% Pd/Al₂O₃ catalyst with a ratio CH₄ : O₂ equal to 1:5. The flows of methane, oxygen and nitrogen are 4 NmL/min, 20 NmL/min and 176 NmL/min.

Set Temp. [°C]	Distance from top of catalyst bed [cm]	Real Temp. [°C]			
		0	1	2	Average
250		205.2	201.3	197.9	201.5
300		248.6	245.1	241.9	245.2
325		279.3	275.7	270.8	275.3
350		308.9	306.3	299.3	304.8
375		337.0	336.5	326.7	333.4
400		403.6	379.8	352.1	378.5
450		442.5	420.6	400.8	421.3
500		486.6	462.0	449.3	466.0

Table 27: Catalyst bed temperature measurements for the first reaction with the 2.0 wt% Pd/Al₂O₃ catalyst with a ratio CH₄ : O₂ equal to 1:5. The flows of methane, oxygen and nitrogen are 4 NmL/min, 20 NmL/min and 176 NmL/min.

Set Temp. [°C]	Distance from top of catalyst bed [cm]	Real Temp. [°C]			
		0	1	2	Average
250		208.1	206.8	207.1	207.3
300		256.8	257.7	258.7	257.7
350		327.4	326.7	327.0	327.0
400		394.6	399.7	400.6	398.3
450		435.4	437.3	437.7	436.8
500		468.5	475.9	475.4	473.3

Table 28: Catalyst bed temperature measurements for the second reaction with 2.0 wt% Pd/Al₂O₃ catalyst with a ratio CH₄ : O₂ equal to 1:5. The flows of methane, oxygen and nitrogen are 4 NmL/min, 20 NmL/min and 176 NmL/min.

Set Temp. [°C]	Distance from top of catalyst bed [cm]	Real Temp. [°C]			
		0	1	2	Average
250		205.9	202.9	198.9	202.6
300		256.6	258.3	253.2	256.0
350		326.2	318.7	304.3	316.4
400		403.2	378.0	355.1	378.8
450		446.2	418.8	401.0	422.0
500		486.7	465.0	449.4	467.0

Table 29: Catalyst bed temperature measurements for the third reaction with 2.0 wt% Pd/Al₂O₃ catalyst with a ratio CH₄ : O₂ equal to 1:10. The flows of methane, oxygen and nitrogen are 2 NmL/min, 20 NmL/min and 178 NmL/min.

Set Temp. [°C]	Distance from top of catalyst bed [cm]	Real Temp. [°C]			
		0	1	2	Average
250		205.6	202.5	197.0	201.7
300		252.2	248.6	244.4	248.4
350		307.3	305.6	297.3	303.4
375		336.5	336.1	325.3	332.6
400		368.7	364.3	350.3	361.1
450		424.0	408.9	398.1	410.3
500		467.3	455.6	445.5	456.1

Table 30: Catalyst bed temperature measurements for the fourth reaction with 2.0 wt% Pd/Al₂O₃ catalyst with a ratio CH₄ : O₂ equal to 1:5. The flows of methane, oxygen and nitrogen are 4 NmL/min, 20 NmL/min and 176 NmL/min.

Set Temp. [°C]	Distance from top of catalyst bed [cm]	Real Temp. [°C]			
		0	1	2	Average
250		205.8	202.6	197.5	202.0
300		253.9	249.1	244.9	249.3
325		282.7	279.5	272.0	278.1
350		317.5	313.0	299.4	310.0
375		364.6	350.5	330.4	348.5
400		403.6	379.8	352.1	378.5
450		450.1	423.1	401.5	424.9
500		489.0	462.0	448.5	466.5

Table 31: Catalyst bed temperature measurements for the fifth reaction with 2.0 wt% Pd/Al₂O₃ catalyst with a ratio CH₄ : O₂ equal to 1:5. The flows of methane, oxygen and nitrogen are 2 NmL/min, 10 NmL/min and 188 NmL/min.

Set Temp. [°C]	Distance from top of catalyst bed [cm]	Real Temp. [°C]			
		0	1	2	Average
200		175.4	166.2	157.0	166.2
250		249.8	245.5	241.1	245.5
325		276.9	273.8	268.9	273.2
350		305.7	303.9	297.9	302.5
375		333.2	332.3	322.6	329.4
400		366.9	366.3	352.0	361.7
450		422.8	413.4	398.4	411.5
500		467.1	454.9	445.3	455.8

Table 32: Catalyst bed temperature measurements for the sixth reaction with 2.0 wt% Pd/Al₂O₃ catalyst with a ratio CH₄ : O₂ equal to 1:5. The flows of methane, oxygen and nitrogen are 1 NmL/min, 5 NmL/min and 194 NmL/min.

Set Temp. [°C]	Distance from top of catalyst bed [cm]	Real Temp. [°C]			
		0	1	2	Average
250		205.8	202.1	197.5	201.8
300		254.5	250.4	246.2	250.4
325		279.0	274.8	271.2	275.0
350		305.3	303.0	297.3	301.9
375		332.2	330.6	323.4	328.7
400		360.1	358.3	349.1	355.8
450		411.3	407.0	396.5	404.9
500		461.2	455.8	448.3	455.1

Table 33: Catalyst bed temperature measurements for the seventh reaction with 2.0 wt% Pd/Al₂O₃ catalyst with a ratio CH₄ : O₂ equal to 1:10. The flows of methane, oxygen and nitrogen are 1 NmL/min, 10 NmL/min and 189 NmL/min.

Set Temp. [°C]	Distance from top of catalyst bed [cm]	Real Temp. [°C]			
		0	1	2	Average
250		205.8	202.1	197.5	201.8
300		249.7	246.0	241.5	245.7
325		273.7	270.5	266.1	270.1
350		302.3	300.2	294.2	298.9
375		331.6	329.2	322.4	327.7
400		360.4	358.5	349.4	356.1
450		413.4	406.8	397.7	406.0

Table 34: Catalyst bed temperature measurements for the eighth reaction with 2.0 wt% Pd/Al₂O₃ catalyst with a ratio CH₄ : O₂ equal to 1:5. The flows of methane, oxygen and nitrogen are 4 NmL/min, 20 NmL/min and 176 NmL/min.

Set Temp. [°C]	Distance from top of catalyst bed [cm]	Real Temp. [°C]			
		0	1	2	Average
250		205.2	201.3	197.9	201.5
300		248.6	245.1	241.9	245.2
325		279.3	275.7	270.8	275.3
350		308.9	306.3	299.3	304.8
375		337.0	336.5	326.7	333.4
400		403.6	379.8	352.1	378.5
450		442.5	420.6	400.8	421.3
500		486.6	462.0	449.3	466.0

Table 35: Catalyst bed temperature measurements for the ninth reaction with 2.0 wt% Pd/Al₂O₃ catalyst with a ratio CH₄ : O₂ equal to 1:5. The flows of methane, oxygen and nitrogen are 0.2 NmL/min, 1 NmL/min and 198.8 NmL/min.

Set Temp. [°C]	Distance from top of catalyst bed [cm]	Real Temp. [°C]			
		0	1	2	Average
200		161.4	158.0	150.4	156.6
250		204.4	201.7	200.1	202.1
275		239.8	232.2	224.7	232.2
300		250.8	247.2	243.8	247.3
325		272.7	267.7	265.8	269.4
350		300.9	298.7	293.7	297.8
400		348.7	344.1	340.3	344.4

Table 36: Catalyst bed temperature measurements for the ninth reaction with 2.0 wt% Pd/Al₂O₃ catalyst with a ratio CH₄ : O₂ equal to 1:10. The flows of methane, oxygen and nitrogen are 0.2 NmL/min, 2 NmL/min and 197.8 NmL/min.

Set Temp. [°C]	Distance from top of catalyst bed [cm]	Real Temp. [°C]			
		0	1	2	Average
200		156.3	153.6	149.5	153.1
250		202.5	198.4	195.6	198.8
300		242.4	240.0	237.6	240.0
325		274.4	270.8	266.9	270.7
350		298.1	294.4	290.0	294.2
375		323.9	319.8	314.9	319.5

The information is used to calculate the conversion as a function of the real catalyst bed

temperature. The conversion was calculated using the methane concentrations at the hold-up times and the inlet concentration:

$$X_{CH_4} = \frac{F_{CH_4,in} - F_{CH_4,out}}{F_{CH_4,in}} \quad (46)$$

where X_{CH_4} is the conversion of methane and $F_{CH_4,in}$ and $F_{CH_4,out}$ are the molar flows of methane at the inlet and the outlet of a specific temperature interval, respectively. The results can be found in Appendix O.

M Gas Hourly Space Velocity calculations

By using Equation 21 in Section 2.6.5, the GHSVs were calculated for each methane oxidation test using fresh catalyst. The weights of the catalysts are found in Appendix D.5 in Table 15.

Table 37: The calculated GHSVs for each methane oxidation reaction using fresh catalyst. Catalysts made for the Specialization Project during fall 2015 and Master's Thesis during spring 2016, are marked as SP and MT, respectively.

Catalyst	Reaction no.	Catalyst weight [g_{cat}]	GHSV [NmL/g_{cat} h]
0.2 wt% Pd/Al ₂ O ₃ SP	1	0.2020	59400
0.2 wt% Pd/Al ₂ O ₃ MT	1	0.2070	58000
2.0 wt% Pd/Al ₂ O ₃ MT	1	0.2040	58800
2.0 wt% Pd/Al ₂ O ₃ MT	2	0.2021	59400

N Results from methane oxidation testing

The catalysts were tested for methane oxidation reactions as explained in Section 3.4 and the results are shown as the percentage of methane converted as a function of catalyst bed temperature. The 0.2 wt% Pd/Al₂O₃ SP was only tested one time under the reference conditions and the results can be found in Section N.1. The 0.2 wt% and 2.0 wt% Pd/Al₂O₃ MT catalysts were tested in series of reactions under different conditions as explained in Table 3 and the results can be found in Sections N.2 and N.3, respectively.

N.1 0.2 wt% Pd/Al₂O₃ SP catalyst

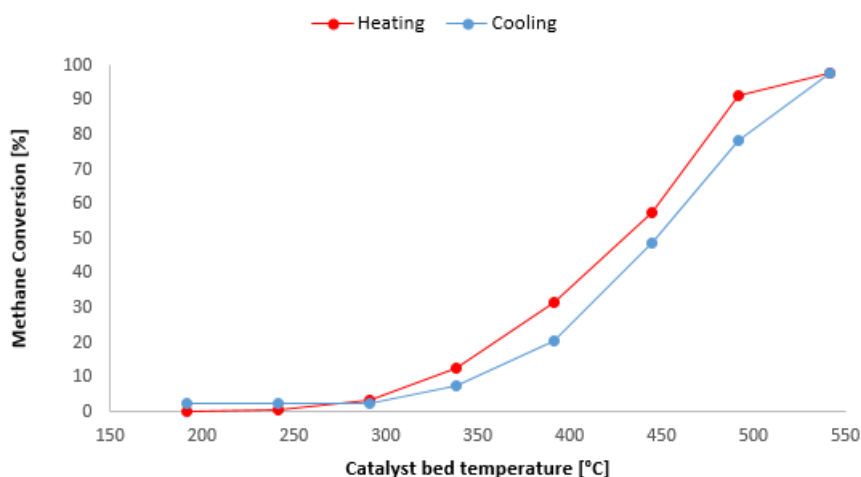


Figure 39: The methane converted (%) in the catalytic combustion of methane over the 0.2 wt% Pd/Al₂O₃ SP catalyst as a function of the catalyst bed temperature (°C) with a GHSV equal to 59400 NmL/g_{cat}h. The temperature was ramped for 5°C/min and the temperature was held for 30 minutes every 50 °C. The feed flow was constant equal 200 NmL/min and the composition of CH₄/O₂/N₂ is 4/20/176 (2%/10%/88%) NmL/min. The red curve symbolizes when the reaction was heated up to 550 °C and the blue curve when it was cooled from 550 °C to 250 °C.

N.2 0.2 wt% Pd/Al₂O₃ MT catalyst

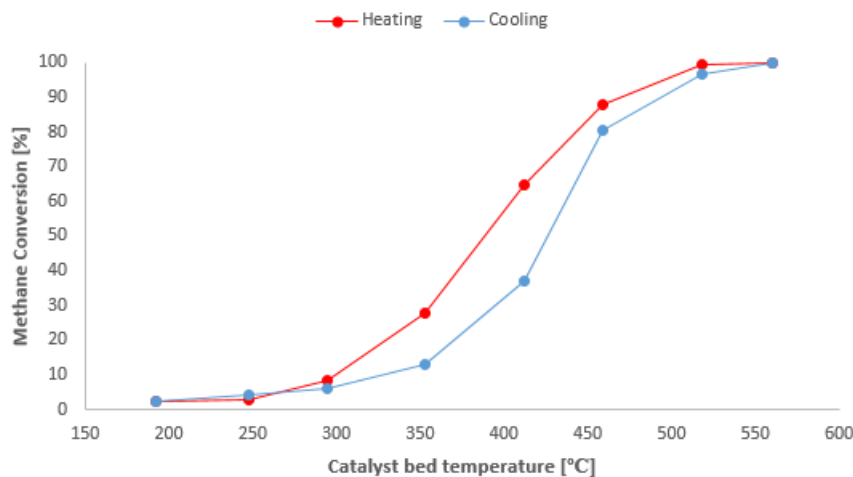


Figure 40: The methane converted (%) in the catalytic combustion of methane over the 0.2 wt% Pd/Al₂O₃ MT catalyst as a function of the catalyst bed temperature (°C) with a GHSV equal to 58000 NmL/g_{cat}h. The temperature was ramped for 5°C/min and the temperature was held for 20 minutes every 50 °C. The flow reactant feed CH₄/O₂/N₂ is 4/20/176 (2%/10%/88%) NmL/min. The red curve symbolizes when the reaction was heated up to 600 °C and the blue curve when it was cooled from 600 °C to 250 °C.

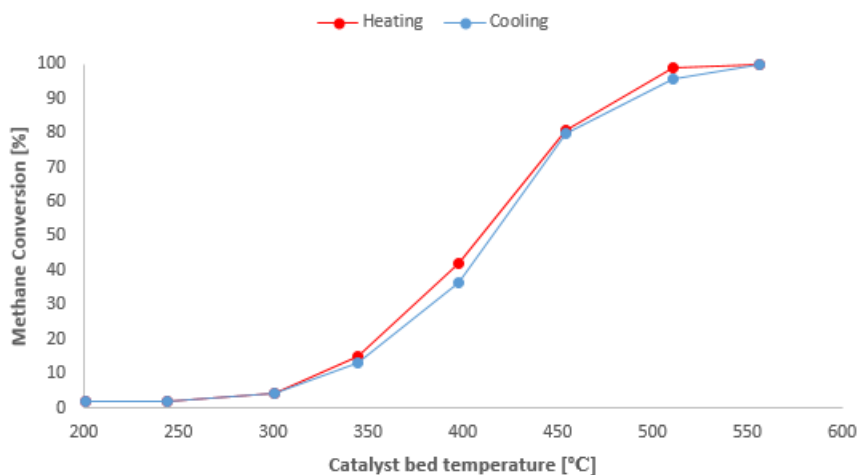


Figure 41: The methane converted (%) in the catalytic combustion of methane over the 0.2 wt% Pd/Al₂O₃ MT catalyst as a function of the catalyst bed temperature (°C) with a GHSV equal to 58000 NmL/g_{cat}h. The temperature was ramped for 5°C/min and the temperature was held for 20 minutes every 50 °C. The flow reactant feed CH₄/O₂/N₂ is 2/20/178 (1%/10%/89%) NmL/min. The red curve symbolizes when the reaction was heated up to 600 °C and the blue curve when it was cooled from 600 °C to 250 °C.

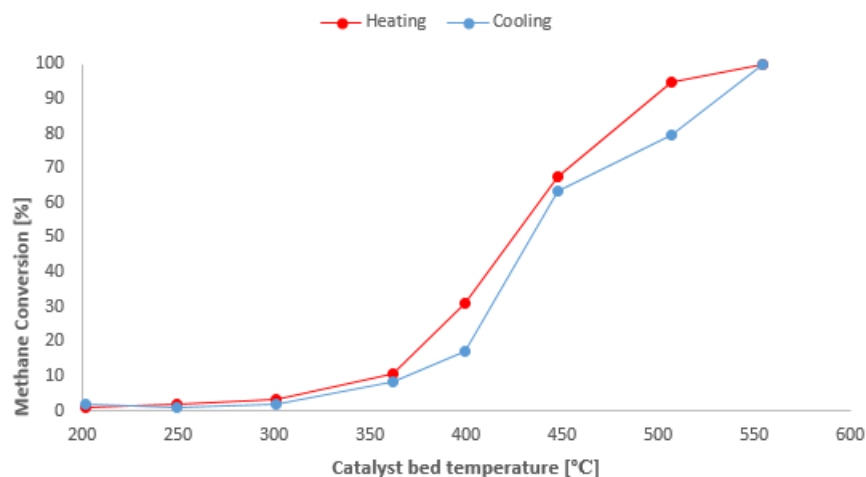


Figure 42: The methane converted (%) in the catalytic combustion of methane over the 0.2 wt% Pd/Al₂O₃ MT catalyst as a function of the catalyst bed temperature (°C) with a GHSV equal to 58000 NmL/g_{cat}h. The temperature was ramped for 5°C/min and the temperature was held for 20 minutes every 50 °C. The flow reactant feed CH₄/O₂/N₂ is 2/10/188 (1%/5%/96%) NmL/min. The red curve symbolizes when the reaction was heated up to 600 °C and the blue curve when it was cooled from 600 °C to 250 °C.

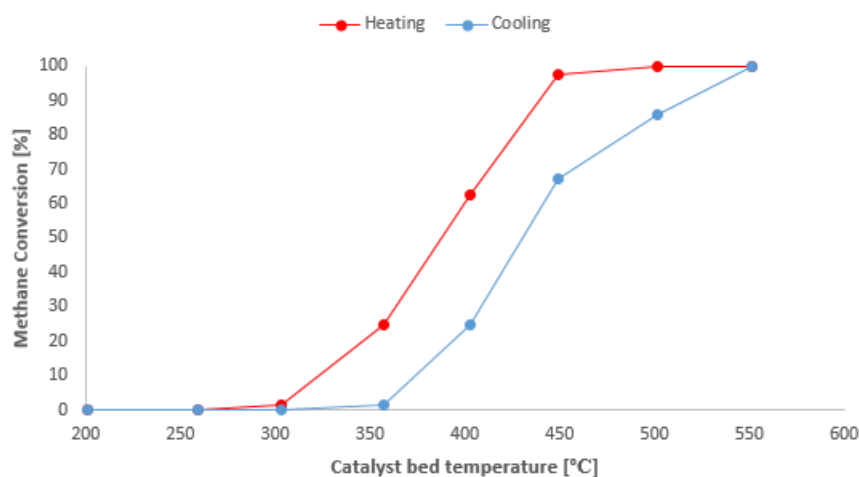


Figure 43: The methane converted (%) in the catalytic combustion of methane over the 0.2 wt% Pd/Al₂O₃ MT catalyst as a function of the catalyst bed temperature (°C) with a GHSV equal to 58000 NmL/g_{cat}h. The temperature was ramped for 5°C/min and the temperature was held for 20 minutes every 50 °C. The flow reactant feed CH₄/O₂/N₂ is 1/5/194 (0.5%/2.5%/97%) NmL/min. The red curve symbolizes when the reaction was heated up to 600 °C and the blue curve when it was cooled from 600 °C to 250 °C.

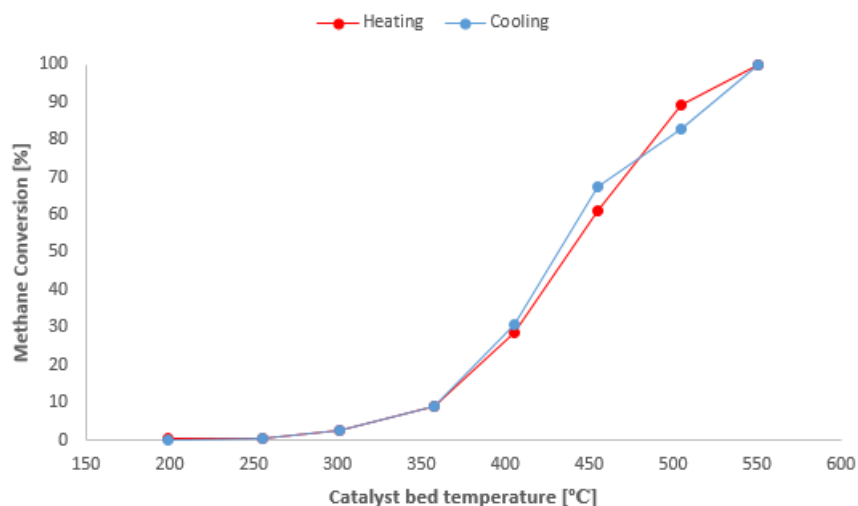


Figure 44: The methane converted (%) in the catalytic combustion of methane over the 0.2 wt% Pd/Al₂O₃ MT catalyst as a function of the catalyst bed temperature (°C) with a GHSV equal to 58000 NmL/g_{cat}h. The temperature was ramped for 5°C/min and the temperature was held for 20 minutes every 25-50 °C. The flow reactant feed CH₄/O₂/N₂ is 1/10/189 (0.5%/5%/97%) NmL/min. The red curve symbolizes when the reaction was heated up to 600 °C and the blue curve when it was cooled from 600 °C to 250 °C.

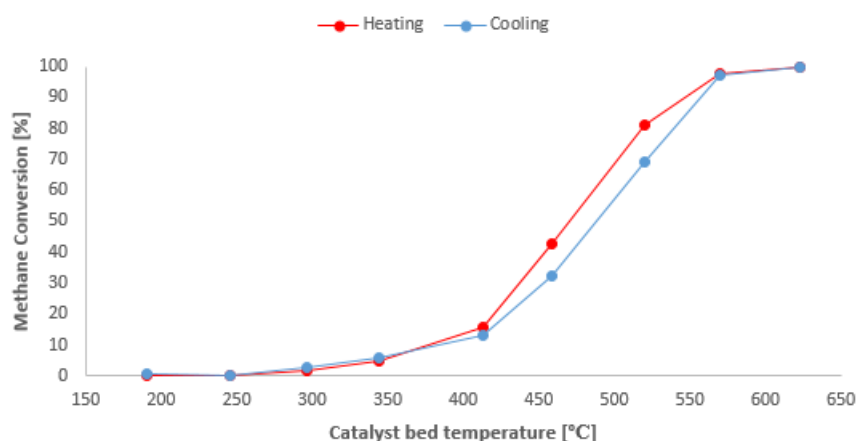


Figure 45: The methane converted (%) in the catalytic combustion of methane over the 0.2 wt% Pd/Al₂O₃ MT catalyst as a function of the catalyst bed temperature (°C) with a GHSV equal to 58000 NmL/g_{cat}h. The temperature was ramped for 5°C/min and the temperature was held for 20 minutes every 25-50 °C. The flow reactant feed CH₄/O₂/N₂ is 4/20/176 (2%/10%/88%) NmL/min. The red curve symbolizes when the reaction was heated up to 650 °C and the blue curve when it was cooled from 650 °C to 250 °C.

N.3 2.0 wt% Pd/Al₂O₃ MT catalyst

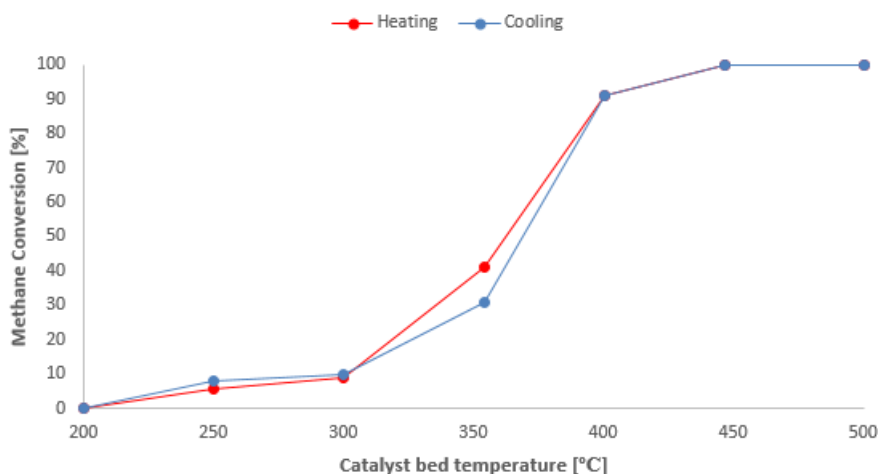


Figure 46: The methane converted (%) in the catalytic combustion of methane over the 2.0 wt% Pd/Al₂O₃ MT catalyst as a function of the catalyst bed temperature (°C) with a GHSV equal to 58800 NmL/g_{cat}h. The temperature was ramped for 5°C/min and the temperature was held for 20 minutes every 50 °C. The flow reactant feed CH₄/O₂/N₂ is 4/20/176 (2%/10%/88%) NmL/min. The red curve symbolizes when the reaction was heated up to 500 °C and the blue curve when it was cooled from 500 °C to 200 °C. The tests were ran in series where this was run number one.

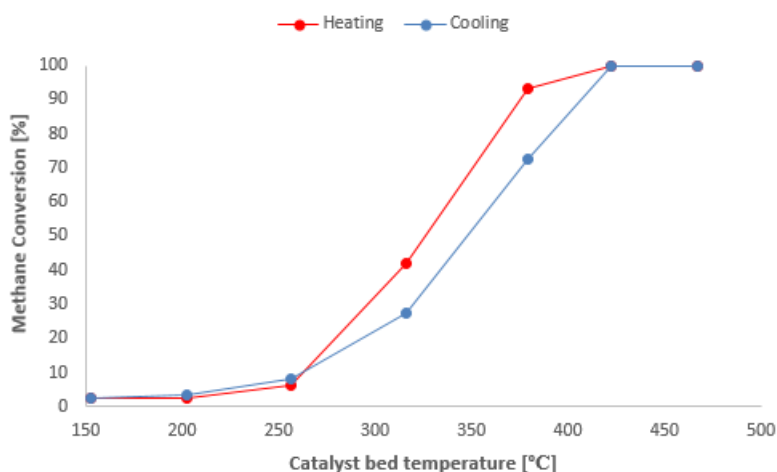


Figure 47: The methane converted (%) in the catalytic combustion of methane over the 2.0 wt% Pd/Al₂O₃ MT catalyst as a function of the catalyst bed temperature (°C) with a GHSV equal to 58800 NmL/g_{cat}h. The temperature was ramped for 5°C/min and the temperature was held for 20 minutes every 50 °C. The flow reactant feed CH₄/O₂/N₂ is 4/20/176 (2%/10%/88%) NmL/min. The red curve symbolizes when the reaction was heated up to 500 °C and the blue curve when it was cooled from 500 °C to 200 °C. The tests were ran in series where this was run number two.

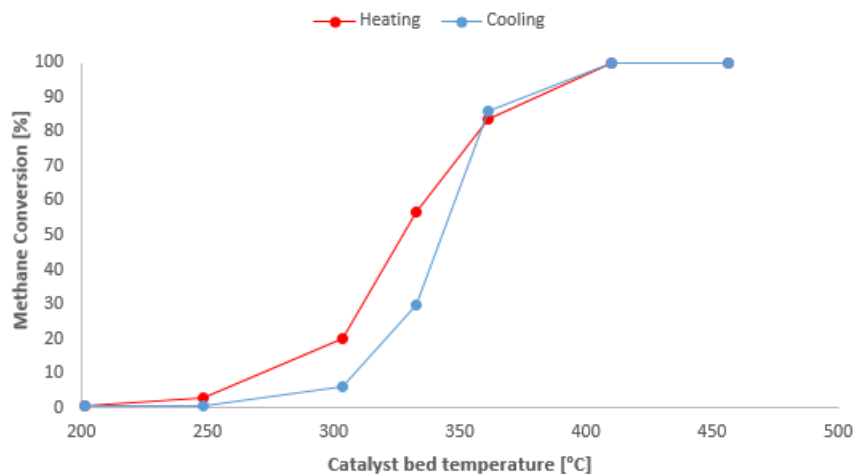


Figure 48: The methane converted (%) in the catalytic combustion of methane over the 2.0 wt% Pd/Al₂O₃ MT catalyst as a function of the catalyst bed temperature (°C) with a GHSV equal to 58800 NmL/g_{cat}h. The temperature was ramped for 5°C/min and the temperature was held for 20 minutes every 50 °C. The flow reactant feed CH₄/O₂/N₂ is 2/20/178 (1%/10%/89%) NmL/min. The red curve symbolizes when the reaction was heated up to 500 °C and the blue curve when it was cooled from 500 °C to 250 °C. The tests were ran in series where this was run number three.

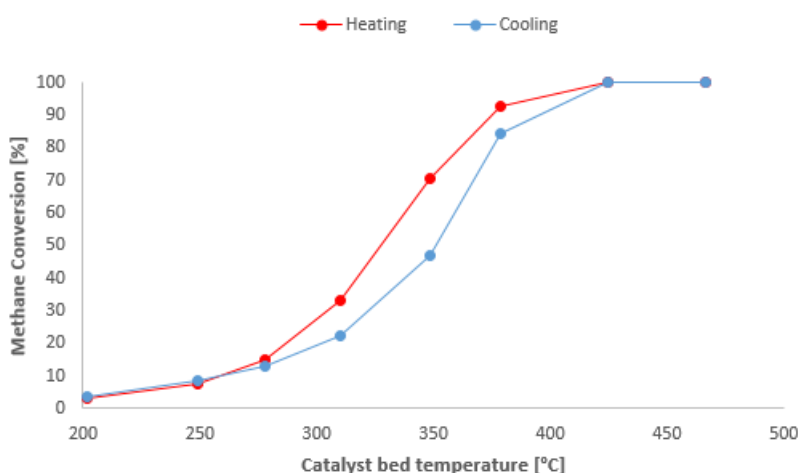


Figure 49: The methane converted (%) in the catalytic combustion of methane over the 2.0 wt% Pd/Al₂O₃ MT catalyst as a function of the catalyst bed temperature (°C) with a GHSV equal to 58800 NmL/g_{cat}h. The temperature was ramped for 5°C/min and the temperature was held for 20 minutes every 50 °C. The flow reactant feed CH₄/O₂/N₂ is 4/20/176 (2%/10%/88%) NmL/min. The red curve symbolizes when the reaction was heated up to 500 °C and the blue curve when it was cooled from 500 °C to 250 °C. The tests were ran in series where this was run number four.

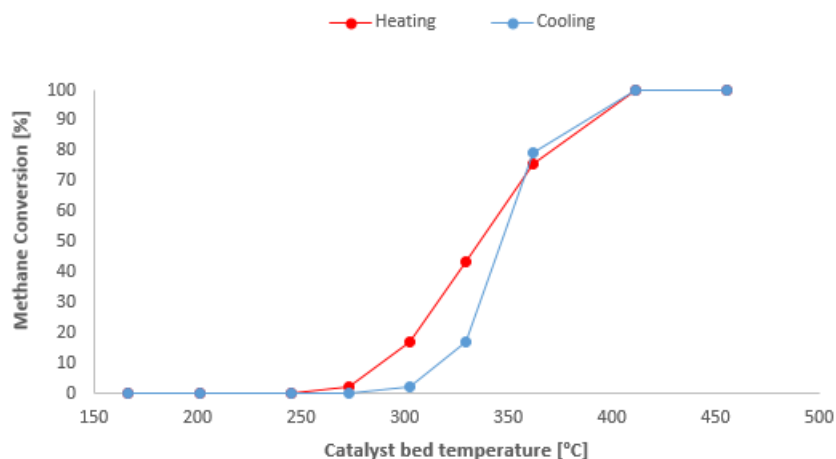


Figure 50: The methane converted (%) in the catalytic combustion of methane over the 2.0 wt% Pd/Al₂O₃ MT catalyst as a function of the catalyst bed temperature (°C) with a GHSV equal to 58800 NmL/g_{cat}h. The temperature was ramped for 5°C/min and the temperature was held for 20 minutes every 50 °C. The flow reactant feed CH₄/O₂/N₂ is 2/10/188 (1%/5%/94%) NmL/min. The red curve symbolizes when the reaction was heated up to 500 °C and the blue curve when it was cooled from 500 °C to 200 °C. The tests were ran in series where this was run number five.

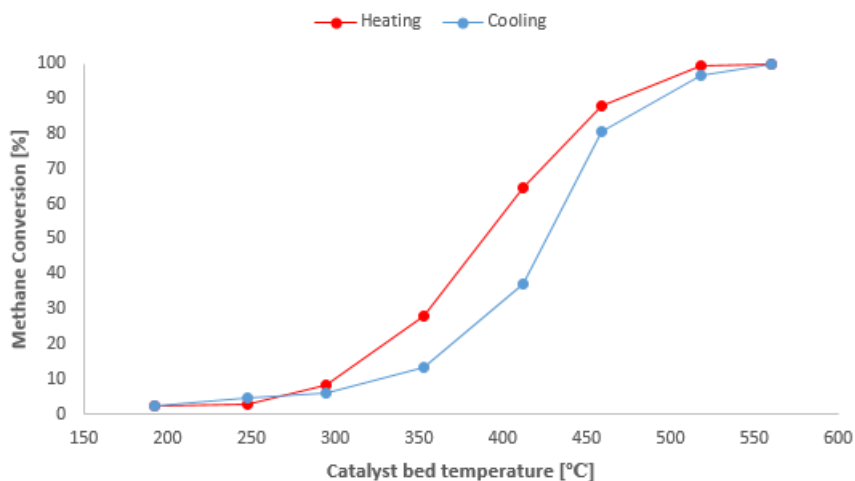


Figure 51: The methane converted (%) in the catalytic combustion of methane over the 2.0 wt% Pd/Al₂O₃ MT catalyst as a function of the catalyst bed temperature (°C) with a GHSV equal to 58800 NmL/g_{cat}h. The temperature was ramped for 5°C/min and the temperature was held for 20 minutes every 50 °C. The flow reactant feed CH₄/O₂/N₂ is 1/5/194 (0.5%/2.5%/97%) NmL/min. The red curve symbolizes when the reaction was heated up to 500 °C and the blue curve when it was cooled from 500 °C to 250 °C. The tests were ran in series where this was run number six.

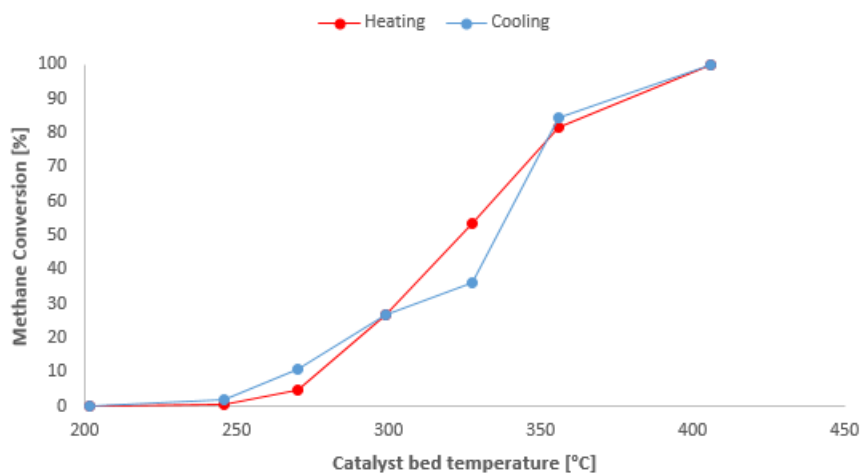


Figure 52: The methane converted (%) in the catalytic combustion of methane over the 2.0 wt% Pd/Al₂O₃ MT catalyst as a function of the catalyst bed temperature (°C) with a GHSV equal to 58800 NmL/g_{cat}h. The temperature was ramped for 5°C/min and the temperature was held for 20 minutes every 50 °C. The flow reactant feed CH₄/O₂/N₂ is 1/10/189 (0.5%/5%/94.5%) NmL/min. The red curve symbolizes when the reaction was heated up to 450 °C and the blue curve when it was cooled from 450 °C to 250 °C. The tests were ran in series where this was run number seven.

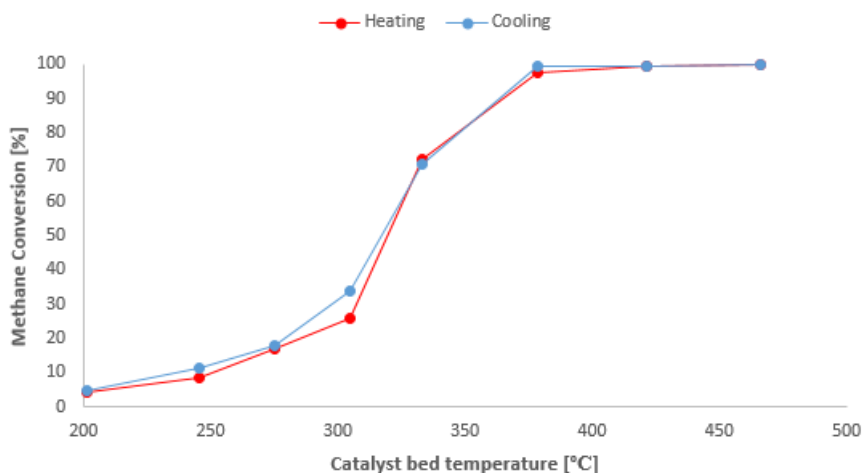


Figure 53: The methane converted (%) in the catalytic combustion of methane over the 2.0 wt% Pd/Al₂O₃ MT catalyst as a function of the catalyst bed temperature (°C) with a GHSV equal to 58800 NmL/g_{cat}h. The temperature was ramped for 5°C/min and the temperature was held for 20 minutes every 50 °C. The flow reactant feed CH₄/O₂/N₂ is 4/20/176 (2%/10%/88%) NmL/min. The red curve symbolizes when the reaction was heated up to 500 °C and the blue curve when it was cooled from 500 °C to 250 °C. The tests were ran in series where this was run number eight.

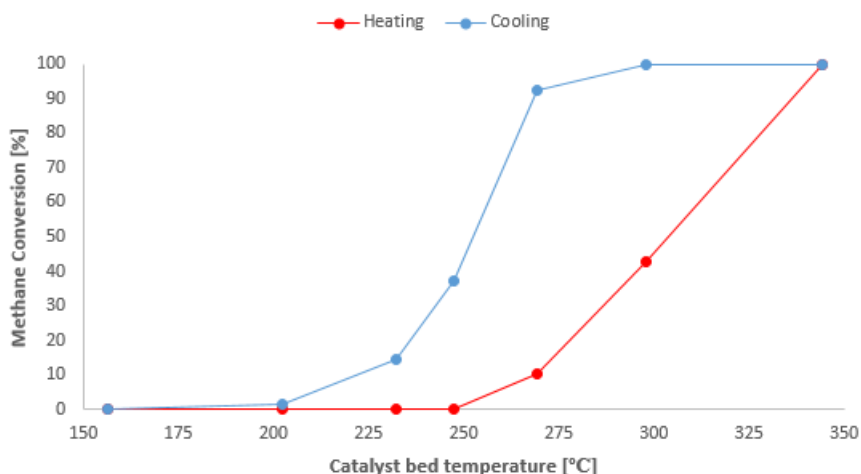


Figure 54: The methane converted (%) in the catalytic combustion of methane over the 2.0 wt% Pd/Al₂O₃ MT catalyst as a function of the catalyst bed temperature (°C) with a GHSV equal to 59400 NmL/g_{cat}h. The temperature was ramped for 5°C/min and the temperature was held for 20 minutes every 50 °C. The flow reactant feed CH₄/O₂/N₂ is 0.2/1/198.8 (0.1%/0.5%/99.4%) NmL/min. The red curve symbolizes when the reaction was heated up to 400 °C and the blue curve when it was cooled from 400 °C to 200 °C. A gas bottle with 5% CH₄ in N₂ was used to achieve lower methane concentrations and were tested using a fresh catalyst.

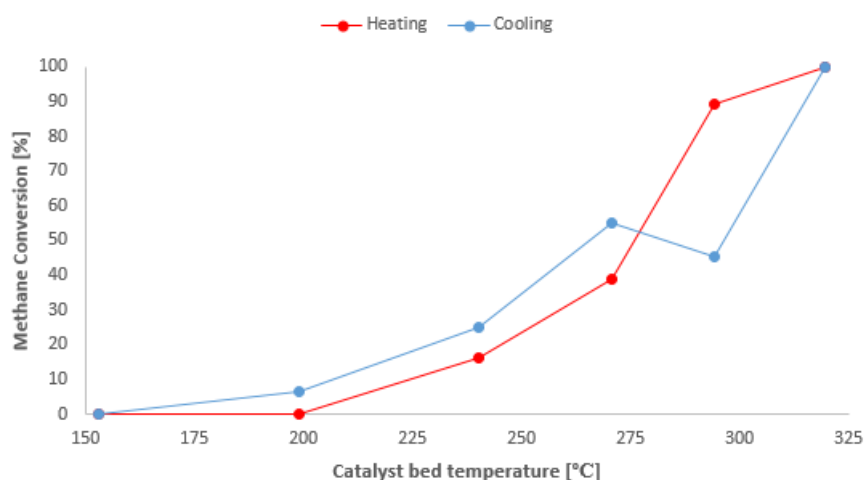


Figure 55: The methane converted (%) in the catalytic combustion of methane over the 2.0 wt% Pd/Al₂O₃ MT catalyst as a function of the catalyst bed temperature (°C) with a GHSV equal to 59400 NmL/g_{cat}h. The temperature was ramped for 5°C/min and the temperature was held for 20 minutes every 50 °C. The flow reactant feed CH₄/O₂/N₂ is 0.2/2/197.8 (0.1%/1%/98.9%) NmL/min. The red curve symbolizes when the reaction was heated up to 375 °C and the blue curve when it was cooled from 375 °C to 200 °C. A gas bottle with 5% CH₄ in N₂ was used to achieve lower methane concentrations. The same catalyst as used to achieve the results in Figure 54 was used.

O Conversion Calculations

The methane conversion as a function of the real catalyst bed temperature were calculated using the data from the GC apparatus, the temperature measurements from Appendix L and Equation 18. The normal volumetric flows of the reactants were 4 NmL/min, 20 NmL/min and 176 NmL/min for methane, synthetic air and nitrogen, respectively, using the reference conditions. The air contains 79% nitrogen and 21% O₂. The normal volumetric flows (NmL/min) were converted to molar flows using standard molar volume of a gas which is defined as the volume occupied by 1 mole of any gas at 0 °C (273 K) and 1 atm (STP), and is equal to 22400 mL, as shown below:

$$F_{tot,in} = \frac{200 \text{ NmL/min}}{22400 \text{ NmL at STP} \cdot 60 \text{ s/min}} = 1.49 \cdot 10^{-4} \text{ mol/s} \quad (47)$$

The total molar flow of the entering inert nitrogen gas is:

$$F_{N_2,in} = F_{N_2,out} = \frac{(176) \text{ NmL/min}}{22400 \text{ NmL at STP} \cdot 60 \text{ s/min}} = 1.31 \cdot 10^{-4} \text{ mol/s} \quad (48)$$

The molar flows of the gases can be found using:

$$F_{i,out} = F_{tot,out} \cdot \text{mol}\%_{i,out} \quad (49)$$

where $F_{i,out}$, $F_{tot,out}$ and $\text{mol}\%_{i,out}$ are the molar out flow of gas i , the total molar out flow and the mol% of gas i , respectively. The total molar out flow can be found using Equation 48 and the mol% of nitrogen detected by the GC:

$$F_{tot,out} = \frac{F_{N_2,out}}{\text{mol}\%_{N_2,out}} = \frac{1.31 \cdot 10^{-4} \text{ mol/s}}{83.9 \text{ mol}\%} = 1.56 \cdot 10^{-6} \text{ mol/s} \quad (50)$$

The $\text{mol}\%_{N_2,out}$ is the average mol% of N₂ out of the reactor detected by the GC. The methane conversion is calculated using Equation 18 for each hold-up temperature, i.e. 200-550 °C with 50 °C intervals. The real catalyst bed temperatures are based on measurements made throughout the catalyst bed and can be found in Appendix L. The GHSVs are calculated and can be found in Appendix M. The calculations are done for each reaction run, i.e. the reactions described in Table 3, for the 0.2 wt% Pd/Al₂O₃ SP, 0.2 wt% Pd/Al₂O₃ MT and 2.0 wt% Pd/Al₂O₃ MT catalysts. The temperatures where 10% and 50% of the methane was converted, T_{10%} and T_{50%}, respectively, was found using linear regression of the combustion curves in Appendix N and the data obtained below. The results can be found in the following tables:

Table 38: The catalytic activities for the methane oxidation reaction, using 0.2 wt% Pd/Al₂O₃ SP catalyst, at each set hold-up temperature, i.e. 200-550 °C with 50 °C intervals and GHSV equal to 59400 NmL/g_{cat}h. The real catalyst bed temperature were found by measuring the temperature throughout the catalyst bed and is 8.4 °C below the real temperature. The reaction conditions can be found in Table 3 as reaction number 1.

Set Temperature [°C]	Real Temperature [°C]	Methane Conversion, X_{CH₄} [%]
200	190	0.0
250	240	0.6
300	290	3.3
350	340	13
400	390	32
450	440	57
500	490	91
550	440	98

Table 39: The catalytic activities for the methane oxidation reaction, using 0.2 wt% Pd/Al₂O₃ MT catalyst, at each set hold-up temperature, i.e. 250-600 °C with 50 °C intervals and GHSV equal to 58000 NmL/g_{cat}h. The real catalyst bed temperature were found by measuring the temperature throughout the catalyst bed and the measurements can be found in Appendix L. The reaction conditions can be found in Table 3 as reaction number 1.

Set Temperature [°C]	Real Temperature [°C]	Methane Conversion, X_{CH₄} [%]
250	190	2.3
300	250	2.9
350	290	8.3
400	350	28
450	410	65
500	460	88
550	520	99
600	560	100

Table 40: The catalytic activities for the methane oxidation reaction, using 0.2 wt% Pd/Al₂O₃ MT catalyst, at each set hold-up temperature, i.e. 250-600 °C with 50 °C intervals and GHSV equal to 58000 NmL/g_{cat}h. The real catalyst bed temperature were found by measuring the temperature throughout the catalyst bed and the measurements can be found in Appendix L. The reaction conditions can be found in Table 3 as reaction number 3.

Set Temperature [°C]	Real Temperature [°C]	Methane Conversion, X_{CH₄} [%]
250	200	2.2
300	240	2.2
350	300	4.4
400	340	15
450	400	42
500	450	81
550	510	99
600	560	100

Table 41: The catalytic activities for the methane oxidation reaction, using 0.2 wt% Pd/Al₂O₃ MT catalyst, at each set hold-up temperature, i.e. 250-600 °C with 50 °C intervals and GHSV equal to 58000 NmL/g_{cat}h. The real catalyst bed temperature were found by measuring the temperature throughout the catalyst bed and the measurements can be found in Appendix L. The reaction conditions can be found in Table 3 as reaction number 5.

Set Temperature [°C]	Real Temperature [°C]	Methane Conversion, X_{CH₄} [%]
250	200	1.0
300	250	2.1
350	300	3.2
400	360	11
450	400	31
500	450	68
550	510	95
600	560	100

Table 42: The catalytic activities for the methane oxidation reaction, using 0.2 wt% Pd/Al₂O₃ MT catalyst, at each set hold-up temperature, i.e. 250-600 °C with 50 °C intervals and GHSV equal to 58000 NmL/g_{cat}h. The real catalyst bed temperature were found by measuring the temperature throughout the catalyst bed and the measurements can be found in Appendix L. The reaction conditions can be found in Table 3 as reaction number 6.

Set Temperature [°C]	Real Temperature [°C]	Methane Conversion, X_{CH₄} [%]
250	200	0.0
300	260	0.0
350	300	1.4
400	360	25
450	400	62
500	450	98
550	500	100
600	550	100

Table 43: The catalytic activities for the methane oxidation reaction, using 0.2 wt% Pd/Al₂O₃ MT catalyst, at each set hold-up temperature, i.e. 250-600 °C with 50 °C intervals and GHSV equal to 58000 NmL/g_{cat}h. The real catalyst bed temperature were found by measuring the temperature throughout the catalyst bed and the measurements can be found in Appendix L. The reaction conditions can be found in Table 3 as reaction number 7.

Set Temperature [°C]	Real Temperature [°C]	Methane Conversion, X_{CH₄} [%]
250	200	0.6
300	250	0.6
350	300	2.8
400	360	9.3
450	410	29
500	460	61
550	500	89
600	560	100

Table 44: The catalytic activities for the methane oxidation reaction, using 0.2 wt% Pd/Al₂O₃ MT catalyst, at each set hold-up temperature, i.e. 250-650 °C with 50 °C intervals and GHSV equal to 58000 NmL/g_{cat}h. The real catalyst bed temperature were found by measuring the temperature throughout the catalyst bed and the measurements can be found in Appendix L. The reaction conditions can be found in Table 3 as reaction number 8.

Set Temperature [°C]	Real Temperature [°C]	Methane Conversion, X _{CH₄} [%]
250	190	0.4
300	250	0.4
350	300	1.5
400	340	4.8
450	410	15
500	460	43
550	520	81
600	570	98
650	620	100

Table 45: The catalytic activities for the methane oxidation reaction, using 2.0 wt% Pd/Al₂O₃ MT catalyst, at each set hold-up temperature, i.e. 200-500 °C with 50 °C intervals and GHSV equal to 58800 NmL/g_{cat}h. The real catalyst bed temperature were found by measuring the temperature throughout the catalyst bed and is 0.3 °C above the real temperature. The reaction conditions can be found in Table 3 as reaction number 1.

Set Temperature [°C]	Real Temperature [°C]	Methane Conversion, X _{CH₄} [%]
200	200	0.0
250	250	5.6
300	300	8.8
350	350	41
400	400	91
450	450	100
500	500	100

Table 46: The catalytic activities for the methane oxidation reaction, using 2.0 wt% Pd/Al₂O₃ MT catalyst, at each set hold-up temperature, i.e. 200-500 °C with 50 °C intervals and GHSV equal to 58800 NmL/g_{cat}h. The real catalyst bed temperature were found by measuring the temperature throughout the catalyst bed and the measurements can be found in Appendix L. The reaction conditions can be found in Table 3 as reaction number 2.

Set Temperature [°C]	Real Temperature [°C]	Methane Conversion, X _{CH₄} [%]
200	150	2.4
250	200	2.4
300	260	6.1
350	320	42
400	380	93
450	420	100
500	470	100

Table 47: The catalytic activities for the methane oxidation reaction, using 2.0 wt% Pd/Al₂O₃ MT catalyst, at each set hold-up temperature, i.e. 250-500 °C with 25-50 °C intervals and GHSV equal to 58800 NmL/g_{cat}h. The real catalyst bed temperature were found by measuring the temperature throughout the catalyst bed and the measurements can be found in Appendix L. The reaction conditions can be found in Table 3 as reaction number 3.

Set Temperature [°C]	Real Temperature [°C]	Methane Conversion, X_{CH₄} [%]
250	200	0.6
300	250	2.8
350	300	20
375	330	57
400	360	84
450	410	100
500	460	100

Table 48: The catalytic activities for the methane oxidation reaction, using 2.0 wt% Pd/Al₂O₃ MT catalyst, at each set hold-up temperature, i.e. 250-500 °C with 25-50 °C intervals and GHSV equal to 58800 NmL/g_{cat}h. The real catalyst bed temperature were found by measuring the temperature throughout the catalyst bed and the measurements can be found in Appendix L. The reaction conditions can be found in Table 3 as reaction number 4.

Set Temperature [°C]	Real Temperature [°C]	Methane Conversion, X_{CH₄} [%]
250	200	3.2
300	250	7.5
325	280	15
350	310	33
375	350	71
400	380	93
450	420	100
500	470	100

Table 49: The catalytic activities for the methane oxidation reaction, using 2.0 wt% Pd/Al₂O₃ MT catalyst, at each set hold-up temperature, i.e. 200-500 °C with 25-50 °C intervals and GHSV equal to 58800 NmL/g_{cat}h. The real catalyst bed temperature were found by measuring the temperature throughout the catalyst bed and the measurements can be found in Appendix L. The reaction conditions can be found in Table 3 as reaction number 5.

Set Temperature [°C]	Real Temperature [°C]	Methane Conversion, X_{CH₄} [%]
200	170	0.0
250	200	0.0
300	250	0.0
325	270	0.0
350	300	17
375	330	44
400	360	76
450	410	100
500	460	100

Table 50: The catalytic activities for the methane oxidation reaction, using 2.0 wt% Pd/Al₂O₃ MT catalyst, at each set hold-up temperature, i.e. 250-600 °C with 50 °C intervals and GHSV equal to 58800 NmL/g_{cat}h. The real catalyst bed temperature were found by measuring the temperature throughout the catalyst bed and the measurements can be found in Appendix L. The reaction conditions can be found in Table 3 as reaction number 6.

Set Temperature [°C]	Real Temperature [°C]	Methane Conversion, X_{CH₄} [%]
250	190	2.3
300	250	2.9
350	290	8.3
400	350	28
450	410	65
500	460	88
550	520	99
600	560	100

Table 51: The catalytic activities for the methane oxidation reaction, using 2.0 wt% Pd/Al₂O₃ MT catalyst, at each set hold-up temperature, i.e. 250-450 °C with 25-50 °C intervals and GHSV equal to 58800 NmL/g_{cat}h. The real catalyst bed temperature were found by measuring the temperature throughout the catalyst bed and the measurements can be found in Appendix L. The reaction conditions can be found in Table 3 as reaction number 7.

Set Temperature [°C]	Real Temperature [°C]	Methane Conversion, X_{CH₄} [%]
250	200	0.0
300	250	0.5
325	270	4.6
350	300	27
375	330	54
400	360	82
450	400	100

Table 52: The catalytic activities for the methane oxidation reaction, using 2.0 wt% Pd/Al₂O₃ MT catalyst, at each set hold-up temperature, i.e. 200-500 °C with 25-50 °C intervals and GHSV equal to 58800 NmL/g_{cat}h. The real catalyst bed temperature were found by measuring the temperature throughout the catalyst bed and the measurements can be found in Appendix L. The reaction conditions can be found in Table 3 as reaction number 8.

Set Temperature [°C]	Real Temperature [°C]	Methane Conversion, X_{CH₄} [%]
200	200	0.0
250	200	4.4
300	250	8.6
325	280	17
350	300	26
375	330	72
400	380	97
450	420	99
500	470	100

Table 53: The catalytic activities for the methane oxidation reaction, using 2.0 wt% Pd/Al₂O₃ MT catalyst, at each set hold-up temperature, i.e. 200-400 °C with 25-50 °C intervals and GHSV equal to 59400 NmL/g_{cat}h. The real catalyst bed temperature were found by measuring the temperature throughout the catalyst bed and the measurements can be found in Appendix L. The reaction conditions can be found in Table 3 as reaction number 9.

Set Temperature [°C]	Real Temperature [°C]	Methane Conversion, X_{CH₄} [%]
200	160	0.0
250	200	0.0
275	230	0.0
300	250	0.0
325	270	10
350	300	43
400	340	100

Table 54: The catalytic activities for the methane oxidation reaction, using 2.0 wt% Pd/Al₂O₃ MT catalyst, at each set hold-up temperature, i.e. 200-375 °C with 25-50 °C intervals and GHSV equal to 59400 NmL/g_{cat}h. The real catalyst bed temperature were found by measuring the temperature throughout the catalyst bed and the measurements can be found in Appendix L. The reaction conditions can be found in Table 3 as reaction number 10.

Set Temperature [°C]	Real Temperature [°C]	Methane Conversion, X_{CH₄} [%]
200	150	0.0
250	200	0.0
300	240	16
325	271	39
350	290	89
375	320	100

P Check of the mass balances from the reaction

Table 55 shows the molar flows detected of CH₄, N₂ and CO₂ by the gas chromatograph when the activity of the 0.2 wt% Pd/Al₂O₃ SP was tested. The water is dried up and therefore not detected. No CO was detected for any of the catalysts tested and O₂ is normally not detected by the GC. The flows of each of the inlet gases are found in Section 3.4 in Table 3. The actual and theoretical molar flows were calculated using the Equations 47, 48 and 49 in Appendix O. When using the 0.2 wt% Pd/Al₂O₃ SP catalyst, only 98% of the methane was converted, as seen in Table 38. The theoretical flows out of the reactor are calculated based on that methane was not fully converted. 2% of the methane is not converted:

$$0.02 \times 3.0 \cdot 10^{-6} \text{ mol/s} = 6.0 \cdot 10^{-8} \text{ mol/s} \quad (51)$$

The rest of the C-atoms will convert to carbon dioxide, since no carbon monoxide is detected, and consequently:

$$0.98 \times 3.0 \cdot 10^{-6} \text{ mol/s} = 2.9 \cdot 10^{-6} \text{ mol/s} \quad (52)$$

98% of the hydrogen in the methane will be converted to water with a stoichiometric ratio of 4:2, and the out flow of water will be:

$$\frac{0.98 \times (1.5 \cdot 10^{-5} - 3.0 \cdot 10^{-6}) \text{ mol/s}}{2} = 5.8 \cdot 10^{-6} \text{ mol/s} \quad (53)$$

The out flow of oxygen is:

$$F_{O_2,out} = F_{O_2,in} - F_{H_2O,out} = (1.5 \cdot 10^{-5} - 5.8 \cdot 10^{-6}) \text{ mol/s} = 9.2 \cdot 10^{-6} \text{ mol/s} \quad (54)$$

Table 55 shows the calculated theoretical out flows of the components for the gases methane, oxygen, nitrogen, carbon dioxide and water, when the methane conversion is 98%. The molar flows out of the reactor detected by the GC and the molar flows calculated based on a 98% methane conversion are fairly similar and are marked in red. Also, the total molar feed flow is equal to the calculated total molar flow out of the reactor, i.e. the mass balance make up, and it is reasonable to conclude that no bi-products are produced. When the 0.2 wt% Pd/Al₂O₃ MT and 2.0 wt% Pd/Al₂O₃ MT catalysts were tested, all the runs achieved complete methane oxidation, i.e. conversion equal to 100%, and therefore it is expected that the mass balances make up. The results suggest that the GC gives reasonable data.

Table 55: The molar flows of the gases CH₄, CO₂ and inert N₂ detected by the gas chromatograph (GC) when testing the 0.2 wt% Pd/Al₂O₃ SP catalyst for the methane oxidation reaction. Water was dried and O₂ is normally not detected by the GC. The composition of the gases in the feed was set to be 4 NmL/min, 20 NmL/min and 176 NmL/min for methane, oxygen and nitrogen, respectively, at 1 bar and GHSV equal to 59400 NmL/g_{cat}h, and the gas compositions at the reactor outlet was calculated when a 98% methane conversion was achieved at 540 °C in the catalyst bed.

Compound	Set molar flow in [mol/s]	Molar flow out (by GC) [mol/s]	Molar flow out (calculated) [mol/s]
CH ₄	$3.0 \cdot 10^{-6}$	$6.1 \cdot 10^{-8}$	$6.0 \cdot 10^{-8}$
N ₂	$1.3 \cdot 10^{-4}$	$1.3 \cdot 10^{-4}$	$1.3 \cdot 10^{-4}$
O ₂	$1.5 \cdot 10^{-5}$	-	$9.2 \cdot 10^{-6}$
CO ₂	0.0	$2.9 \cdot 10^{-6}$	$2.9 \cdot 10^{-6}$
H ₂ O	0.0	-	$5.8 \cdot 10^{-6}$
Total	$1.5 \cdot 10^{-4}$	$1.3 \cdot 10^{-4}$	$1.5 \cdot 10^{-4}$